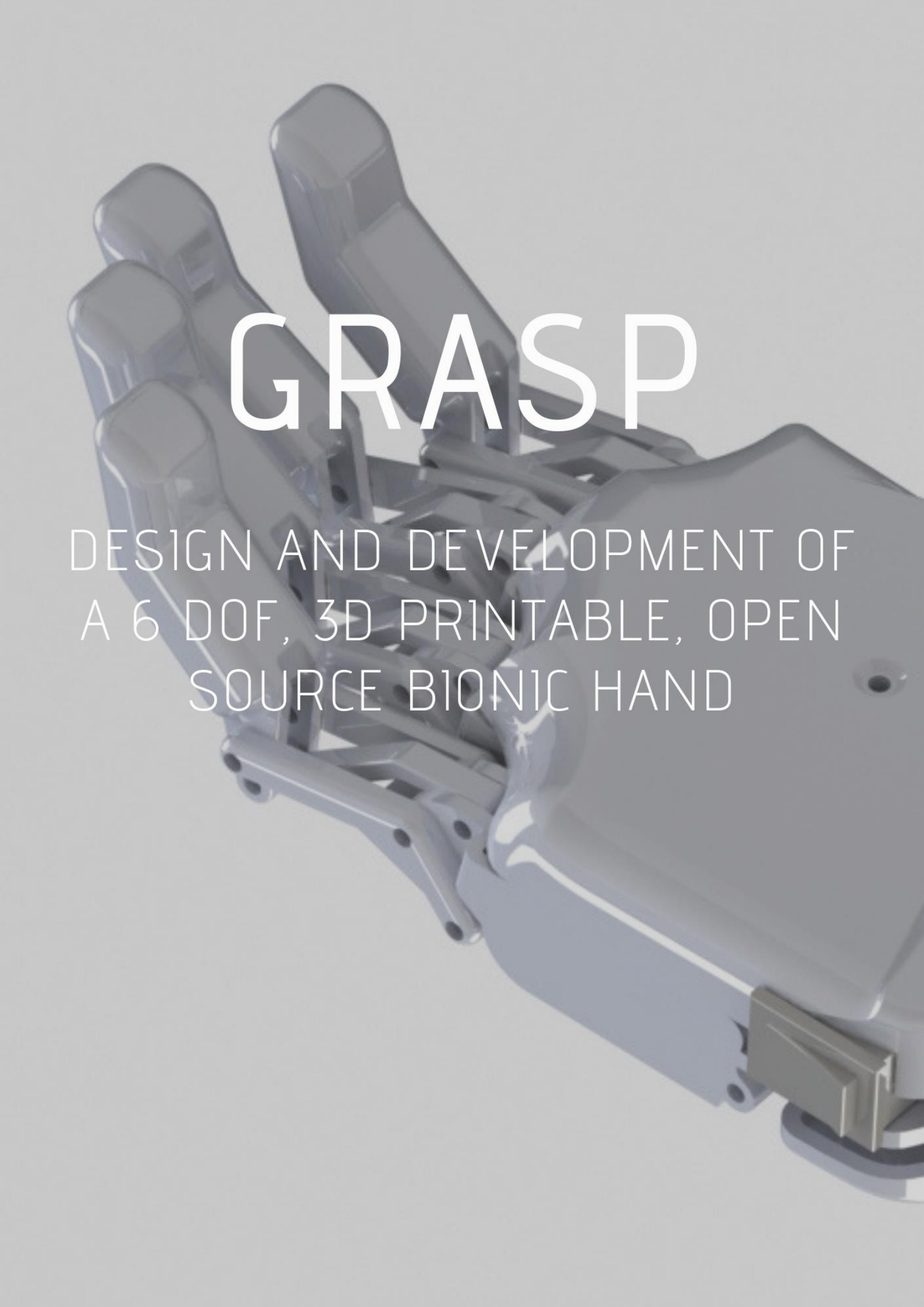


GRASP



DESIGN AND DEVELOPMENT OF
A 6 DOF, 3D PRINTABLE, OPEN
SOURCE BIONIC HAND

Abstract

There are 3 millions of upper limb amputees worldwide, and this represents a minority of 5% of the total number of amputees. For this reason, the costs of production of an advanced bionic limb are so elevated. This impacts on the acquisition prices, setting them between 25.000 and 75.000 €. The main motivation of the present work has been to create a design of a bionic hand with 6 degrees of freedom (DOF), which can be 3D printed with competitive features respect to the best commercial models available in the market in terms of flexion-extension speed and force.

Each of the aims of the project has been a different technological challenge. The main objectives can be summarised as follows: (1) the bionic hand must be able to reproduce the 6 most important types of grips required in order to carry out activities of daily life; (2) all the components: electronics and actuators should be included into the palm of the hand to reduce the possible space occupied in the forearm; (3) the hand mass should be less than 400g, which is the weight critical for the user to be considered too heavy; (4) the bionic hand should be easily assembled and programmed by the same user once you have downloaded the open source files; (5) the total cost of the hand must be below 500 € including all components. Finally, the greatest challenge is to achieve all these objectives and at the same time be competitive with respect to existing commercial projects.

The project includes the development of various designs and 3D printable prototypes that have been carried out during the previous 4 years. All the experience and knowledge acquired with these prior designs culminated in Grasp: the latest design, presented in this work. Grasp sets out to achieve all the objectives that have emerged from the needs that must be covered to provide a product with the optimal quality and functionality.

List of abbreviations

DOF	Degrees of freedom
BP	Body powered
EP	Externally powered
ADL's	Activities of daily living
EMG	Electromyography
FDM	Fused deposition modelling
DC	Direct current
PWM	Pulse width modulation
CAD	Computer aided design
CMC	Carpometacarpal
MCP	Metacarpal
IP	Interphalangeal
DIP	Distal interphalangeal
PIP	Proximal interphalangeal
Li-Po	Lithium Polymer
PLA	Polylactic acid
ABS	Acrylonitrile butadiene styrene
SLA	Stereo lithography
PCB	Printed circuit board
FEM	Finite element method
IDE	Integrated development environment
CE	European conformity
EMI	Electromagnetic interference
EMC	Electromagnetic compatibility
ISO	International Organization for Standardization
EU	European Union

Contents

introduction	12
Planning.....	13
The problem	15
Amputation causes.....	15
Upper limb amputation levels	15
Advantages of digital manufacturing technologies	16
Issues of digital manufacturing technologies	16
Project goals	16
Project scope.....	17
Aim of the project.....	17
State of the art.....	18
3D printed bionic hands.....	19
Non 3d printed bionic hands.....	20
Influences	22
Influences	23
Project evolution.....	24
Grasp project from 2014 to 2018.....	25
First myoelectric design	26
First palm electronics and actuator integration.....	28
Low cost	29
Grasp 0	31
Grasp beta.....	33
The human hand	34
Anthropometrics of the human hand	35
Grip forces.....	35
Anatomy of the human hand	36
Human hand kinematics	38
Creating a model of the human finger	39
Design process.....	40
Verification and validation	41
Selected dimensions for the standard hand design	41
Types of actuators and mechanical systems	42
Palm electronics integration	43
Providing grip to the distal phalanges	45

Mechanical design iterations	45
Components of the final design.....	46
Prototyping	46
Different sizes.....	48
Left hand.....	48
Drawings	49
Components and materials	50
Components.....	51
Rotary dc micro servo motor: tower pro MG90S.....	51
Linear micro servo motor: actuonix PQ12R.....	51
Microcontroller: arduino nano v3	52
Emg analog sensor: dfrobot oymotion SKU:SEN0240 or emg analog sensor: advancer technologies myoware	52
Pololu step-down voltage regulator D24V25F6.....	53
Turnigy nano-tech 6.0 battery	53
Pololu switch on/off	54
Dfrobot DFR0029-B pushbutton module	54
Imax B6 DC charger.....	54
Materials	55
Rigid material	55
Flexible material: silicone elastomer A-103.....	55
Electronics design.....	56
Electrical design	57
Results	59
Schematics.....	60
PCB design.....	62
Electrical safety	63
Kinematics.....	64
Workspace	65
Finger flexion-extension speed.....	67
Mechanical static study	69
Finger static study.....	70
Free solid diagram	71
Results	72
Thumb static study	78
Free solid diagram	79
Results	80
Stress study.....	81

The finite element method.....	82
Material mechanical properties	82
Strong form.....	82
Boundary conditions.....	82
Load-stress relationship study	83
Convergence study	84
Validation	86
Grip type test	87
Real tests with limbless subjects	88
Fingertip force experimental data.....	89
Finger flexion-extension speed.....	94
Maximum resistance experimental data	96
Control.....	98
EMG morphology of different types of grasps	99
Analog sensor input – linear servo output system calibration.....	100
EMG analog sensor calibration	101
Functions of the main program.....	102
Graphical user interface.....	104
Graphical user interface.....	105
Regulatory framework.....	107
Device classification according to the directive	108
Declaration of conformity	108
Sustainability	110
Environmental cost comparing 3d printing and molding injection	111
Budget	112
Device construction budget	113
Energy consumption budget	114
Publications and divulgation	115
Publications	116
Assembly instructions	117
Grasp 1.0 assembly instructions	118
Discussion	135
Grasp performance	136
Conclusions	140
Conclusions	141
Future work	142
What is next.....	143

References	144
References	145
Appendices	149
Appendix A: finger model script.....	150
Appendix B: micro servo comparison table	151
Appendix C: matlab code for the hand current simulation.....	152
Appendix D1: matlab code for the finger static study	152
Appendix D2: matlab code for the thumb static study	154
Appendix E: FEM solidworks simulation stress study results.	155
Appendix F: FSR calibration equation values using $g = 9.81 \text{ m/s}^2$	155
Appendix G: fingertip force values from the finger model.	155
Appendix H: fingertip force values from the thumb model.	156
Appendix I: arduino script for serial EMG data acquisition using matlab and arduino.	156
Appendix J: matlab function for serial emg data acquisition using matlab and arduino.....	156
Appendix K: matlab script to plot the results of the emg acquisition.....	157
Appendix L: matlab script to plot the solidworks kinematics simulation.	161
Appendix M: tables of finger speed values for the index finger.	164
Appendix N: matlab script to compare the index finger of grasp and the model hand.	165
Appendix O: real values of fingers speed.....	166
Appendix P: hand control program.	166
Appendix Q: graphical user interface code.	171

List of figures

Figure 1: Upper limb amputation types.....	15
Figure 2: Traditional manufacturing vs digital manufacturing production costs.	16
Figure 3: Main types of grasps to perform the ADL's.....	17
Figure 4: From left to right, Tact Hand [8], Hero Arm [16], Exiii Hackberry [13] and One single actuator hand [10].	19
Figure 5: From left to right, Vincent Hand [61], Bebionic 3 [62], i-limb ultra [63], Taska Hand [15], Michelangelo [64] and Sensor Hand [68].....	20
Figure 6: Project Influences in chronological order of discovery, Open Hand Project [7], Flexi Hand [65], i-Limb ultra [63], Bebionic3 [62], Exiii Hackberry [13], Compliant Hand [9], Brunell Hand [16] and AR-10 Hand [66].....	23
Figure 7: Different designs of the project from 2014 to 2019 since the first myoelectric design to the last design of Grasp.....	25
Figure 8: CAD model of the first myoelectric design (left) and 3D printed model (right).	26
Figure 9: First myoelectric design printable components.....	27
Figure 10: Assembly method between flexible joints and rigid segments.	27
Figure 11: Electrical design.....	27
Figure 12: Second myoelectric design printed (right) and designed on CAD (left).....	28
Figure 13: Second myoelectric design components.	28
Figure 14: Second myoelectric hand electrical design.	29
Figure 15: Low cost model in CAD (left) and 3D printed model (right).	29
Figure 16: Low cost model components.....	30
Figure 17: Low cost model circuit.....	30
Figure 18: Grasp 0 3D printed model (left) and CAD design (right).....	31
Figure 19: Grasp 0 3D printable components.....	31
Figure 20: Grasp 0 electrical circuit.	32
Figure 21: Brass worm gear for the combination of plastic metal power transmission [23].....	32
Figure 22: Voltage regulator L78 series recommended capacitors [22].....	32
Figure 23: Grasp 0 finger worm gear mechanical system detail.	32
Figure 24: Grasp Beta 3D printed model and CAD model.	33
Figure 25: Human hand dimensions adapted from [24].	35
Figure 26: Human hand full grasp [25] and fingertip grasp [26] respectively.	35
Figure 27: From above to below, human hand Extension/Flexion, Abduction/Adduction movements and thumb Retroposition/opposition.	36
Figure 28: Dorsal view of the bones of the human hand [69].	37
Figure 29: Palmar view of the muscles and connectivity tissues of the human hand [70].	37
Figure 30: Model of the finger.	39
Figure 31: Finger simulation trajectory.....	39
Figure 32: Design approach schematic.....	41
Figure 33: Dimensions of the Grasp Bionic Hand.	41
Figure 34: Six types of grasps effectuated virtually.	42
Figure 35: Iterations across different types of actuators and mechanicals systems.....	42
Figure 36: Differences in the dimensions of the two micro linear actuators Actuonix [20] (left) and Mighty ZAP [33] (right).....	43
Figure 37: Rotary servo motor selection criteria.	43
Figure 38: From left to right model on Fusion 360 and Solidworks.	44

Figure 39: PCB and Arduino Nano Grabcad model [35] assembled in Solidworks and assembled with the hand.....	44
Figure 40: The two mold models in CAD (above) and the printed part and the result of the silicone cover manufactured (below).....	45
Figure 41: Changes suffered by the thumb finger: length of the distal phalanx and another point of attachment.	45
Figure 42: Grasp 1.0 components.....	46
Figure 43: Grasp 1.0 first prototype 3D printed.....	46
Figure 44: PCB prototype with the soldered pins.....	47
Figure 45: Grasp 1.0 assembled with the PCB and the pushbutton inserted in the bottom cover.....	47
Figure 46: Distal phalanx size L and the standard compared with the L size.....	48
Figure 47: Left and right hand models.....	48
Figure 48: MG90S DC servo motor [34].....	51
Figure 49: Actuonix PQ12R micro linear servo motor [20].....	51
Figure 50: Arduino Nano [19].....	52
Figure 51: Arduino Nano pinout [19].....	52
Figure 52: Myoware EMG analog sensor [21].....	52
Figure 53: OYMotion EMG sensor [39]	53
Figure 54: Pololu D24V25F6 voltage regulator [17].....	53
Figure 55: Battery Nano-tech 6.0 [40].....	53
Figure 56: Pololu Rocket swith [17]	54
Figure 57: DFR0029-B pushbutton [39]	54
Figure 58: Li-po charger [40]	54
Figure 59: Medical grade ABS [41]	55
Figure 60: Medical grade silicone compound [42].....	55
Figure 61: Actuonix PQ-12R current curves values [20].....	57
Figure 62: Pololu D24V25F6 voltage regulator efficiency curves at different voltages [17]	57
Figure 63: Simulink diagram for the current cycles simulation.....	59
Figure 64: Two periods of current over time representation	59
Figure 65: Electric schematic of the Myoware sensors configuration.....	60
Figure 66: Electric schematic of the OYMotion sensors configuration	61
Figure 67: Electric schematic on Eagle	62
Figure 68: PCB board.....	62
Figure 69: PCB board manufacture appearance top and bottom layers	63
Figure 70: PCB board drill holes.....	63
Figure 71: EMG Myoware sensor safety recommendations	63
Figure 72: Finger displacement sequence	65
Figure 73: Origin of coordinates of the simulation in black.....	65
Figure 74: Full hand simulation values	66
Figure 75: Fingers (index, middle, ring and small) simulation values visualized in the three-dimensional space and on the different planes ..	66
Figure 76: Thumb simulation values visualized in the three-dimensional space and on the different planes... ..	67
Figure 77: Speed of the index finger in the x (left) and y (right) axis.....	68
Figure 78: The finger forces diagram with the nodes from A to F and the external load applied W (above). The distances x and y between the nodes (below).....	70
Figure 79: Reaction forces on the nodes in the initial hypothesis.....	71
Figure 80: Finger equation weight vs actuator force.....	72
Figure 81: The thumb forces diagram with the nodes from G to I and the external load applied W(above). The distances x and y between the nodes (below).....	78
Figure 82: Reaction forces on the nodes in the initial hypothesis	79
Figure 83: Thumb actuator fingertip force	80

Figure 84: Boundary conditions applied in both systems.....	83
Figure 85: Finger function of von Mises stresses under applied load.	83
Figure 86: Thumb function of von Mises stresses under applied load.	84
Figure 87: Finger (above) and thumb (below) initial and final mesh.....	84
Figure 88: Finger convergence maximum value of von Mises stress increasing the number of nodes.	85
Figure 89: Thumb increasing value of von Mises stress maximum value while increase the number of nodes.	85
Figure 90: Different types of grasps validated.	87
Figure 91: Myoware electrode skin placement.....	88
Figure 92: Myoelectric control of the prosthetic device using an old socket.	88
Figure 93: FSR 402 sensor [49].....	89
Figure 94: The voltage divider circuit.	89
Figure 95: Sensor calibration curve.....	90
Figure 96: Breadboard schematic of the fingertip force experiment setup.	90
Figure 97: Schematic of the fingertip force experiment setup.	91
Figure 98: Experimental setup.....	92
Figure 99: Finger and Thumb CAD benches models respectively.....	92
Figure 100: Finger and Thumb assembled in their respective benches.	92
Figure 101: Experimental setup.....	94
Figure 102: Opposition trajectory and angle.	94
Figure 103: Flexion trajectory and angle.....	95
Figure 104: Experimental setup for the destructive essay.	96
Figure 105: Finger (left) and thumb (right) positioning.	97
Figure 106: Fracture of the finger model.....	97
Figure 107: Amplitude of the different types of grasps.....	99
Figure 108: Flexion contraction muscles of the hand send the EMG signal to the microcontroller.	99
Figure 109: Two different ranges in the input and the output signals.	100
Figure 110: PQ12R linear servo calibration schematic with a 10KΩ resistor.....	100
Figure 111: PQ12R linear servo and MG90S rotary servo calibration equations for the potentiometer range.	100
Figure 112: PQ12R linear servo calibration schematic with the EMG Myoware sensor.	101
Figure 113: Main loop function of the Grasp hand.	102
Figure 114: Grasp type function structure.	103
Figure 115: Grasp EMG calibration test changing the type of grip with the pushbutton and controlling the flexion-extension movement of the fingers with the EMG linear function.	103
Figure 116: Step one (left) first appearance of the GUI and step two, the value of time is introduced by the user (right).	105
Figure 117: The “EMG signal button is pressed” (left) and the plot starts showing the values of the signal (right).	105
Figure 118: The “Update maximum” button is pressed and the static text shows the maximum value of the EMG signal recorded.....	106
Figure 119: Conformity assessment procedure for a class I medical device.	108
Figure 120: Symbols of the label organized in the order of the previous description from left to right [16]..	109
Figure 121: Image from the website [57] and Youtube channel.	116
Figure 122: The project published in Hackaday [60] on the left and Thingiverse [59] on the right.	116
Figure 123: Regular finger assembly of four steps.....	120
Figure 124: Thumb assembly of three steps.	121
Figure 125: Linear and rotary servos assembly with the palm.	123
Figure 126: Linear actuators and thumb assembly.	124
Figure 127: Fingers and palm assembly.	125
Figure 128: The silicone is applied between the two parts of the finger mold.	126

Figure 129: The silicone is applied between the two parts of the thumb mold.	126
Figure 130: The fingertip covers are glued with super gule.	127
Figure 131: PCB assembly for the two sensors: Myoware and DFRobot.	128
Figure 132: Connector and pin connection (bottom) PCB connections GND (grey) Vcc (red) and signal (white) on top.	129
Figure 133: Schematic for safety recommendations.	129
Figure 134: Assembly of the top and bottom covers.	130
Figure 135: Forearm-EMG sensor example connection.	131
Figure 136: First view of the graphical user interface.	131
Figure 137: Time window introduced by the user.	132
Figure 138: EMG signal displayed in the graph window.	132
Figure 139: Maximum of the EMG signal showed in the end of the recording.	133
Figure 140: Grasp code open in the Arduino IDE.	133
Figure 141: EMG maximum value introduced in the constant variable of the program.	134
Figure 142: Mass comparison between Grasp and the other projects.	136
Figure 143: DOF comparison between Grasp and the other projects.	137
Figure 144: Fingertip force comparison between Grasp and the other projects.	137
Figure 145: Finger flexion-extension speed comparison between Grasp and the other projects.	138
Figure 146: Comparison of the model hand index finger (red) and Grasp index finger (blue).	138
Figure 147: Comparison of the Solidworks simulation finger (blue) and the real Grasp index finger analysed using Kinovea (red) normalized.	139
Figure 148: EMG Myoware sensor with simultaneous connection with the grid safety recommendations.	143
Figure 149: Image of the Matlab GUI editor.	171

List of tables

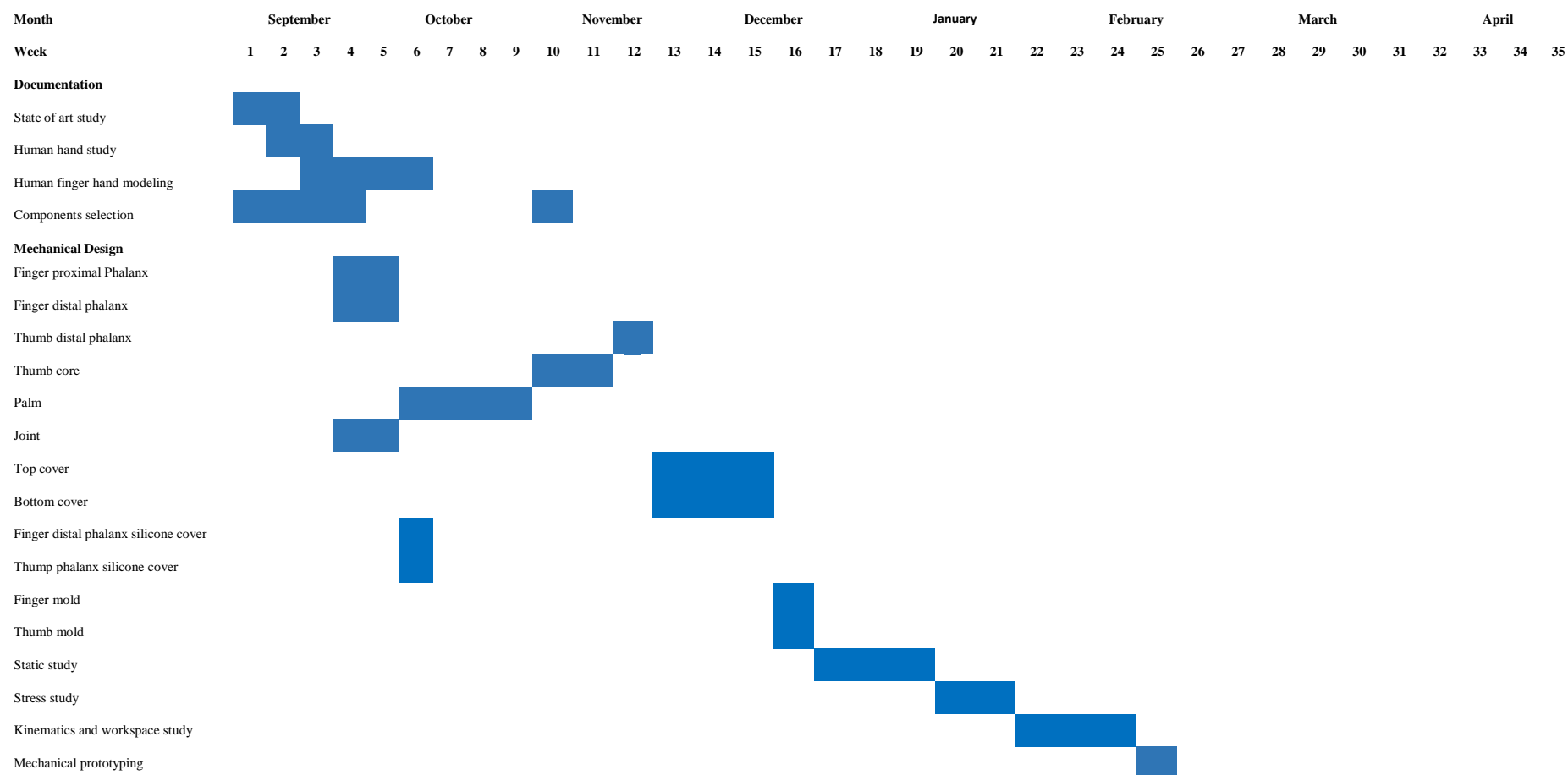
Table 1: Planning.....	13
Table 2: Collected data from open source and non-open source 6 DOF prosthetic hands [14], [8], [12], [9] & [16].	21
Table 3: Designs and iterations of the different bionic hands during the project.....	26
Table 4: 3D printable components of the first myoelectric design.....	27
Table 5: Second myoelectric design printed (right) and designed on CAD (left).....	28
Table 6: 3D printable components of the low cost design.....	30
Table 7: 3D printable components of the Grasp 0 design.	31
Table 8: Table 5.1: Anthropometric values for both sexes [24]......	35
Table 9: Range of motion of the thumb in degrees [28]:.....	38
Table 10: Range of motion of the index, middle, ring and small fingers in degrees [28]:	38
Table 11: Speed of the three phalanges of the human hand [30]:	38
Table 12: Angles of the finger model joints.....	39
Table 13: Standard dimensions of Grasp:.....	41
Table 14: Final number of elements that conform the final design of Grasp and have to be 3D printed:.....	46
Table 15: Features of MG90S [34]......	51
Table 16: Features of PQ12R [20].....	51
Table 17: Features of Arduino Nano [19].	52
Table 18: Features of Myoware sensor [21]......	52
Table 19: Features of the signal transmitter board [39].....	53
Table 20: Features of the dry electrode board [39].	53
Table 21: Features of the D24V25F6 [17].....	53
Table 22: Battery specifications [40].....	53
Table 23: Switch features [17].	54
Table 24: Pushbutton features [39]......	54
Table 25: Charger features [40].....	54
Table 26: ABS medical grade specifications [41]......	55
Table 27: Finger initial conditions.	65
Table 28: Thumb initial conditions.	65
Table 29: Environmental Impact of Mold injection in Asia.....	111
Table 30: Environmental Impact of 3D printing in Europe.....	111
Table 31: 3D printed components budget.....	113
Table 32: Electric components budget.	113
Table 33: Other components budget.....	114
Table 34: Energy consumption budget.....	114
Table 35: Grasp 1.0 features.....	136

Introduction

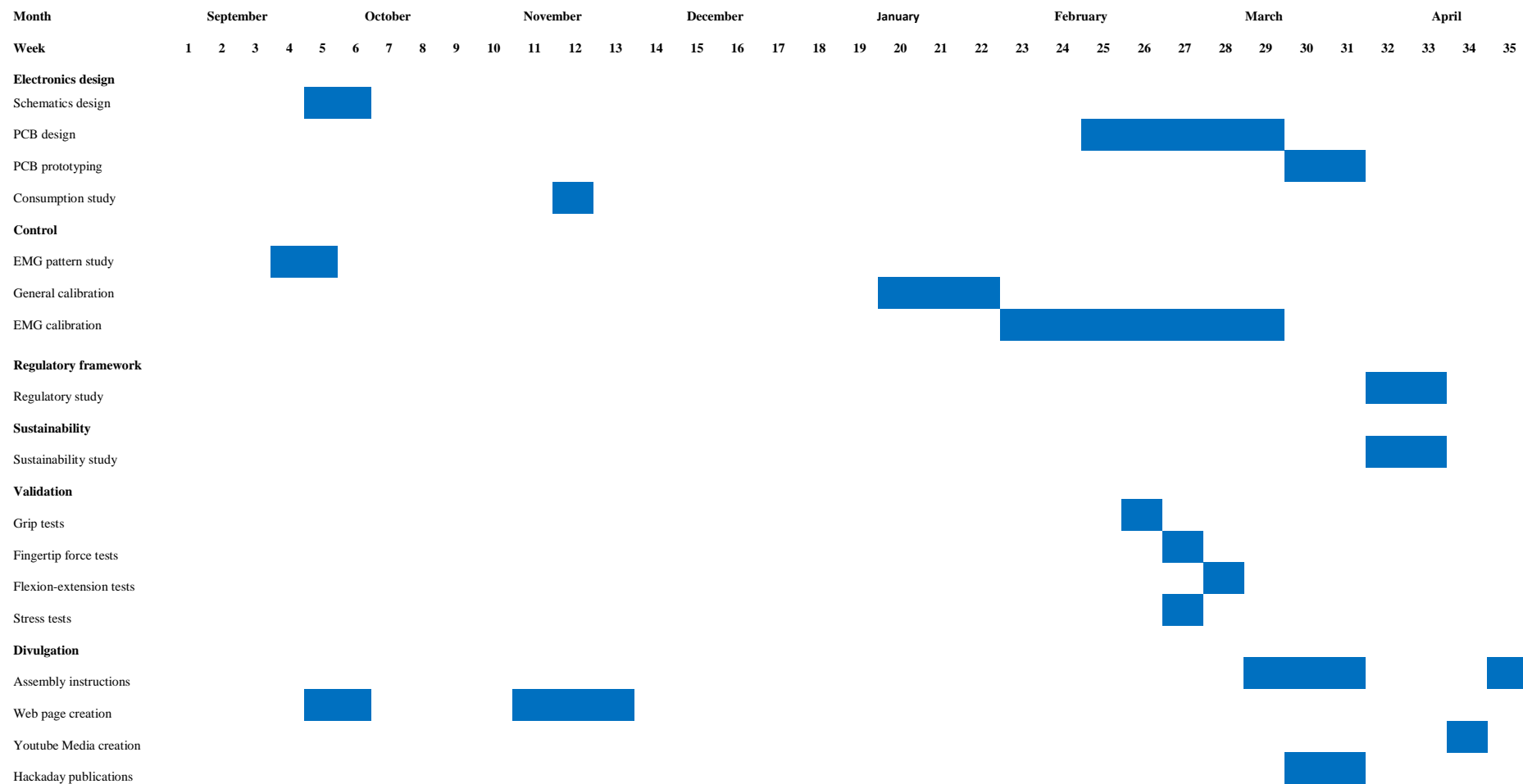
PLANNING

The present work stars with the whole eight-month planning in order to achieve all the steps to finish and test the prototypes. The planning is divided in eight main parts: documentation, mechanical design, electronics design, control, regulatory framework, sustainability, validation and divulgation.

Table 1: Planning.



Design and development of a 6 DOF, 3D printable, open source bionic hand



THE PROBLEM

The incidence of amputation is 1.5 per 1000, the arm amputees in the world represent 3 million people and 2,4 of this are in developed countries. Over the 59% of these amputees suffer an amputation below the elbow, the 28% above the elbow, the 8 % have a shoulder disarticulation and the 5% a wrist disarticulation or partial hand amputation [1]. In Spain, based on 2007 data, there are 5,477 upper limb amputees, it represents the 3,67% of the country's amputees [2]. Nowadays the main problem is the cost of a commercial prosthesis, the cost of a body powered prosthetic device can range from 4.000 to 10.000 dollars and the cost of an externally powered prosthetic hand can range from 25.000 to 75.000 dollars [3]. The number of upper limb amputees is much lower than the lower limb amputees, for this reason the bionic hands that are produced by traditional industry have high prices, because the production costs and investment on development are high for a low population. For that reason, there are inaccessible prices for the 6 degrees of freedom (DOF) Electromyography (EMG) controlled prosthetic hands.

AMPUTATION CAUSES

In general, the most common causes of amputation in countries with no belic conflicts are: Congenital (present at birth) limb deficiency occurs when an infant is born without part or all of a limb. In the United States, 82% of amputations are due to vascular disease, 22% to trauma, 4% are congenital, and 4% are due to tumours. In upper limb amputations the main cause is trauma, over 75% that is because the cardiovascular and diabetes related cases are more common in lower extremities [4].

UPPER LIMB AMPUTATION LEVELS

We can specify different levels of amputations (Figure 1) which can be separated in eight types [5]:

- **Forequarter:** Amputation of the entire arm with the scapula and clavicle.
- **Shoulder disarticulation.**
- **Transhumeral:** Humerus amputation.
- **Elbow disarticulation**
- **Transradial:** Radius amputation.
- **Wrist disarticulation.**
- **Partial hand:** Carpus or metacarpal bones amputation.
- **Fingers.**

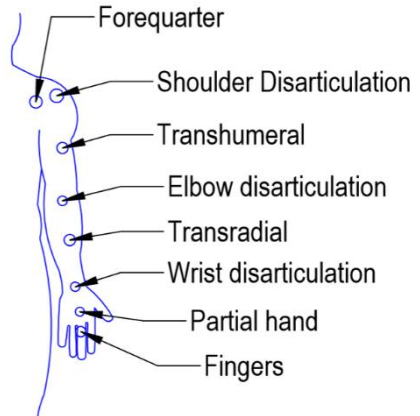


Figure 1: Upper limb amputation types.

ADVANTAGES OF DIGITAL MANUFACTURING TECHNOLOGIES

The main 3D-printing advantages compared to other traditional manufacturing technologies can be summarised as follows:

- The huge design freedom, highly complex geometries can be made.
- Designs can be personalized and customized in an easy way.
- Parts can be produced quickly from an idea to a prototype and from this to a product and make fast changes in the design [3].

The traditional manufacturing method where the molds have to be included in the price of the units to sell with the blue line (Figure 2) can be compared with the case of 3D-printed case in a constant value of the red line at the same figure [6]. In the first case more than 1000 units have to be sold to get the same unit cost as with the 3D printing production.

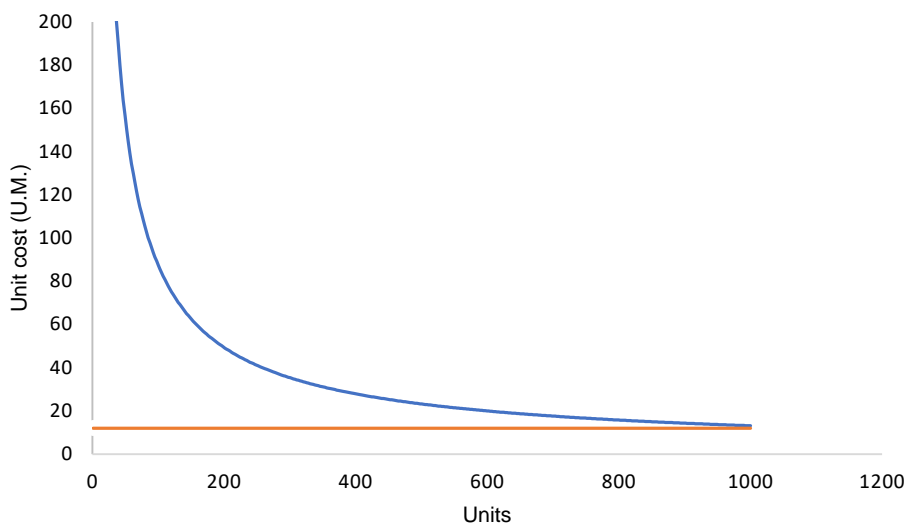


Figure 2: Traditional manufacturing vs digital manufacturing production costs.

ISSUES OF DIGITAL MANUFACTURING TECHNOLOGIES

- The mechanical properties are very hard to predict.
- The accuracy is highly affected by material shrinkage; errors can be induced by CAD/CAM software.

PROJECT GOALS

This project has several goals to be achieved:

- Usable for three type of upper limb amputations: wrist disarticulation, trans humeral and trans radial amputations.
- 3D-printable using a fused deposition modelling (FDM) 3D printer.
- Self-repairing. Everyone can repair or acquire the components separately.
- Self-programmable. Everyone can program their own code.
- Open hardware and software.
- Low cost: under 500€ including all components.

- Separate finger movements: 6 degrees of freedom (DOF).
- Myoelectric control: surface electromyography (EMG).
- Electronics included in the palm of the hand.
- Equivalent features of the commercial ones.
- Not far from the human hand average weight of 400g.
- The hand has to be able to do the six types of grasps that represent most of the activities of daily living (ADLs): spherical grip, hook grip, lateral grip, tip grip, tripod or palmar grip and cylindrical grip [3] (Figure 3).

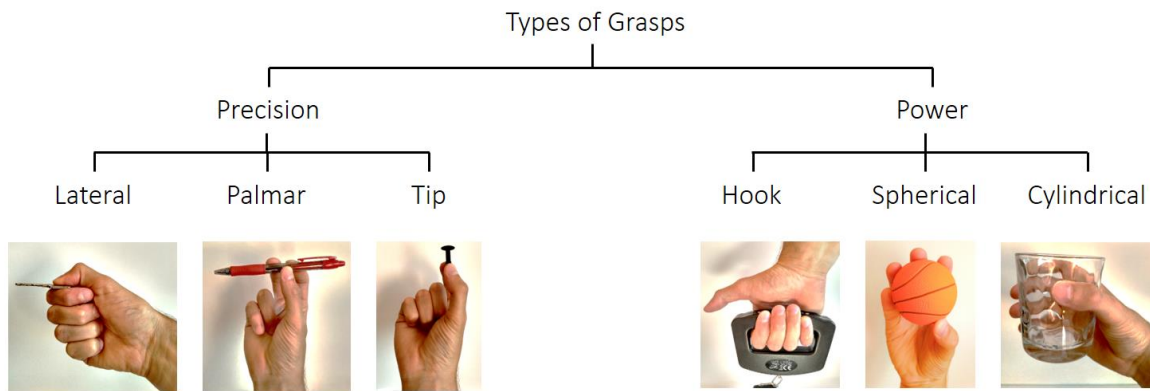


Figure 3: Main types of grasps to perform the ADL's.

PROJECT SCOPE

Grasp Bionic Hand can be used in many different fields as:

- It can be an implantation project in a Medical Centre or Hospital, where patients can access a prosthetic element at cost or subsidized by the state.
- It can also be used as a platform to reach people who have been victims of wars suffering amputations.
- For persons of developing countries who have been born with some joint deficit and who cannot access a biomedical implant of these characteristics.
- For use as an educational element in engineering universities.
- As a platform for research in machine learning.

AIM OF THE PROJECT

But the main idea of the final design can be resumed in three points:

- Propose a new design and mechanical system with equivalent features of the best commercial prosthetic hands.
- An affordable prosthetic limb attachable to a previous used socket or a 3D printable one.
- A simple kit that can be repaired and assembled in the easiest way.

State of the art

3D PRINTED BIONIC HANDS

Until 2016, 51 prosthetic devices could be found in the literature divided in 30 body-powered (BP) prosthesis and 22 externally-powered (EP) [3]. The interests in the present work are for the externally powered (EP) hands controlled through electromyography (EMG). Most of these projects are only suitable for upper arm amputations (above the elbow), for this reason in the next description are only included the most interesting designs for the purpose of this project. The most interesting designs of this first period of development are the Dextrus Hand from Open Hand Project [7] now, Open Bionics which is the pioneer design in this field, and Tact Hand, a project from the University of Illinois an affordable prosthetic hand that combines four bar linkage systems with DC motors that pull the system using wires [8].

After the last mentioned publication can be added nowadays, 3 more prosthesis published during the last two years. These three prostheses are The Compliant Hand [9] an evolution of Tact Hand [8], a six degrees of freedom (DOF) and high-performance prosthetic hand a powered 3D printed prosthetic hand for Transmetacarpal amputees as the same way as the compliant with the same DOF and metallic gears, a four-bar linkage system actuated by DC motors, encoders and pressure sensors for a precisely control of grasping patterns an applied forces to objects with a cost of 553.06 \$ including all components. The last paper published this last year is a revolutionary design of a one single actuator hand that can reproduce the main movements of the human hand changing the distribution of the mechanical system, it is the first prosthetic hand that achieved the 34.5 N using a pinch grasp, this is an important fact because this values are close to the real human hand [10].



Figure 4: From left to right, Tact Hand [8], Hero Arm [16], Exiii Hackberry [13] and One single actuator hand [10].

The most influential designs on the field can be divided by their actuator type, there are three devices that use linear actuators, concretely the most famous of the market: Ada, Brunell and Hero Hands from Open Bionics which use the same system that consist in iron wires pulled by linear actuators. Another hand that uses a linear actuator as the Open Bionics models is Tact Hand [8], developed by the University of Illinois in 2015 and now this project has evolved to Psyonic. Youbionic is the name of the last prosthetic device to introduce linear actuators placed in the dorsal part of the hand but, now the project has changed and its focused on increase the human abilities and other robotic applications [11]. Other devices use DC motors with an external position sensor, actuating a worm gear system, is the case of the Compliant hand cited previously [9] and the Hand from Transmetacarpal Amputees from the PUCP in Perú [12]. On the other hand the Exiii Hackberry, the Japanese project that uses DC servo motors with spur gears [13]. Tact hand, Hero arm, Exiii Hackberry and the single actuator hand are illustrated in the Figure 4.

NON 3D PRINTED BIONIC HANDS

The non-3D printed anthropomorphic hands that can be found in the market are: Sensor Hand, Vincent Hand, iLimb, Bebionic, Michelangelo and Ottobock's Sensor Hand. These hands have six DOF except Michelangelo and Sensor Hand, which have two and one respectively. The weights have different values depending on the size but, can range from 350 to 615 g. The dimensions of these models are between 180 and 198 mm length and 75 to 90 mm width. The average finger flexion speed values are around 103,3 % s for the Vincent Hand (ring, middle or index finger), 95,3 % s for the I-limb (index finger), 96,4 % s for the Bebionic (ring, middle or index finger), and 86,9 for the Michelangelo (ring, middle or index finger). The five hands have different tip grip forces which range from 8,44 N for Vincent Hand (ring, middle or index finger) to 12,47 N at Bebionic (index). The actuation method is different in Michelangelo that uses a single finger segment actuated only at a single point like the metacarpal phalange (MCP) joint, for the other hands the system is similar to the human hand two phalanges one at the MCP joint and another distal phalange that has both human proximal interphalange (PIP) and distal interphalange (DIP) [14]. At 2018 a new prosthetic device has arrived, the Taska Hand [15] but features are not tested and published in a scientific paper but, a big advance of this design is the waterproof feature (Figure 5).



Figure 5: From left to right, Vincent Hand [61], Bebionic 3 [62], i-limb ultra [63], Taska Hand [15], Michelangelo [64] and Sensor Hand [68].

This models present high fingertip force and speed values that will be difficult to achieve with six degrees of freedom, the critical point of the larger sizes of this hands are the weight of Bebionic and i-Limb which exceed the value of 500 g and that could be a reason for rejection. This manufacturers use medical grade Maxon DC motors that provide high efficiency and allow precise control but also higher costs up to 208 \$ [8]. In the Table 2 is collected the data available of the main prosthetic devices with high performance that have been published until now.

Table 2: Collected data from open source and non-open source 6 DOF prosthetic hands [14], [8], [12], [9] & [16].

Hand	Developer	Flexion/extension speed (°/s)	Fingertip Force (N)	Mass (g)	Number of Joints	DOF	Number of Actuators	Actuation method	Dimensions (length x width x thickness, mm)
Bebionic (2011)	RSL Stepper	36.6 - 96.4	12.25 - 16.11	495 - 539	11	6	6	DC Motor -Lead Screw	190-200 x 84 - 92 x 50
iLimb (2010)	Touch Bionics	60.5 - 110.6	3.09 - 11.18	460 - 615	11	6	6	DC Motor -Worm Gear	180-182 x 75 - 80 x 35 - 45
Vincent Hand (2010)	Vincent Systems	87.9 - 103.3	3.00 - 8.44	-	11	6	6	DC Motor -Worm Gear	-
Dextrus (2013)	Open Hand Project	175.4	1.71	428	15	6	6	DC Motor -Tendons	205 x 88 x 45
Tact (2015)	University of Illinois	249.8	4.21		11	6	6	DC Motor -Tendons	200 x 98 x 27
Transmetacarpal Hand (2017)	PUCP	97.9 - 180.8	2.42 - 1.16	-	10	6	6	DC Motor -Worm Gear	-
Compliant Hand (2017)	Psyonic	-	-		10	6	6	DC Motor -Worm Gear	-
Brunel Hand (2018)	Open Bionics	-	-	332	9	5	5	Linear Actuator - Tendons	198 x 127 x 55

This values are important to define the main steps of the project to get similar values of dimensions, fingertip forces, flexion/extension speeds, Number of actuators, possible actuation methods, DOF or number of joints and get quantitative values to be achieved on the present work.

Influences

INFLUENCES

From the projects that have inspired “Grasp bionic hand” (Figure 6) Open Hand Project, now Open Bionics, which is the most recognized and pioneer company in the development of open source 3D-printable prosthetic hands, set the motivation to create affordable bionic hands. This incredible project and its hands: Dextrus (2013), Ada (2015) and Brunel (2018) has won all the innovation awards of recent years in the field. Most of Open Bionics hands use as a mechanical system, DC motors (Dextrus) or micro linear actuators (Ada and Brunel) that pull from steel cables (Tendons). Probably the most innovative aspects in their designs are the combination of different 3D printing materials and flexible filaments for the biggest part of the hand providing an easy assembly to their models. Nowadays Open Bionics has become the first company to test their newest 3D printable prosthetic device (Hero Arm) in clinical trials achieving the CE mark and the class I medical device label.

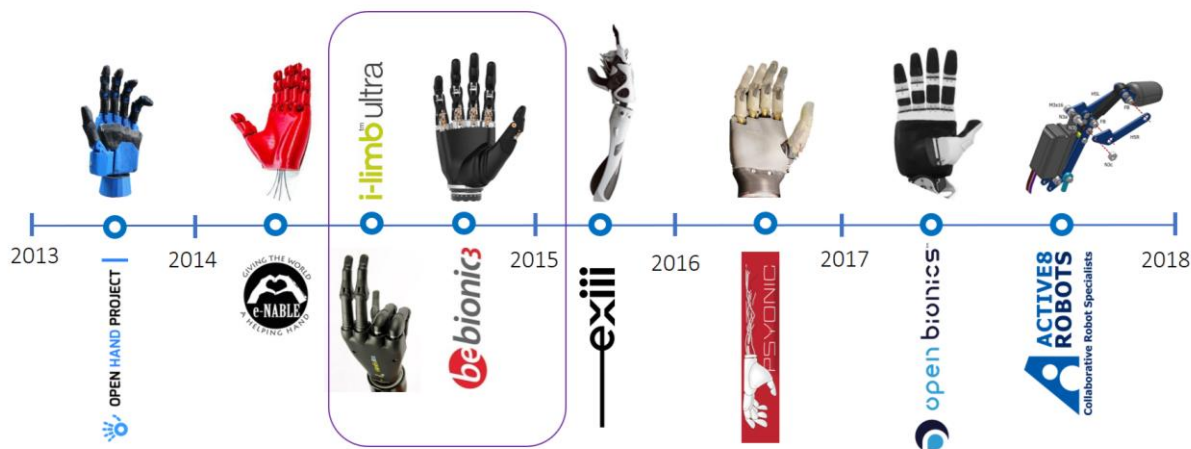


Figure 6: Project Influences in chronological order of discovery, Open Hand Project [7], Flexi Hand [65], i-Limb ultra [63], Bebionic3 [62], Exiii Hackberry [13], Compliant Hand [9], Brunell Hand [16] and AR-10 Hand [66].

After this first discovery, in 2014 an international organisation of volunteers, Enabling the future, published the Flexi Hand, designed by Steve Wood, the first mechanical prosthetic hand that introduces elastic joints and rigid segments. There are two non 3D printed and non-open source hands, which can be considered as the best prosthetic hands in the world, Bebionic3 and i-Limb which set the state of the art in the field and the goal of the present project is to achieve their features in the closest way. After 2015 the most important approach to a potential medical devices have done by Exiii a Japanese start-up with its hand, hackberry, a 3D printable prosthetic hand capable to do different types of grasps with the combination of two different ways of actuation one for the tip grasp an another for the power grasp. Probably the most advanced design until that date was made in 2017 from a Psyonic’s hand, with the Compliant hand.

Other non-prosthetic devices like the robot hand with 10 DOF AR-10 hand developed by Active Robots have been an inspiration to design the mechanical system of the “Grasp 1.0” hand.

Project evolution

GRASP PROJECT FROM 2014 TO 2018

The design of “Grasp Bionic Hand” went through several stages of iteration and optimization. The first myoelectric design is from 2014, inspired in the Flexi Hand from Steve Wood, is a hand with 5 DOF actuated by micro servos pulling from tendons and located in the forearm. One year later, after this first experiment, the next challenge was include the actuators and electronics inside the palm of the hand, is at that point when using the same mechanical system of flexible joints and rigid phalanges, the actuators have been changed from DC servo motors, to Pololu 50:1 DC micro metal geared motors [17], with more range of motion than the previous actuators used and a Hitec Nano servo HS-35HD [18] to let the opposition of the Thumb finger.

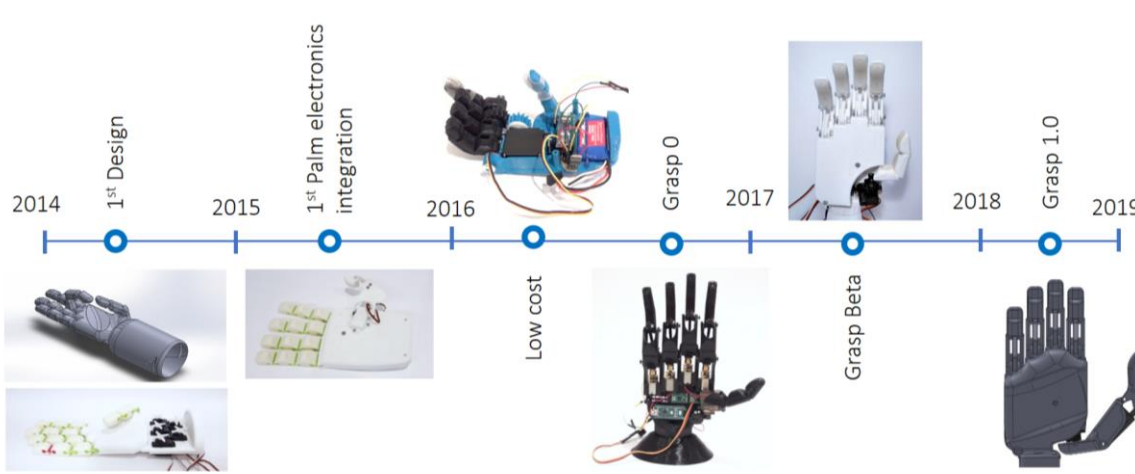


Figure 7: Different designs of the project from 2014 to 2019 since the first myoelectric design to the last design of Grasp.

After two different tests of 5 DOF bionic hands the “Low cost” design was developed to minimize the costs as less as was possible using only one actuator to get two different functions: the tip grasp and the cylindrical grasp. That hand used a spur gear actuated by a standard size servo motor Hitec HS-322HD to be able to do the flexion of the four fingers. The thumb is positioned orthogonal respect to the palm and index finger is slightly extended to be coincident with the thumb when the flexion of the four fingers. The first big improvement starts with Grasp 0 based in the Compliant Hand [9] introducing the stiff bar system actuated by a metallic (brass) worm gear and Pololu 30:1 DC micro metal geared motors and controlled via two Pololu DRV8833 dual motor driver carrier [17], that system makes the hand more robust but the main issue is the measure of the position of the finger, must be added the rotary encoders to measure the position of the fingers and the used board Arduino Nano [19] has no enough digital I/O. The last iteration is Grasp Beta, in the current paradigm using the Actuonix PQ-12R [20] linear servos that include the position sensor inside. This last design, maintain the robustness and gets one of most important goals, easy assimilability (Figure 7). The most important features of this several designs are grouped in the Table 3.

Table 3: Designs and iterations of the different bionic hands during the project.

Hand	Flexion/extension speed (°/s)	Fingertip Force (N)	Mass (g)	Number of Joints	DOF	Number of Actuators	Actuation method	Dimensions (length x width x thickness, mm)	Cost (€)
1 st Myoelectric design (2014)	-	-	245	14	5	5	DC Servo Motor - Tendons	198 x 91 x 44	229.77
1 st Palm Integration (2015)	-	-	221	13	6	6	DC Motor - Tendons	189 x 117 x 37	222.94
Low cost (2016)	400	-	198	1	1	1	DC Motor - Spur Gear	192 x 82 x 69	108.89
Grasp 0 (2016)	93	-	253	9	5	5	DC Motor – Worm Gear	188 x 84 x 35	282.17
Grasp Beta (2017)	72	-	339	9	5	5	DC Motor – Linear Servo	166 x 80 x 38	394.24

First myoelectric design

The first project, starts in October of 2014, the challenge was to design a prosthetic device that met the following requirements:

- Printable in 3D.
- Easy assembly and assembly.
- Self-programmable by the user.
- Open source and available on the network.
- Maximum anthropometric similarity with the human hand.
- Maximum functional similarity with the human hand (flexion and individual extension of the fingers).
- Controlled by servo motors, one to operate each finger.

In this design, Nylon cables pass through the palm and arrive to the servo motors placed in the forearm (Figure 8). The hand is composed by four essential parts because the fingers have the same dimensions (Figure 9 and Table 4).



Figure 8: CAD model of the first myoelectric design (left) and 3D printed model (right).

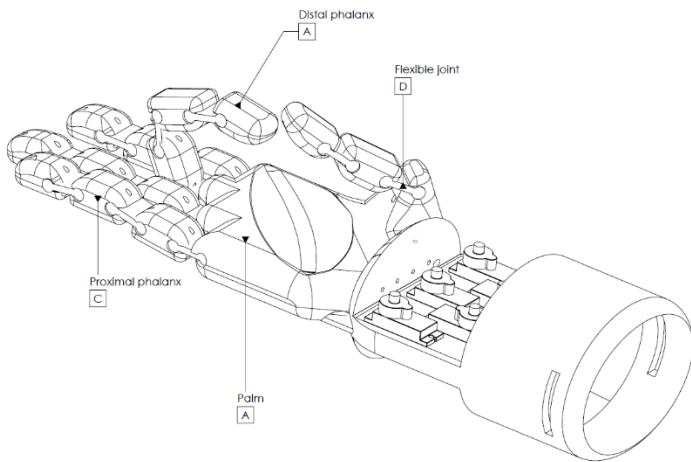


Figure 9: First myoelectric design printable components.

This hand uses elastic interphalangeal joints, as Steve Wood's Flexi Hand does since it was inspired by the American model and is a key aspect for a very fast assembly (Figure 10). This design raises the concern of integrating electronics and actuators into the palm of your hand. After numerous tests. An iteration procedure to find the correct thickness to get ther extension movement of the finger when the servo motor is not applying force was done. This hand and Advancer technologies muscle sensor v3 [21], the first low cost EMG sensor, which required a symmetric power supply (Figure 11).

Table 4: 3D printable components of the first myoelectric design.

Reference	Name	Quantity
A	Distal Phalanx	5
B	Palm	1
C	Proximal Phalanx	9
D	Flexible joint	14

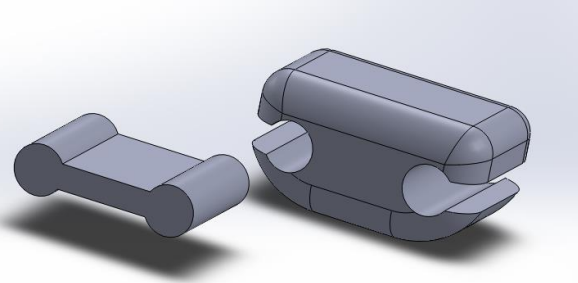


Figure 10: Assembly method between flexible joints and rigid segments.

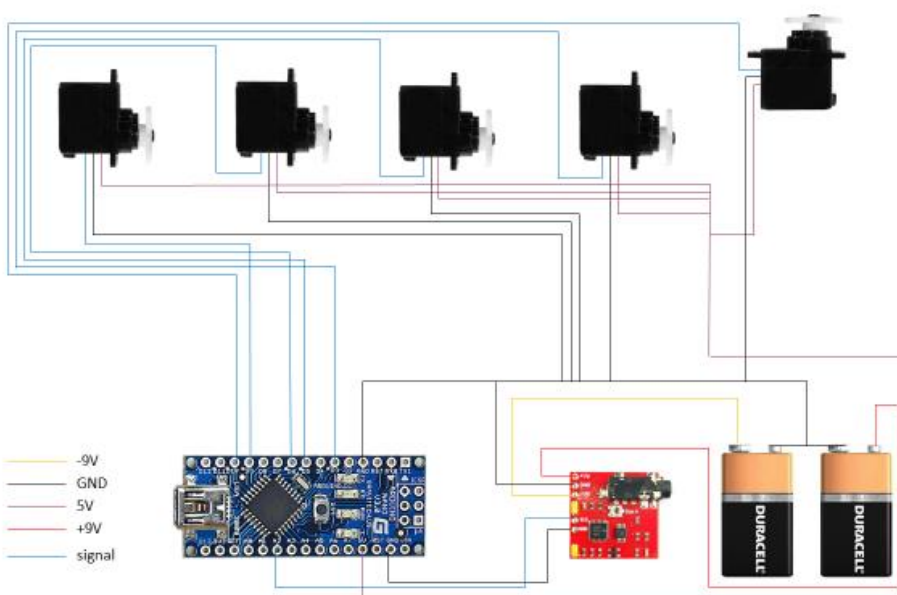


Figure 11: Electrical design.

First palm electronics and actuator integration

After the first design, six months later, the main idea was to insert the electronics inside the palm of the myoelectric hand using the same mechanical system of strings or wires but, this time with a tiny DC motors with great features commonly used in hobby robotics (Figure 12). This motivation is due to get a device suitable for wrist disarticulation amputees.

In this second design the original idea of the first one is maintained but with the following improvements:

- Insertion of control electronics in the palm of the hand
- Insertion of the power electronics in the palm of the hand
- Insertion of the actuators in the palm of the hand
- Opposition movement of the thumb.
- Replacement of servo motors with DC motors with better performance from $2.4 \text{ kg}\cdot\text{cm}$ to $5 \text{ kg}\cdot\text{cm}$ to get higher fingertip forces. Actuating worm gear shape pulleys and reusing the flexible joints (Figure 13).

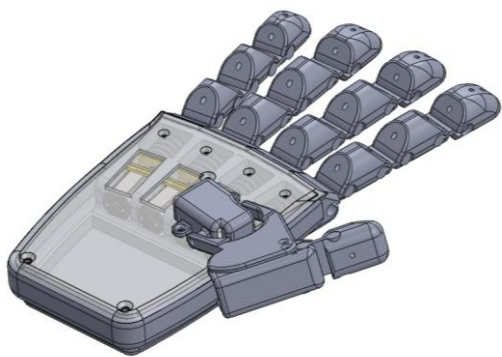


Figure 12: Second myoelectric design printed (right) and designed on CAD (left).

Table 5: Second myoelectric design printed (right) and designed on CAD (left).

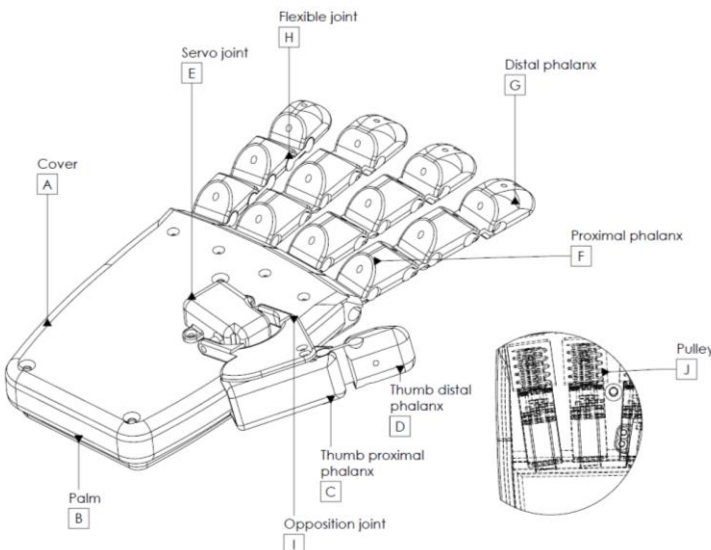


Figure 13: Second myoelectric design components.

Reference	Name	Quantity
A	Cover	1
B	Palm	1
C	Thumb proximal phalanx	1
D	Thumb distal phalanx	1
E	Servo joint	1
F	Proximal phalanx	8
G	Distal phalanx	4
H	Flexible joint	13
I	Opposition Joint	1
J	Pulley	4

This design introduces the DC motor drivers for the motor control, the Jameco Voltage regulator L78 series [22] and the Myoware EMG sensor [21] (Figure 14).

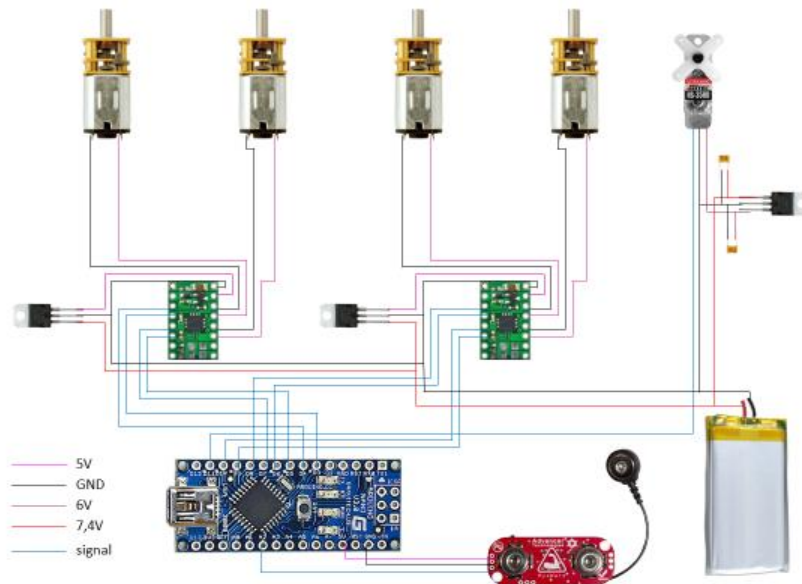


Figure 14: Second myoelectric hand electrical design.

Low cost

This step of the project arises from the idea of achieve maximum functionality and the best features with a single degree of freedom (Figure 4.9) due to the observation of current and previous designs. Raising the question of whether it is possible through a specific placement of the index and the rest of the fingers get a fine grip for smaller objects and a strong grip for bags or larger objects, with a single actuator in a robust way. For this reason, have been gathered the following characteristics:

- A single actuator, in this case a standard size DC rotary servo motor with metal gears, high torque and rotation speed ($11 \text{ kg} \cdot \text{cm}$ and $400 \text{ }^{\circ}/\text{s}$).
- The hand is made up of only 5 printable elements.
- The transmission is more robust, with only two spur gear system that connects the fingers with the palm when rotating with respect to an axis, also providing a finer and more robust control.
- Controlled by a single electromyographic analogue sensor that allows the signal to be continuously transmitted to the hand and to make an optimal regulation with few resources.
- A total budget that does not exceed 120 €, thus designing a myoelectric prosthesis with a lower cost.

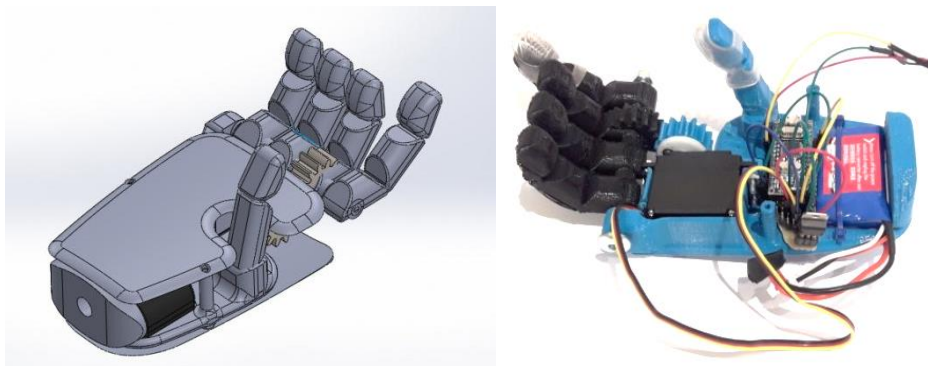


Figure 15: Low cost model in CAD (left) and 3D printed model (right).

The number of components needed to build the hand (Table 6) are only five, here the idea of making something very simple, assembled in some steps, becomes stronger. The index finger is displaced 30 degrees from the other fingers in order to be able to make the fingertip (precision) grasp but, also existing the possibility to grasp bigger objects with a cylindrical grasp. The second spur gear is also part of the four finger “block” (Figure 16).

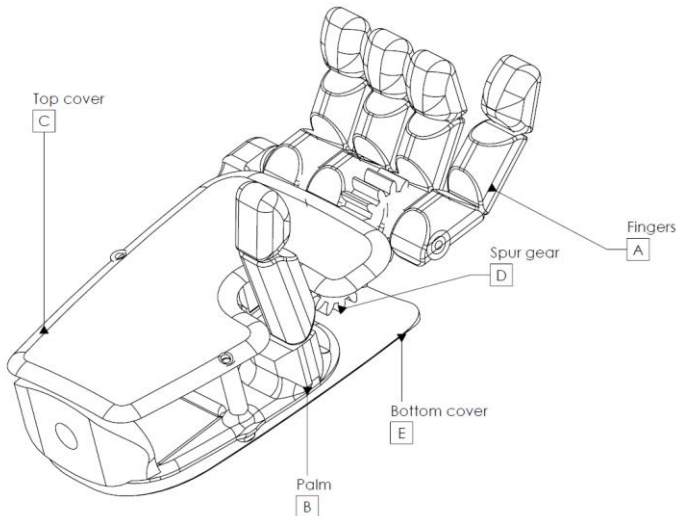


Table 6: 3D printable components of the low cost design.

Reference	Name	Quantity
1	Fingers	1
2	Spur Gear	1
3	Palm	1
4	Top Cover	1
5	Bottom cover	1

Figure 16: Low cost model components.

Also, the number of electronic components is also the minimum, only one rotary DC servo motor, a voltage regulator to get 6 volts from 7.4 volts of the Li-Po battery, integrated on the palm and the Arduino Nano board (Figure 17).

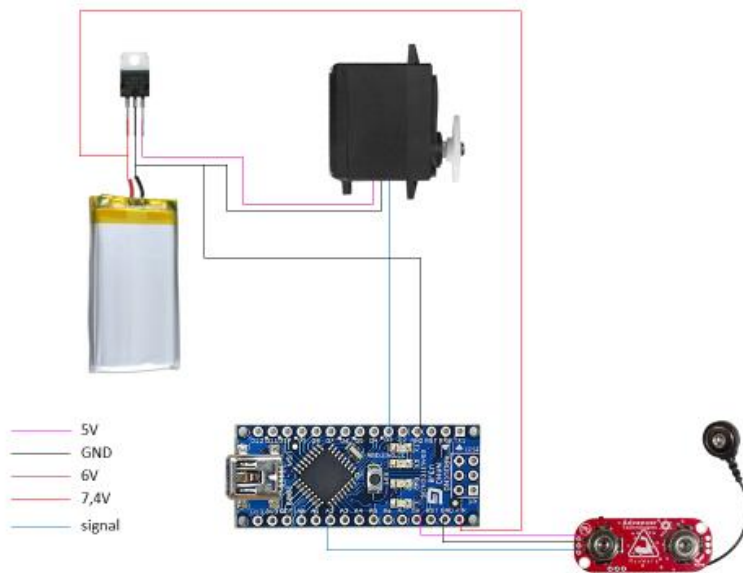


Figure 17: Low cost model circuit.

Grasp 0

This model designed in 2016 is the first hand that achieves competitive features. Also combines different materials to reduce frictions in the power transmission using brass worm gears from Mootio components [23] and 3D printed plastic helicoidal gears integrated in the proximal phalanx. This model represents a big technical improvement against the past steps of the project (Figure 18). The hand is composed by 8 different parts (Figure 19).

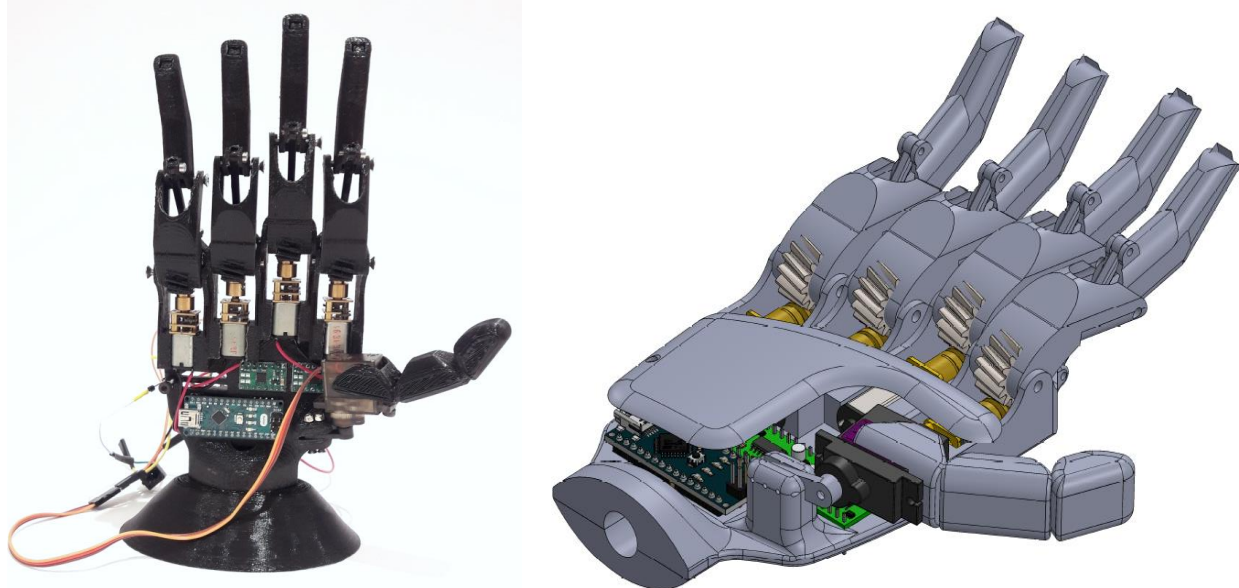


Figure 18: Grasp 0 3D printed model (left) and CAD design (right).

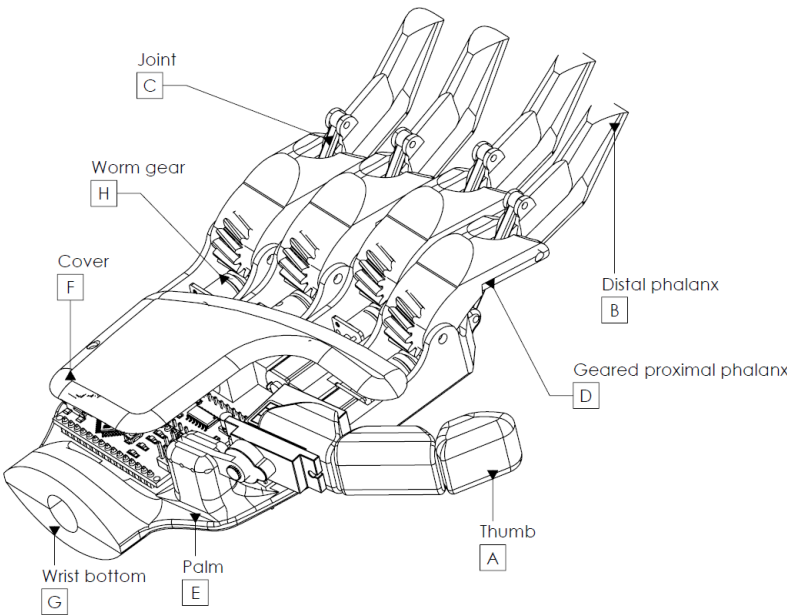


Figure 19: Grasp 0 3D printable components.

Table 7: 3D printable components of the Grasp 0 design.

Reference	Name	Quantity
A	Thumb	1
B	Distal Phalanx	4
C	Joint	4
D	Geared proximal phalanx	4
E	Palm	1
F	Cover	1
G	Wrist bottom	1
H	Worm gear	4

The actuators selected for that hand had been four Pololu micro DC brushed micro metal gear motors with 30:1 gear ratio actuated by two Pololu DRV8835 dual motor driver carrier [17] (Figure 20) and one MG90S micro rotary servo motor for the opposition movement of the thumb. Each Pololu motor incorporates a brass worm gear (Figure 4.15) and actuates the system presented in the four linkage bar system presented in the Figure 23.

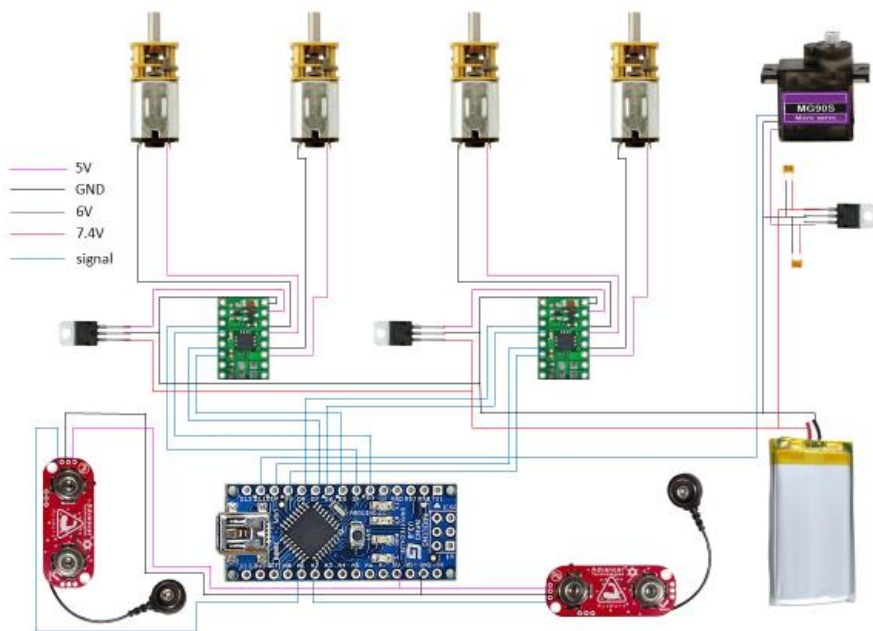


Figure 20: Grasp 0 electrical circuit.

The main issue of this model was the need to use encoders or potentiometers to control the position of the fingers, that means more digital inputs that the I/O pins that we have in the Arduino Nano or so many electric wires in the case of potentiometers. The conclusion after this was to search some actuator that had the position sensor included and at the same time, had the correct volume to be included in the palm of the hand with the electronics.



Figure 21: Brass worm gear for the combination of plastic metal power transmission [23].

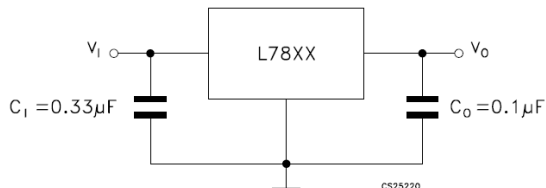


Figure 22: Voltage regulator L78 series recommended capacitors [22].

Two capacitors have been selected to filter the possible noise produced by the voltage regulator towards the micro servomotor. As indicated by the manufacturer in the datasheet, one of 330nF capacity connected to the input and another of 100nF with connection to the output has been selected (Figure 22).

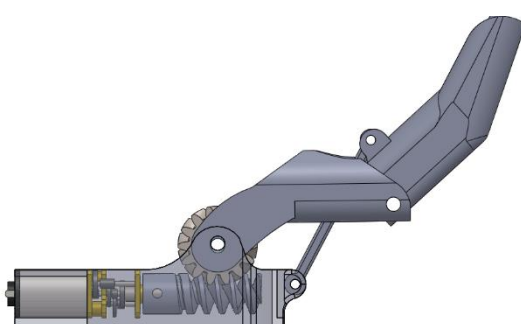


Figure 23: Grasp 0 finger worm gear mechanical system detail.

Grasp Beta

Grasp Beta is the first step to get the current design, with 5 DOF one less than Grasp 1.0 and is the first time in the project where DC linear servos as an actuators have been used. A rotary servo motor is used like in Grasp 0 to make the opposition movement of the thumb which has only this degree of actuation. The details of this hand are inherent to the main design of this project (Figure 24).

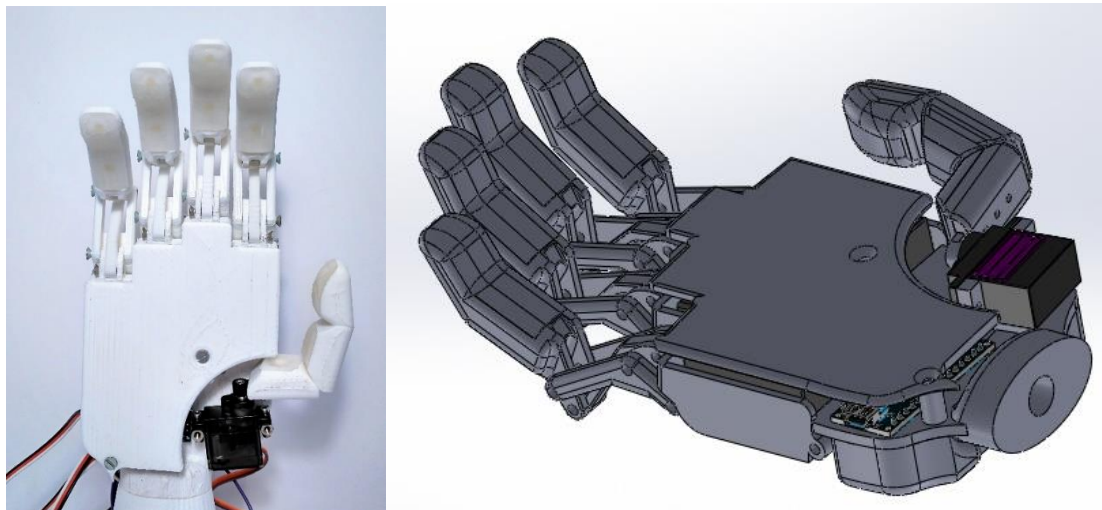


Figure 24: Grasp Beta 3D printed model and CAD model.

The human hand

ANTROPHOMETRICS OF THE HUMAN HAND

Anthropometric human data were extracted from a study carried out measuring 46 people, 22 men and 24 women, all of them between 20 and 30 years of age and most of them of Spanish or European nationality (Table 8). The data collection was done using the digital hand scanning technique, this procedure was performed with a high-resolution scanner (Figure 25). For the recording of the hand individuals were asked to support the hand in pronation on the scanner platform, with the fingers straight and together and special care was taken in that the posture did not adopt radial or cubital deviations [24].

Table 8: Table 5.1: Anthropometric values for both sexes [24].

	Male	Female
Hand length (mm)	183 ± 17	178 ± 9
Palm length (mm)	105 ± 12	102 ± 6
Thumb length (mm)	62 ± 7	61 ± 5
Hand width (mm)	104 ± 10	95 ± 5
Palm Width (mm)	82 ± 8	76 ± 2

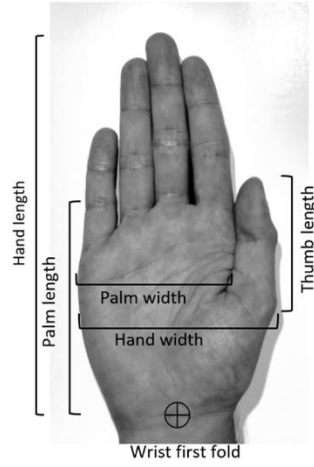


Figure 25: Human hand dimensions adapted from [24].

GRIP FORCES

The forces applied against an object when it is grasped by the human hand can be measured using a dynamometer, the data founded in the literature suggest that the grip force in adults N = 21 (10 male and 11 female) are 412 ± 93 N for the men and 235 ± 50 N for the woman [25]. Otherwise the force registered during a fingertip grasp exercise can go up to 30 N using one finger and measured with a magnetic force sensor [26] (Figure 26).

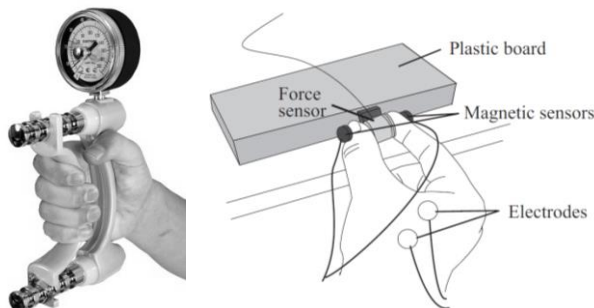


Figure 26: Human hand full grasp [25] and fingertip grasp [26] respectively.

ANATOMY OF THE HUMAN HAND

In the human hand we will first describe the bones that will be the solid and rigid segments on which the muscles, ligaments and tendons apply the forces to be able to generate rotations of this rigid segments [27].

The hand has 27 bones; 8 bones are located in the wrist, 3 are located in the thumb (1 metacarpal and 2 phalanx) and 4 metacarpal and 12 phalanxes are located in the other fingers [28]. The most important movements of the human hand are the all fingers flexion/extension and abduction/adduction and the opposition/retroposition of the thumb (Figure 27). This project aims to get the flexion/extension movement of the fingers and the opposition/retroposition of the thumb not the abduction-adduction, because requires more actuators.

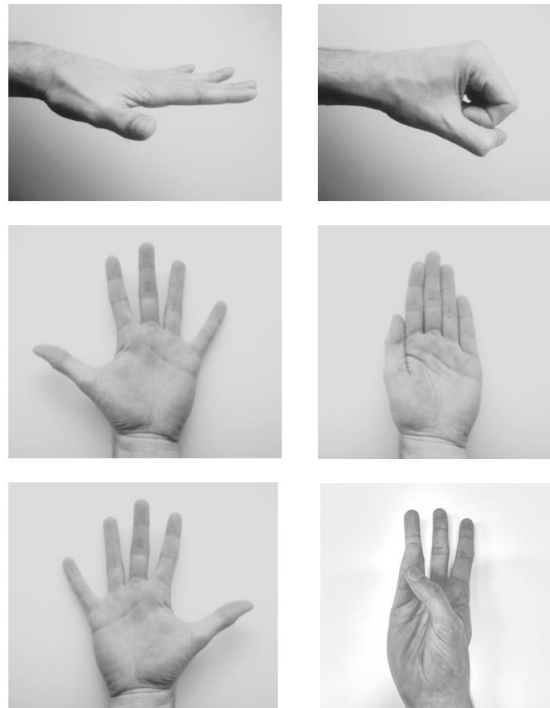


Figure 27: From above to below, human hand Extension/Flexion, Abduction/Adduction movements and thumb Retroposition/opposition.

The bones of the human hand are classified from proximal (closer to the mid-line of the body) being the first bones after the wrist, the bones of the carpus, the bones of the metacarpus and the phalanges from proximal to distal (Figure 28).

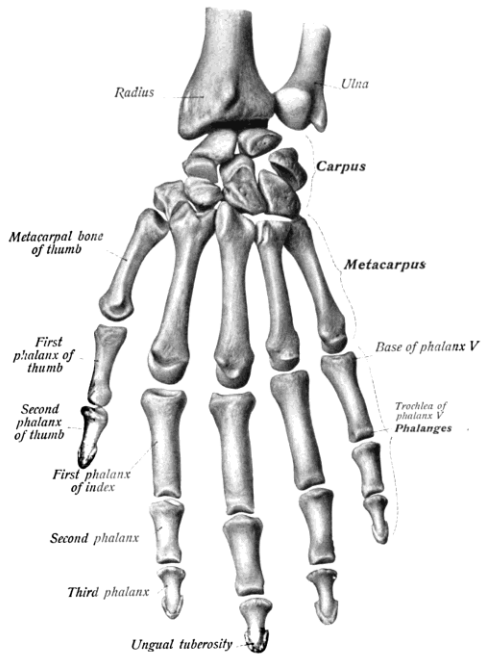


Figure 28: Dorsal view of the bones of the human hand [69].

Most of the human hand muscles are located on the forearm, this fact provides the human hand with high capabilities of strength speed, precision and 25 DOF, for this reason the reproducibility of the hand functions is a complex problem. The ligaments of fingers are the union between segments in the joints and we can distinguish for each joint: a palmar, collateral ligaments and articular capsule. Carpal ligaments limit the mobility of the carpal bones. The forearm muscles can be grouped by the flexors and abductors in the palmar side and the extensors and adductors in the dorsal side of the forearm (Figure 29).

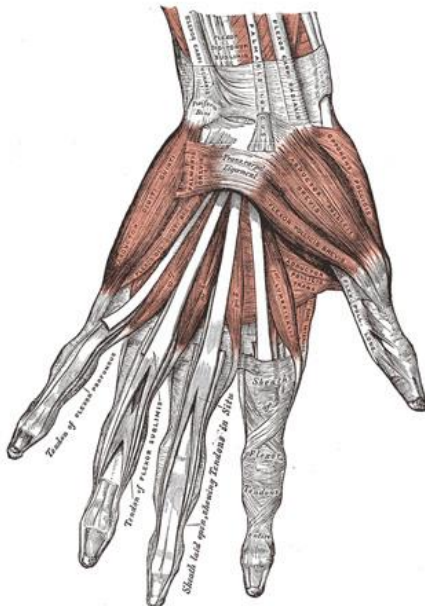


Figure 29: Palmar view of the muscles and connective tissues of the human hand [70].

HUMAN HAND KINEMATICS

The human hand can be defined as a 25 DOF system without considering the wrist movements. The thumb has five DOF, the fingers have 4 DOF each, 2 DOF for the metacarpophalangeal (MCP) 2 for the interphalangeal (IP) and four more DOF for the carpometacarpal (CMC) joints [28] (Tables 9 and 10).

Table 9: Range of motion of the thumb in degrees [28]:

Joint	Movement type	Range
CMC	Adduction/abduction	0(contact)/60
CMC	Extension/flexion	25/35
MCP	Extension/flexion	10H/55
MCP	Adduction/abduction	0/60
IP	Extension/flexion	15H/80

Table 10: Range of motion of the index, middle, ring and small fingers in degrees [28]:

Finger	MCP (E/F)	PIP (E/F)	DIP (E/F)	MCP (Ab/Ad)
Index	0/80	0/100	10H/90	13/42
Middle	0/80	0/100	10H/90	8/35
Ring	0/80	0/100	20H/90	14/20
Small	0/80	0/100	30H/90	19/33

Using a biomechanics software Kinovea [29] for video analysis in 2D and tracking the joints path we can find the finger displacements and linear velocities during the flexion and extension movement [30] (Table 11). These velocities would be the desired value for a hypothetic prosthetic device.

Table 11: Speed of the three phalanges of the human hand [30]:

Joint	Velocity (m/s)
Distal	0,47
Middle	0,28
Proximal	0,16

CREATING A MODEL OF THE HUMAN FINGER

The most common models found in the bibliography are 22 DOF [31]. Thus, 22 is the most common number used in modelling of the human hand. One of the questions to ask in the present work is how is the trajectory of a simulated bionic finger compared with the trajectory of a real human finger. To answer this question, the model of a human finger has been created ignoring the abduction-adduction movement and simulating only the movement in the xy plane.

The finger modelling is based on the two dimensional and three segment robot in their general form [32]. All the joints have a range of 90 degrees (Table 12) and the length of the segments are 40, 22 and 25 mm for l1, l2 and l3 respectively (Figure 30).

Table 12: Angles of the finger model joints.

Joint	Angle (°)
MCP (E/F)	0/90
PIP (E/F)	0/90
DIP (E/F)	0/90

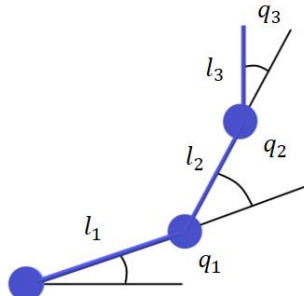


Figure 30: Model of the finger.

The equations used in the Matlab script are:

$$\begin{aligned}x &= l_1 \cdot \cos(q_1) + l_2 \cdot \cos(q_1 + q_2) + l_3 \cdot \cos(q_1 + q_2 + q_3) \\y &= l_1 \cdot \sin(q_1) + l_2 \cdot \sin(q_1 + q_2) + l_3 \cdot \sin(q_1 + q_2 + q_3) \\z &= 0\end{aligned}$$

In order to compare the trajectory of one of Grasp bionic hand fingers with one of this theoretical human hand finger, the movement of one finger has been simulated (Appendix A) and the resultant trajectory is shown in the Figure 31.

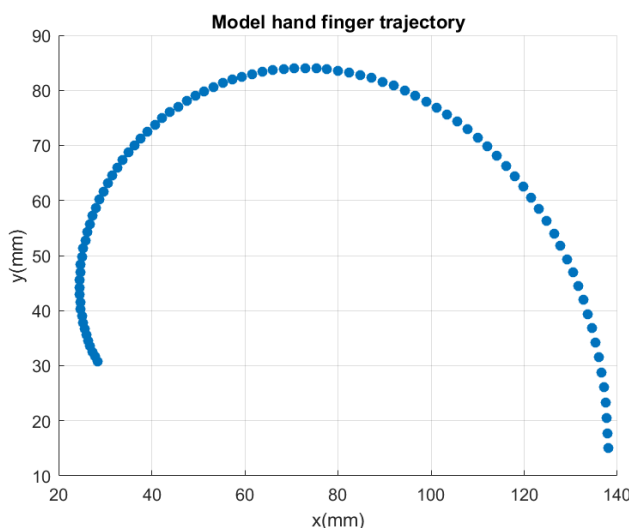


Figure 31: Finger simulation trajectory.

Design process

VERIFICATION AND VALIDATION

The procedure followed in the design process is composed of two stages: verification and validation. First of all, the verification of the design outputs is needed to evaluate if the bionic hand is able to do actions defined as the most important for the most common daily activities, with guarantees. The design process suffers a lot of iterations in this verification part of the design process. Once the goals of the project have been verified using calculations, simulations and qualitative evaluations is time for the prototyping. Then the second stage, validation, takes place (Figure 32) by experiments and real essays with the assembled prototype.

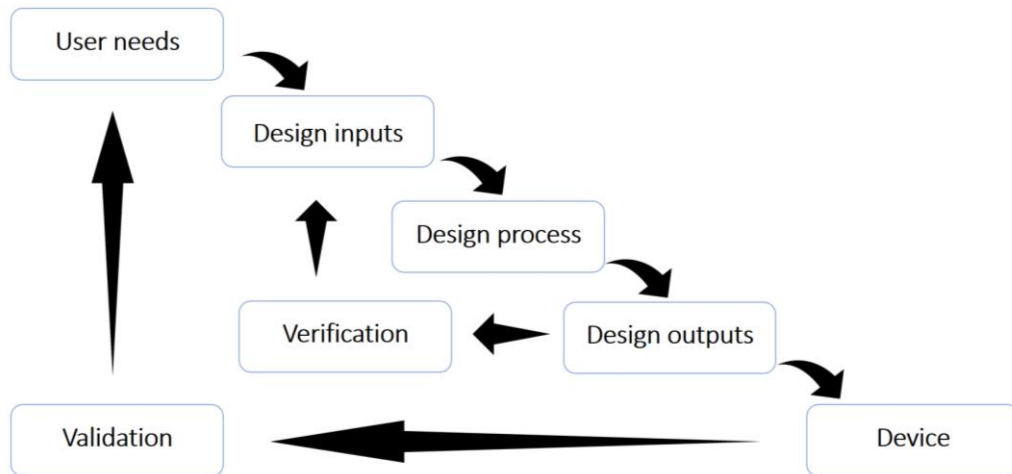


Figure 32: Design approach schematic.

SELECTED DIMENSIONS FOR THE STANDARD HAND DESIGN

From the data extracted from the anthropometric studies and from the limitations found during the design due to the size of the components included in the device, the selected measures are close to the average human hand dimensions (Table 13).

Table 13: Standard dimensions of Grasp:

Dimension	Size
Hand length (mm)	190
Palm length (mm)	104
Thumb length (mm)	97
Hand width (mm)	141
Palm width (mm)	82

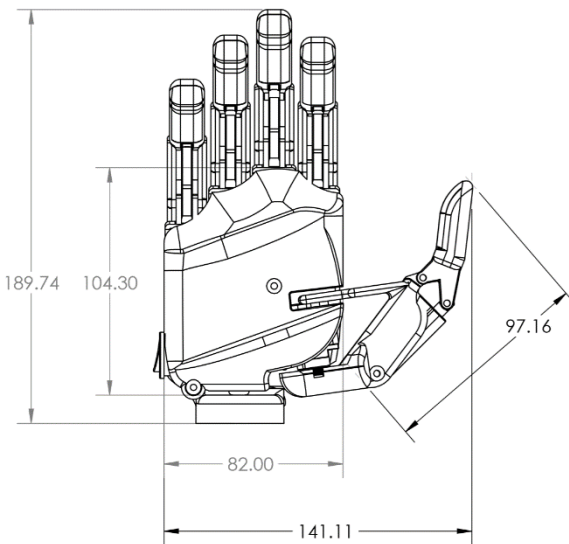


Figure 33: Dimensions of the Grasp Bionic Hand.

The dimensions also, have been constrained for the types of grasps that the hand must be able to do, being that ones the six described previously. The dimensions of the fingers and the palm have been changing with the aim to reproduce virtually this six types of grasps (Figure 34).

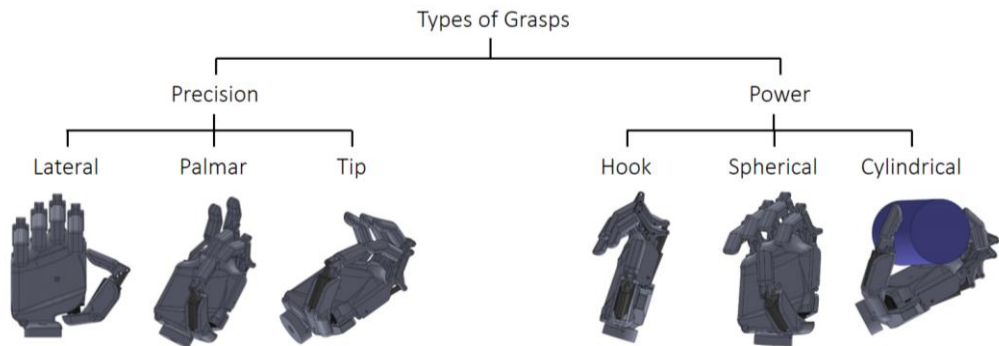


Figure 34: Six types of grasps effectuated virtually.

TYPES OF ACTUATORS AND MECHANICAL SYSTEMS

From the beginning of the project, the DOF and the requirements of the hand have been increased, for that reason the mechanical system of the hand has evolved from the simplest system that can be used to a more complex system. The firsts myoelectric designs had as actuators brushed DC micro servo motors with low torque and a lot of space outside of the palm of the hand was needed, the control of the fingers was also not so much robust. With Grasp 0 model, a 4 bar linkage system was implemented using DC motors with very good relationship between cost and speed/torque ratio, but again the main inconvenient was the absence of a position sensor, and external sensor would have been included but that increased the number of wires or digital pins used in the case of rotational encoders and also increased the number of steps to assemble the hand. After this designs a linear servo with very good features (45 N of force and 15 mm/s of speed) was found and the system was designed maintaining the four bar linkage system (Figure 35).

Brushed Servo Motor (2014)

- It requires an external mechanical system
- It takes too much space

DC Motor (2016)

- The position is unknown

Linear Actuator (Current)

- The position is known
- High force
- Space distribution
- Faster assembly

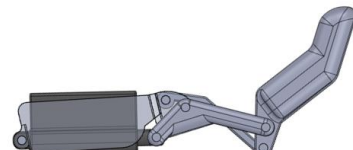
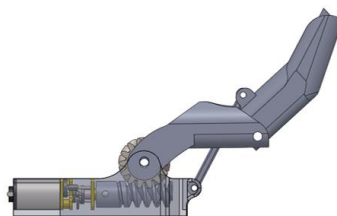
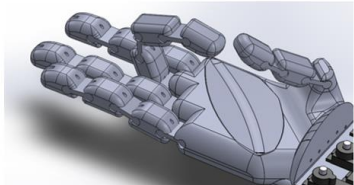


Figure 35: Iterations across different types of actuators and mechanical systems.

Another important step in the design process is the selection of the different components to get the best features, for example to choose the linear servos. There are in the market two manufacturers of this micro linear actuators, Actuonix PQ12 series [20], selected for the present work, and the Mighty ZAP micro linear actuators [33]. These are the two options of linear actuators with configurations of more than 20 N of stall force and a price under 100\$ in the worldwide market. The Actuonix model was selected for the price 70\$ against 85\$ and the dimensions, the length of the servo was significantly different to get space for the electronics in the palm of the hand (Figure 36).

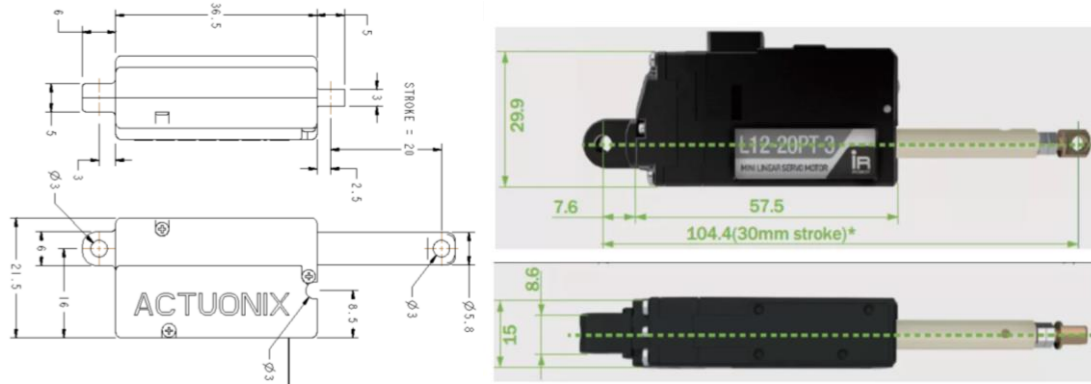


Figure 36: Differences in the dimensions of the two micro linear actuators Actuonix [20] (left) and Mighty ZAP [33] (right).

For the rotary servo selection, the decision was more difficult because there are much more options with the same standard dimensions and high range of features and prices. Is at that point when an statistical analysis have been taken (Appendix B), 41 micro servo motors were compared and the best option in terms of torque/cost was selected and that was the model MG90S of Tower Pro [34] showed in darker blue (Figure 37).

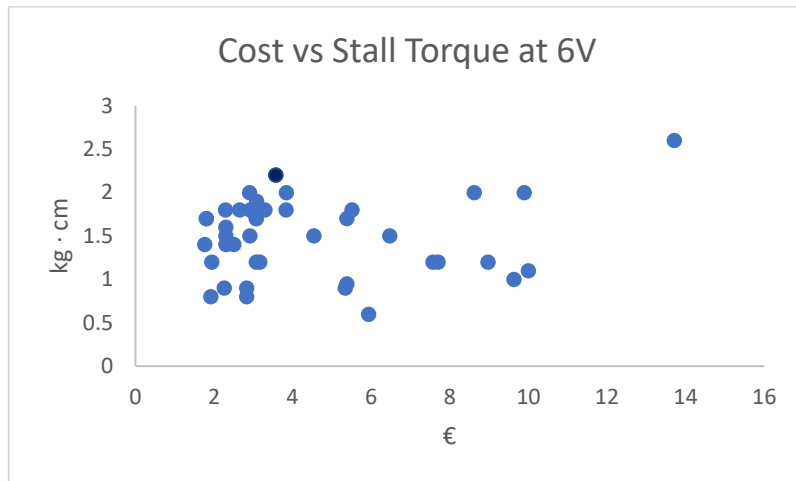


Figure 37: Rotary servo motor selection criteria.

PALM ELECTRONICS INTEGRATION

The decision of the selection of the micro controller have been taken based in two different points: it must be small to fit in the palm of the hand and it must be accessible for any person that wanted to change the firmware on their own. With this two features, Arduino Nano [19] is the best option, because is the most extended micro controller with infinite tutorials to learn online, it is easy to use, is cheap and is very small.

On the other hand, in order to check if the dimensions of the different iterations on the PCB design fit in the palm of the hand the model was created in the virtual environment. The 3D model of the PCB has been obtained using the option of Eagle to export to Autodesk Fusion 360 (Figure 38), from this CAD software, the file has been saved in the step. format and then opened with Solidworks and then introduced in to the assembly.

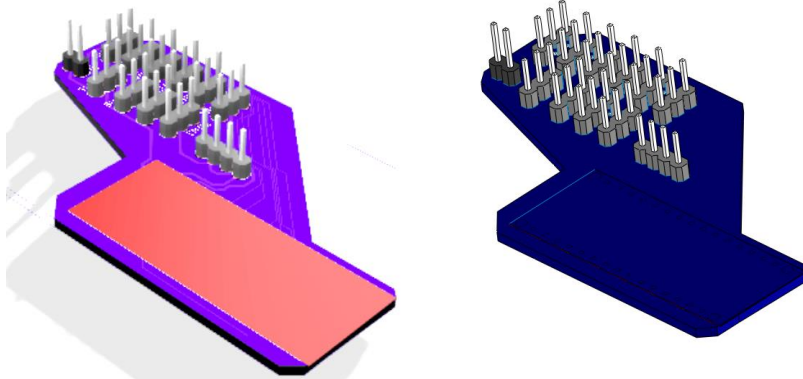


Figure 38: From left to right model on Fusion 360 and Solidworks.

The designed PCB model has been assembled with the Arduino Nano model found in Grabcad [35]. Also these two components are introduced into the Global assembly in order to prove if the dimensions are correct (Figure 39), that step has been done several times until the correct dimensions have been found.



Figure 39: PCB and Arduino Nano Grabcad model [35] assembled in Solidworks and assembled with the hand.

PROVIDING GRIP TO THE DISTAL PHALANGES

Other important part of any bionic hand is to have a soft surface with high coefficient of friction, in order to get grip to catch objects. Two molds for the two different types of finger distal phalanx have been created using the Solidworks mold tools: core and cavity (Figure 40).



Figure 40: The two mold models in CAD (above) and the printed part and the result of the silicone cover manufactured (below).

MECHANICAL DESIGN ITERATIONS

The design process has gone through several iterations to fit electronics in the palm of the hand but, also after the FEM and static simulations in order to increase the radius of the fillets and reduce stresses at some critical points. Other changes have been done for kinematics requirements, for example, the length of the distal phalanx of the thumb has been increased to get the lateral grasp. But the most relevant change after the first prototype has been the addition of another point of attachment of the thumb to provide this finger with equivalent resistance to the other elements of the hand (Figure 41). Other modifications, for example in the covers, have been done for aesthetic purposes.



Figure 41: Changes suffered by the thumb finger: length of the distal phalanx and another point of attachment.

COMPONENTS OF THE FINAL DESIGN

The hand is finally conformed by 10 different components (Figure 42) that can be printed using different types of 3D printers. Also we can consider the molds as four more components making a total of 14 different parts knowing that the phalanges of the fingers and the joint must be printed four times, one time for each finger and the Finger covers that also must be casted 4 times one for each finger (Table 14).

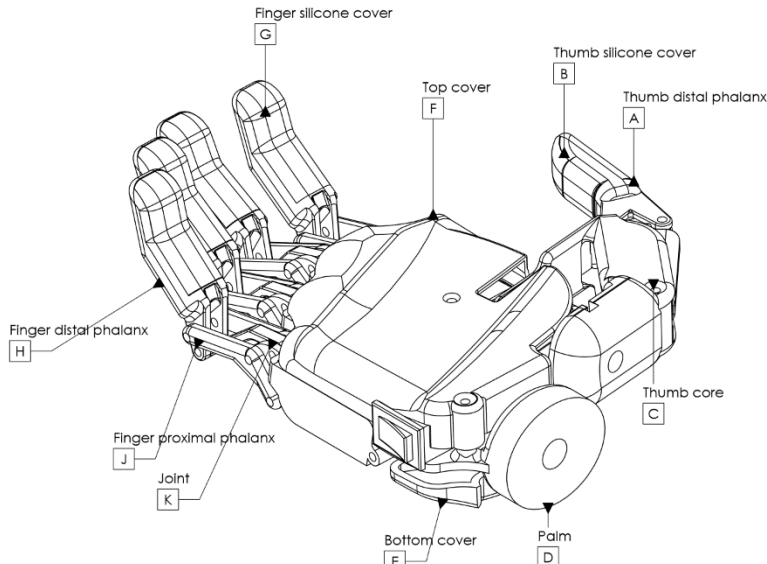


Figure 42: Grasp 1.0 components.

Table 14: Final number of elements that conform the final design of Grasp and have to be 3D printed:

Reference	Component	Quantity
A	Thumb distal phalanx	1
B	Thumb silicone cover	4
C	Thumb core	1
D	Palm	1
E	Bottom cover	1
F	Top cover	1
G	Finger silicone cover	4
H	Finger distal phalanx	4
J	Finger proximal phalanx	4
K	Joint	4

PROTOTYPING

After the past designs of hands a first full prototype of Grasp 1.0 have been printed with PLA 3D850 [36] in an BQ Hepstero 2 [37] in order to check the different types of grasps, the functionality of the hand, if the hand is easy to be assembled, and to make the different tests with the firmware (Figure 43).

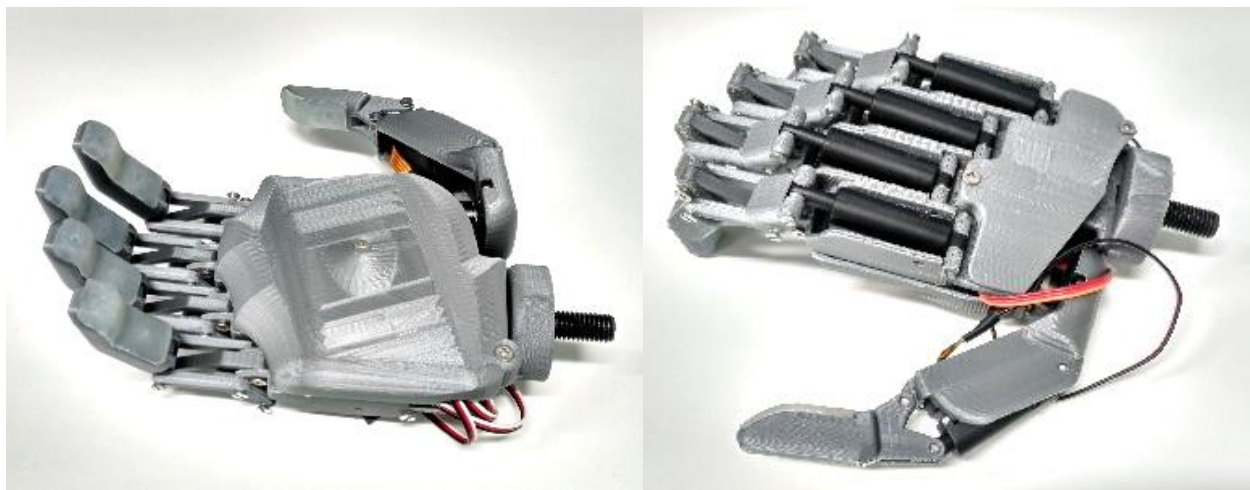


Figure 43: Grasp 1.0 first prototype 3D printed.

A PCB to be connected directly to six volts power supply have been manufactured by the supplier PCBgo [38], to make the test with a model of the full hand, proceed to generate the control algorithms and validate the full bionic device (Figure 44).

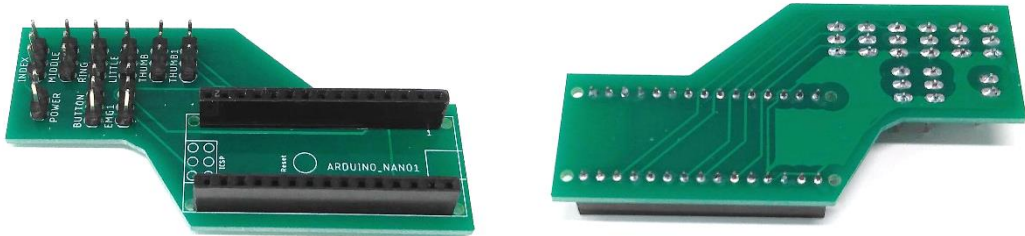


Figure 44: PCB prototype with the soldered pins.

The next step has been the assembly of the PCB prototype with the 3D printed hand (Figure 45) and get the complete Grasp bionic hand. The test was completely successful.

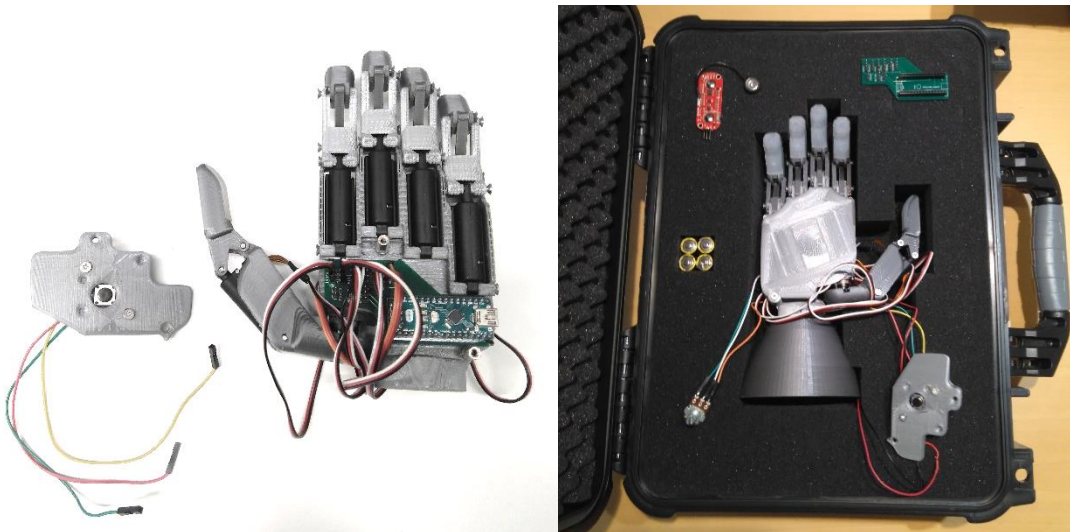


Figure 45: Grasp 1.0 assembled with the PCB and the pushbutton inserted in the bottom cover.

DIFFERENT SIZES

Grasp has been designed in two different sizes, the standard one, presented in this study on the drawings and another larger size, Grasp L (Figure 46) for people with bigger hands. Smaller sizes have not designed because the standard size is the minimum to catch common daily life objects. The parts of the hand that have been increased on their length are the distal phalanx and the distal phalanx cover, in fact are 6 mm longer which is close to the difference between the palm length and the hand length standard deviations (5 mm) viewed in the chapter, the human hand.

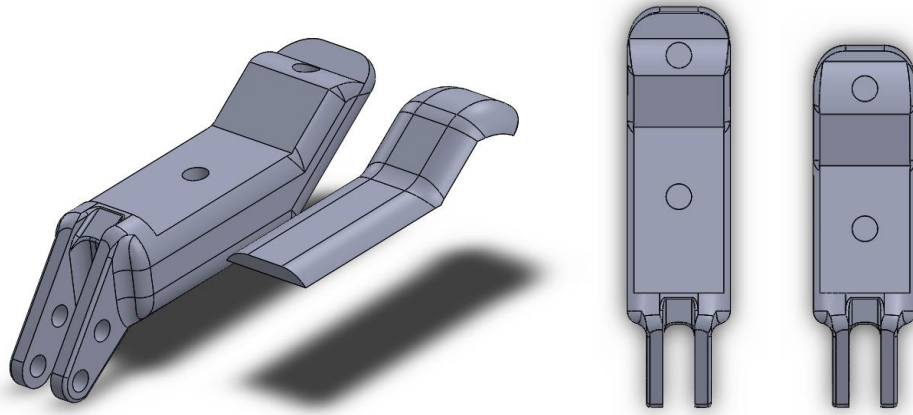


Figure 46: Distal phalanx size L and the standard compared with the L size.

LEFT HAND

The left hand has been created using the symmetry feature on the assembly (Figure 47). This feature has been done for the non-symmetric parts: the palm, the top cover and the bottom cover.

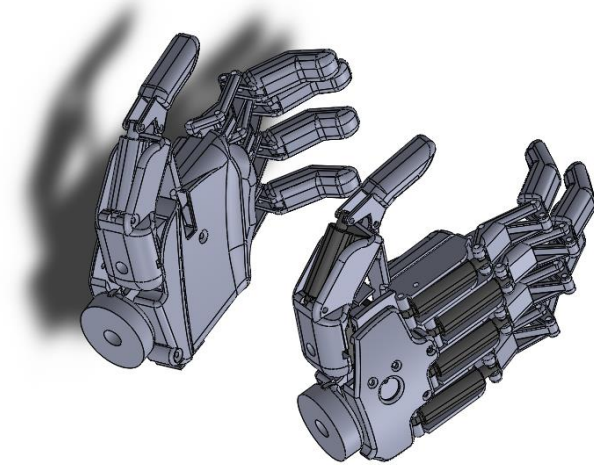


Figure 47: Left and right hand models.

Drawings

Components and materials

COMPONENTS

Rotary DC micro servo motor: Tower Pro MG90S

As can be seen in the previous chapter, the micro-servo MG-90S which offers very good benefits for very good price because it has a price of € 3.57 / unit on the internet and has gears metallic, providing a Torque of 2.2 kg·cm, much higher than the average (1.48 kg · cm) in this type of engines and a rotation speed also higher.

Table 15: Features of MG90S [34].

Dimensions (mm)	22,5 x 12 x 35,5
Weight (g)	13,4
Operating voltage (V)	6
Rotation time (s/60°) at 6V	0,08
Stall torque (kg·cm) at 6V	2,2
Cost (€)	3,57



Figure 48: MG90S DC servo motor [34].

Linear micro servo motor: Actuonix PQ12R

The Actuonix PQ12R (Figure 49) is the only linear servo with potentiometer to track the position with high performance features and the smallest dimensions.

Table 16: Features of PQ12R [20].

Gearing option	63:1
Peak power point	30N @ 8 mm/s
Peak efficiency point	8N @ 12 mm/s
Max speed (no load)	15 mm/s
Max force (lifted) (N)	45
Max side load (N)	10
Back drive force (N)	25
Stroke (mm)	20
Input voltage (V)	6
Stall current (mA)	550
Mass (g)	15
Operating temperature (°C)	-10 to +50
Positional Repeatability (mm)	±0,1
Mechanical Backlash (mm)	0,25
Audible noise (dB)	55
Ingress protection	IP-54
Feedback potentiometer (kΩ)	5±50%
Limit switches (μA)	8
Maximum duty cycle	20%



Figure 49: Actuonix PQ12R micro linear servo motor [20].

Microcontroller: Arduino Nano V3

The Arduino Nano micro controller based on the ATmega 328 offers enough digital PWM outputs to control the six servo motors and the perfect size to be fitted in the palm of the hand (Table 17).

Table 17: Features of Arduino Nano [19].

Micro-controller	ATmega 328
Operating voltage (V)	5
Input voltage (V)	7-12
Maximum input voltage (V)	6-20
Digital pins I/O	14 (6 with PWM)
Analog Input pins	8
Maximum current (mA)	40
Flash memory (KB)	32
SRAM (KB)	2
EPROM (KB)	1
Clock speed (MHz)	16
Dimensions (mm)	18,54 x 43,18

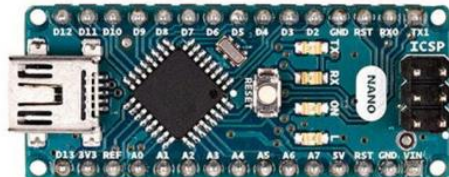


Figure 50: Arduino Nano [19].

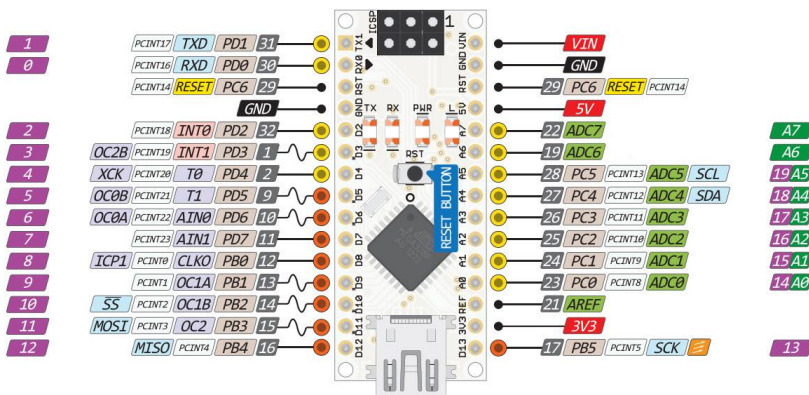


Figure 51: Arduino Nano pinout [19].

EMG analog sensor: DFRobot OYMotion SKU:SEN0240 or EMG analog sensor: Advancer Technologies Myoware

In this project, one electromyographic sensor is used to provide the analog input that will actuate the actuators to bend and extend the fingers. There are two different EMG sensors compatible with the hand: OYMotion and Myoware. OYMotion [39] uses a dry electrode with the skin proper for the daily use instead of adhesives. It would be a good option to have the bionic device in contact with the skin for several hours. Otherwise, Myoware sensor [21] has all the electronics integrated on the electrodes board, but uses adhesive surface, which would be a better electrode for research or occasional use (Figure 52).

Table 18: Features of Myoware sensor [21].

Parameter	Min.	Typ.	Max.
Supply Voltage	2,9V	3,3 o 5V	5,7V
Adjustable Gain Potentiometer	0,01 Ω	50 Ω	100 Ω
Input impedance	-	110 GΩ	-
Supply current	-	9 mA	14 mA
CMRR	-	110	-



Figure 52: Myoware EMG analog sensor [21].

Table 19: Features of the signal transmitter board [39].

Supply Voltage (V)	3.3~5.5
Operating Voltage (V)	+3.0
Detection Range (mV)	± 1.5
Electrode Connector	PJ-342
Module Connector	PH2.0-3P
Output Voltage (V)	0~3.0
Operating Temperature (°C)	0~50
Size (mm)	22 x 35

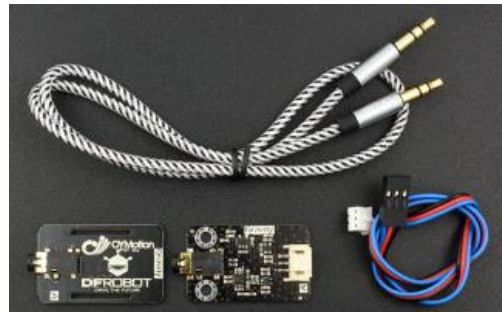


Figure 53: OYMotion EMG sensor [39].

Table 20: Features of the dry electrode board [39].

Electrode Connector	PJ-342
Wire Length (cm)	50
Plate Size (mm)	22 x 35
Weight (g)	36

Pololu step-down voltage regulator D24V25F6

The voltage needed to supply the servo motors and the power circuit is 6 V and the Lithium batteries are 7.4 V, the Pololu D24V25F6 offers high efficiency voltage regulation and up to 2.5 A continuous output current (Table 21) perfect features taking into account the electrical calculations described in the next chapter.

Table 21: Features of the D24V25F6 [17].

Minimum operating voltage (V)	7
Maximum operating voltage (V)	38
Continuous output current (A)	2.5
Output voltage (V)	6
Reverse voltage protection?	Yes
Maximum quiescent current (mA)	0.7
Size (mm)	17.8 x 17.8 x 8.87
Weight (g)	2,6



Figure 54: Pololu D24V25F6 voltage regulator [17].

Turnigy nano-tech 6.0 battery

The battery is selected to get 8 hours of autonomy with a voltage close to 6 volts to get efficiency on the voltage conversion and without a high cost (Table 22).

Table 22: Battery specifications [40].

Model	Nano-tech 6.0
Capacity (mAh)	6000
Voltage (V)	7.4
Discharge (C)	25 Constant / 50 Burst
Weight (g)	333
Dimensions (mm)	155 x 49 x 20



Figure 55: Battery Nano-tech 6.0 [40].

Pololu switch on/off

Knowing which will be the maximum current in the system, the selection of the main ON/OFF switch can be done, and Rocket switch of the manufacturer Pololu [17] in this case the maximum current is four times bigger than the current needed for this application (Table 23).

Table 23: Switch features [17].

Max. current (mA)	10000
Dimensions (mm)	21.2 x 15.1 x 22.4



Figure 56: Pololu Rocket switch [17].

DFRobot DFR0029-B Pushbutton module

The selected pushbutton module integrates the voltage divider resistor in the circuit and has appropriate dimensions to go under the bottom cover (Table 24).

Table 24: Pushbutton features [39].

Dimensions (mm)	22 x 30
Supply Voltage (V)	5



Figure 57: DFR0029-B pushbutton [39].

IMAX B6 DC Charger

The last component to be selected is a Li-Po battery charger (Table 25).

Table 25: Charger features [40].

Input Voltage (V)	11~18
Circuit Power: Max charge/ max discharge (W)	50/5
Charge Current Range (A):	0.1~5.0
Discharge Current Range (A):	0.1~1.0
Li-ion/ LiPoly Cells	1~6
Weight (g)	227
Dimensions (mm)	133 x 87 x 33



Figure 58: Li-po charger [40].

MATERIALS

Rigid material

The hand can be printed in different materials using FDM and SLA. In the present work, all the parts have been printed in the most common used FDM filament: Polylactic acid (PLA) and the properties of this material has been used in the FEM stress simulations.

Otherwise, the recommended material for applications with regular contacts with the human skin is the Medical Grade Acrylonitrile butadiene styrene (ABS), which is biocompatible and recyclable. As an example, the ABS medical from the manufacturer Smartfil presents a High quality filament specially designed for medical applications. This material is compliant with the UPS Class VI or ISO 10993-1 certification (Table 26). This allow the manufacturers to make components that can be in touch with the human body [41]. Also is recyclable and compliant with the sustainability goals of the project.

Table 26: ABS medical grade specifications [41].

Material Density (g/cm³)	1.05
Tensile Yield Strength (Mpa)	36.5
Tensile Modulus (Gpa)	2.55
Print Temperature (°C)	240 ± 10
Hot Pad (°C)	80 ± 100
Biocompatible	Yes /ISO 10993-1
Recyclable	Yes



Figure 59: Medical grade ABS [41].

Flexible material: Silicone elastomer A-103

For the finger distal phalanx grip covers the most recommended material is an elastomeric material that could be cast in the mold designed for its use. The Silicone Elastomer A-103 (Figure 60) datasheet specifies no significant irritation expected form single short term exposure [42]. The main function of this material is to provide the grip that makes the hand able to catch objects with firmness.



Figure 60: Medical grade silicone compound [42].

Electronics design

ELECTRICAL DESIGN

The electrical design starts with the selection of actuators. Once defined the mechanical requirements, the model of actuator PQ-12R of the manufacturer Actuonix [20] and the MG90S micro servo [34] are chosen. The maximum requirement for each linear servo is the stall force current which is the maximum value that the motor can consume for a short period of time. This value is not a value to consider for the common use but can set the maximum value required for the five DC linear servos and the rotary DC servo motor. The maximum current is 450 mA at 6 V DC (Figure 61) and 200 mA at 6V DC for the linear and rotary servo motors respectively.

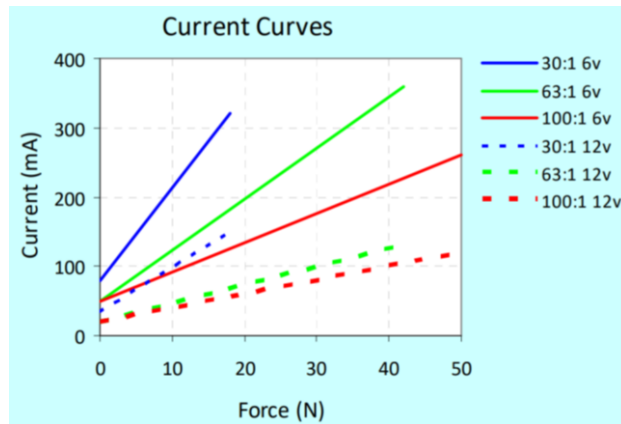


Figure 61: Actuonix PQ-12R current curves values [20].

The total current demand done by the six actuators must be added to the current demanded by the Arduino Nano board this is the Atmega 328 maximum current, 200 mA [19] where are included the two DFRobot Gravity EMG sensor and the Pushbutton [39]:

$$I_{max} = \sum_{i=1}^n I_i$$

$$I_{max} = I_{MG90S} + 5 \cdot (I_{PQ-12R}) + I_{Arduino\ Nano}$$

$$I_{max} = 200\ mA + 5 \cdot (450\ mA) + 200\ mA = 2650\ mA$$

This huge value requires a huge voltage regulator in terms of space, it doesn't be able to be found with the project space constrains and the best option became the Pololu step down voltage regulator D24V25F6 which can supply 2.5A at 6V and has good efficiency curves (Figure 62):

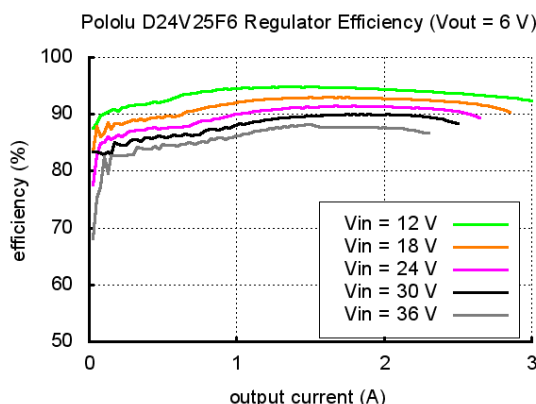


Figure 62: Pololu D24V25F6 voltage regulator efficiency curves at different voltages [17].

As observed in the Figure 62, the efficiency from 12 V to 6 V range between 90 % to 95 % there are no values for the 7.4 V to 6 V regulation curve. Therefore, it can be assumed that the efficiency is close to 100 % because the voltage drop-off is smaller. It will be considered an efficiency of 98 % in the voltage regulation.

The minimum values of current can also be calculated in the same way as:

$$I_{min} = \sum_{i=1}^n I_i$$

$$I_{min} = I_{MG90S} + 5 \cdot (I_{PQ-12R}) + I_{Arduino\ Nano}$$

$$I_{min} = 40\ mA + 5 \cdot (50\ mA) + 40\ mA = 330\ mA$$

And the power extremes at 6 V:

$$P_{max} = V \cdot I_{max}$$

$$P_{max} = 6\ V \cdot 2.65\ A = 15.90\ W$$

$$P_{min} = V \cdot I_{min}$$

$$P_{min} = 6\ V \cdot 0.33\ A = 1.98\ W$$

The source power can be calculated as follows where the performance is $\gamma = 0.98$:

$$P_\gamma = \frac{P}{\gamma}$$

$$P_{max\gamma} = \frac{15.90\ W}{0.98} = 16.22\ W$$

$$P_{min\gamma} = \frac{1.98\ W}{0.98} = 2.02\ W$$

And the source current as:

$$I_{max\gamma} = \frac{16.22\ W}{7.4\ V} = 2191\ mA$$

$$I_{min\gamma} = \frac{2.02\ W}{7.4\ V} = 272\ mA$$

The Battery load required for 8 hours in the two scenarios will be:

$$C_{max} = 2191\ mA \cdot 8\ h = 17528\ mAh$$

$$C_{min} = 272\ mA \cdot 8\ h = 2176\ mAh$$

The C_{max} is an inaccessible value for a prosthetic device, in this case can be considered a rectified oscillating function that ranges from the previous extreme values, from 272 mA to 2191 mA in order to simulate a performance test where the hand is catching and leaving an object as a possible test to make as an approximation of a cyclic use in the daily living activities.

In this case the average current required can be approximated as the integral of the current over time during a wave period:

$$I_{av} = \frac{1}{T} \int_0^T I \cdot dt$$

The previous approach has been implemented in Simulink (Figure 63) (Appendix B) to approximate the hand use during 1 hour, using a switch to rectify the sine wave and send the resulting signal to the Matlab [43] workspace.

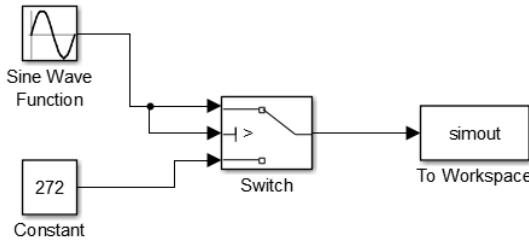


Figure 63: Simulink diagram for the current cycles simulation.

RESULTS

After the simulation (Figure 64), the load required to guarantee the usability of the hand during the most important part of the day is considerable.

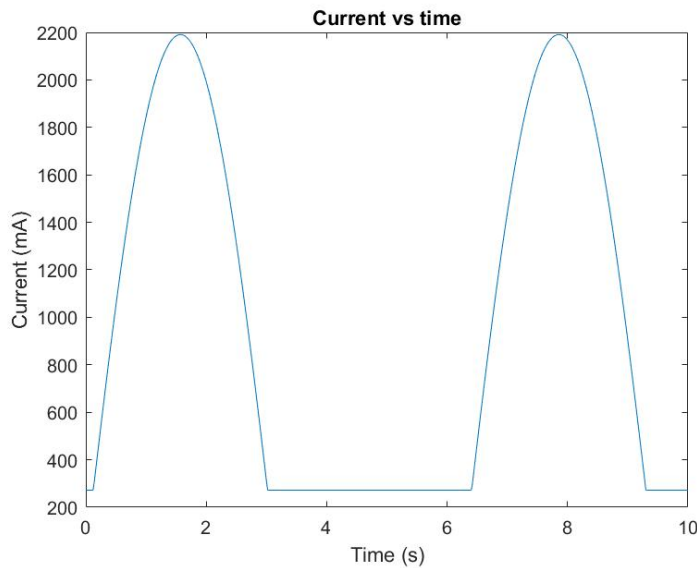


Figure 64: Two periods of current over time representation.

$$I_{av} = 838.78 \text{ mA}$$

The total load necessary to supply an 8-hour activity with this pattern would be:

$$C = I_{av} \cdot 8 \text{ h}$$

$$C = 838.78 \text{ mA} \cdot 8 \text{ h}$$

$$C = 6710 \text{ mAh}$$

Once the previous parameters are defined, the batteries can be chosen and there are no many manufacturers of batteries with this high load then, the battery chosen, 6000 mAh at 7.4 V fits very well with the economical

constraints. Knowing which will be the maximum current in the system, the selection of the main ON/OFF switch can be done, and Rocket switch of the manufacturer Pololu [17].

SCHEMATICS

The electronics configuration starts with conceptual schematics both are the following, for the two different analog EMG sensors available in the market, with the Myoware EMG sensor (Figure 65) and the DFRobot EMG sensor (Figure 66).

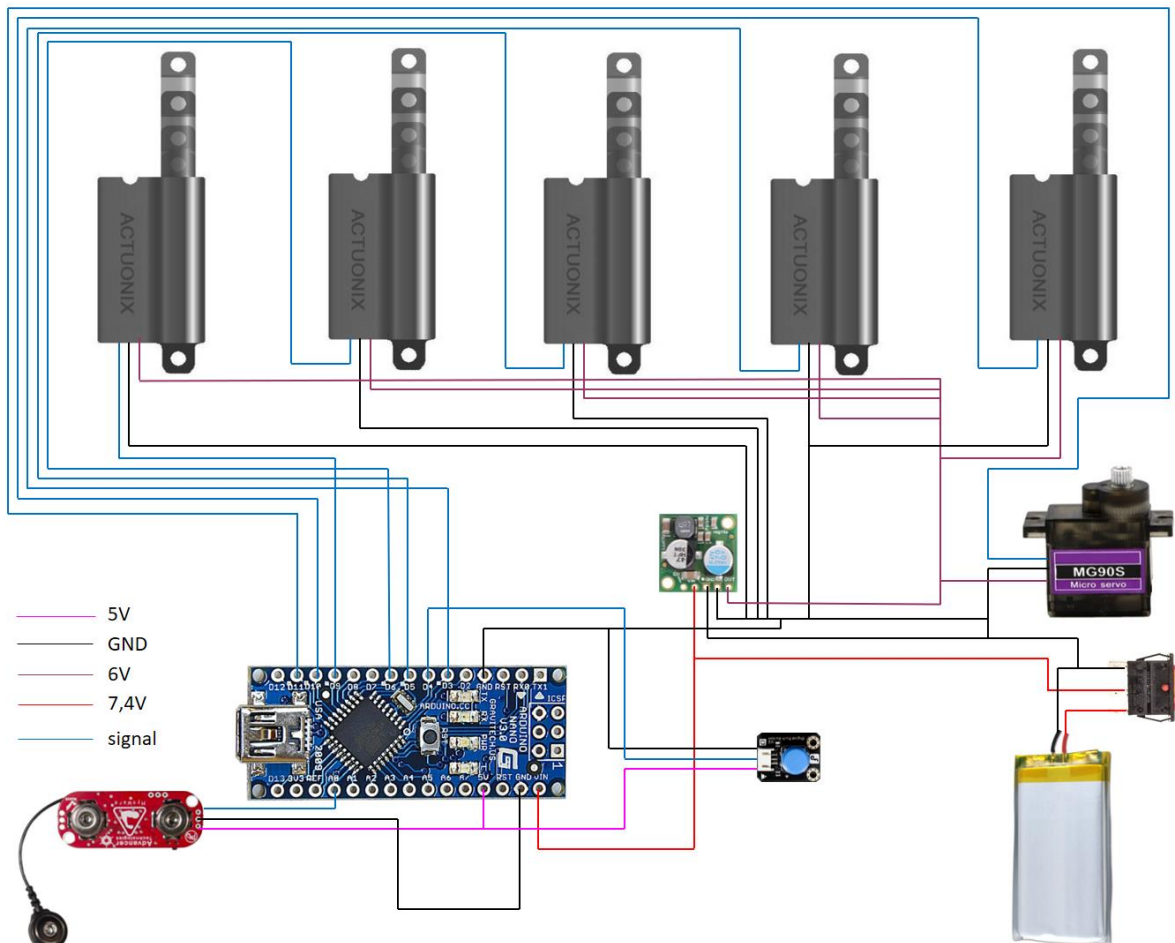


Figure 65: Electric schematic of the Myoware sensors configuration.

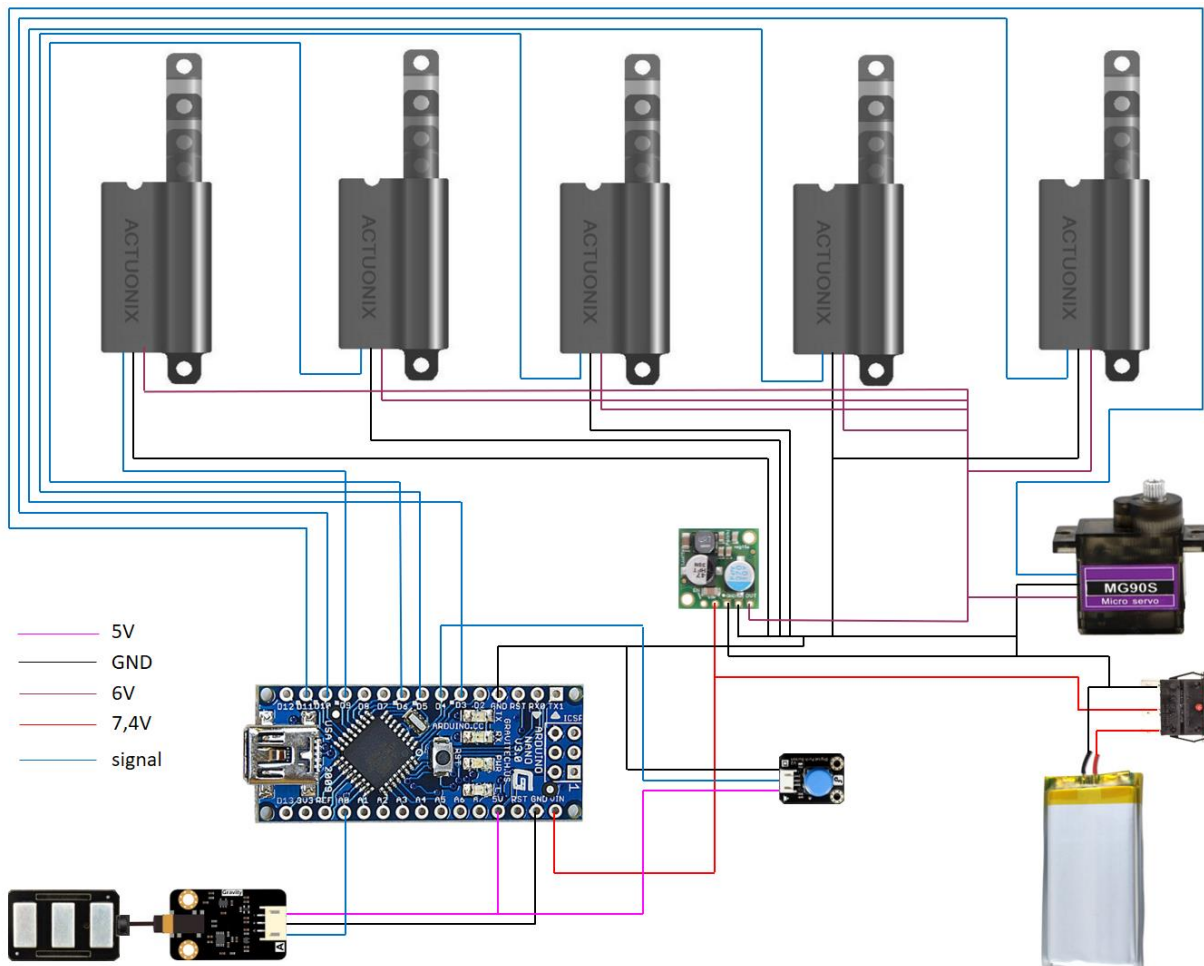


Figure 66: Electric schematic of the OYMotion sensors configuration.

PCB DESIGN

The PCB design contains the option to connect another EMG sensor for more advanced configurations. The previous schematic is drawn in the PCB software Eagle [44] (Figure 67):

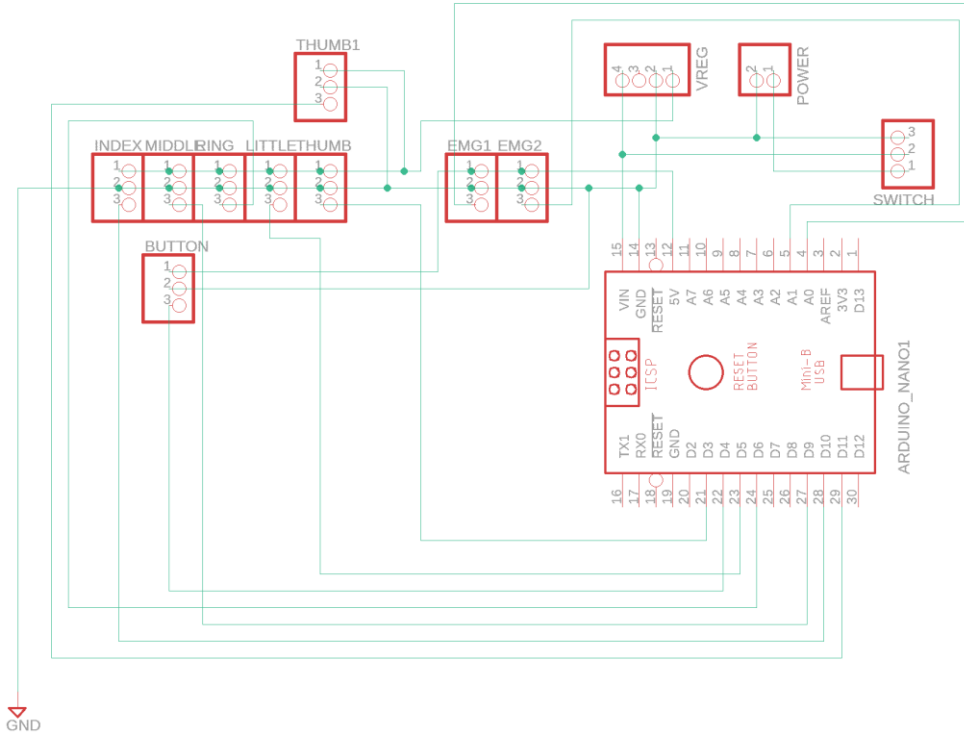


Figure 67: Electric schematic on Eagle.

This schematic is developed as a board taking into account two considerations: the minimal spacing between tracks in the layout is 0.317 mm for voltages under 30 V. Otherwise, applying a security factor of 2, the maximum current goes up to 4382 and the corresponding track thickness for 5 A is 0.512 mm for the supply tracks and 0.15 mm thickness for the other tracks which maximum current will be under 500 mA [45]. A GND plane has been created with an isolation of 0.4064 mm between tracks. The dimensions of the PCB are constrained by the space available in the palm of the hand, and for that reason the geometry and dimensions of the board must be under 80 mm length and 50 mm height (Figures 68, 69 and 70).

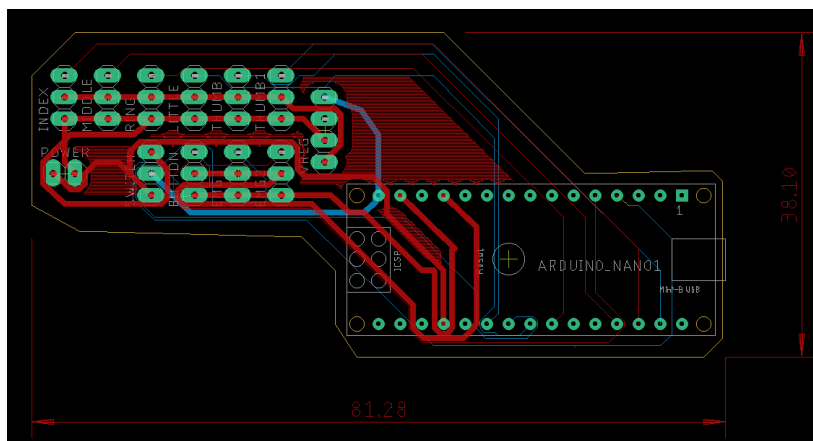


Figure 68: PCB board.

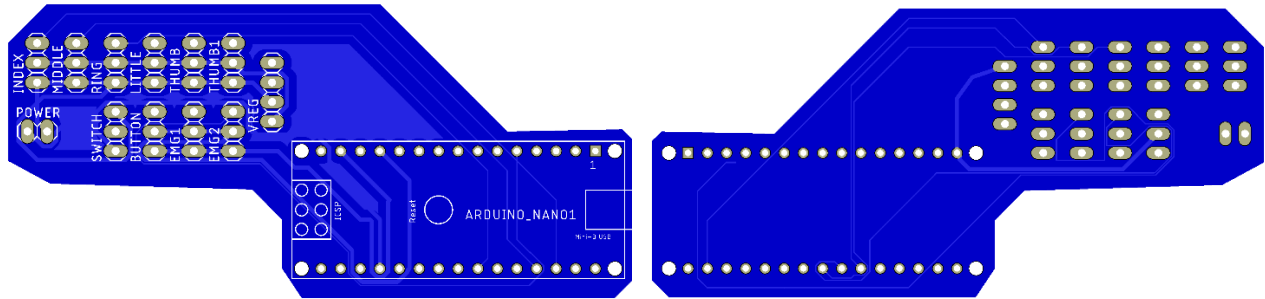


Figure 69: PCB board manufacture appearance top and bottom layers.

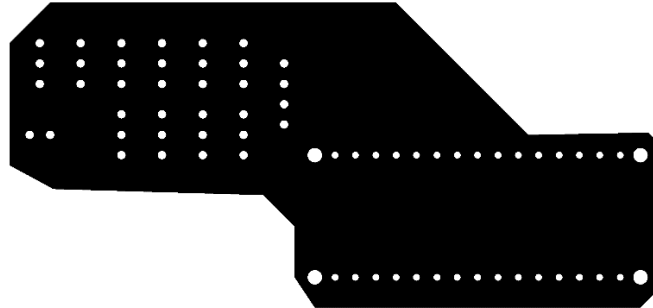


Figure 70: PCB board drill holes.

ELECTRICAL SAFETY

The previous electric design was conceived taking into account the safety recommendations of the EMG sensor [21] which specifies that the recommended use of the sensor is with the Arduino connected to a battery while the sensor is connected to the body, and not connecting it to the USB port and body parts simultaneously if the PC is connected to the grid. That point is specified in the user instructions as a safety warning (Figure 71).

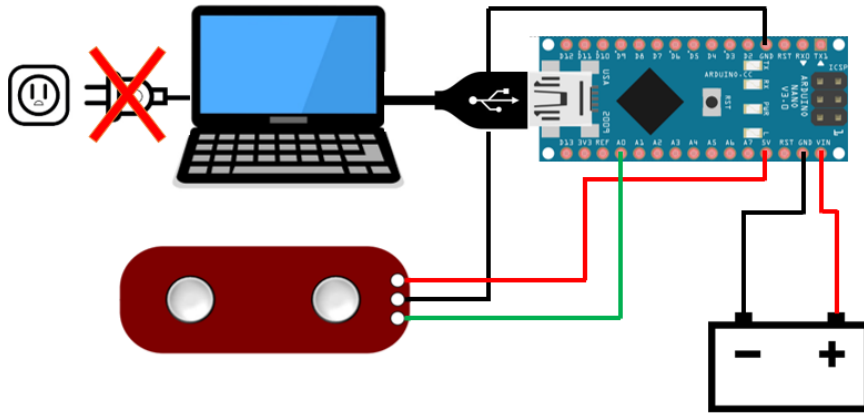


Figure 71: EMG Myoware sensor safety recommendations.

Kinematics

WORKSPACE

In order to get an indicator of the quality movement of the bionic hand and the speed of the flexion-extension movements of the fingers kinematics study has been done. The simulations of the displacements of each finger in the three-dimensional space have been done virtually using the Solidworks simulation package [46] and once the data has been obtained as a csv. has been stored in Excel sheets and plotted using a Matlab script (Appendix L). The initial and final conditions have been set up in the Table 27.

Table 27: Finger initial conditions.

Condition	Value
Finger initial piston displacement (mm)	4
Finger final piston displacement (mm)	19
Actuator speed (mm/s)	15
Time of displacement (s)	1

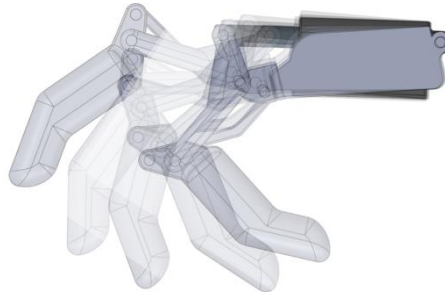


Figure 72: Finger displacement sequence.

The thumb has two DOF and the simulation must be done for each increment of the angle of the rotary servo motor, in other words the flexion movement of the finger has been simulated in 10 different positions in combination with the opposition movement of the thumb (Table 28).

Table 28: Thumb initial conditions.

Condition	Value
Linear servo positions (mm)	[1,2,4,6,8,10,12,14,16,18,20]
Rotary servo initial position (°)	0
Rotary servo final position (°)	90
Rotary servo speed (°/s)	75
Time of displacement (s)	1.2

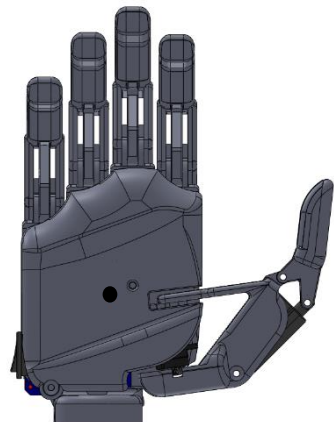


Figure 73: Origin of coordinates of the simulation in black.

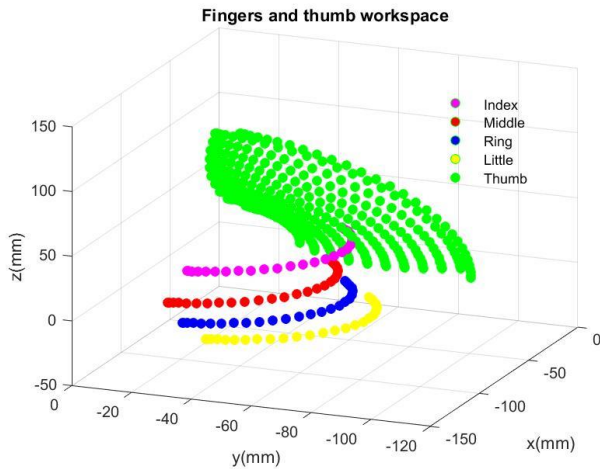


Figure 74: Full hand simulation values.

The trajectories of the hand fingers in the space are a good indicator of how the hand is capable to catch different objects and on the discussion will be used to be compared with the human finger workspace approximation of the chapter “The human hand”.

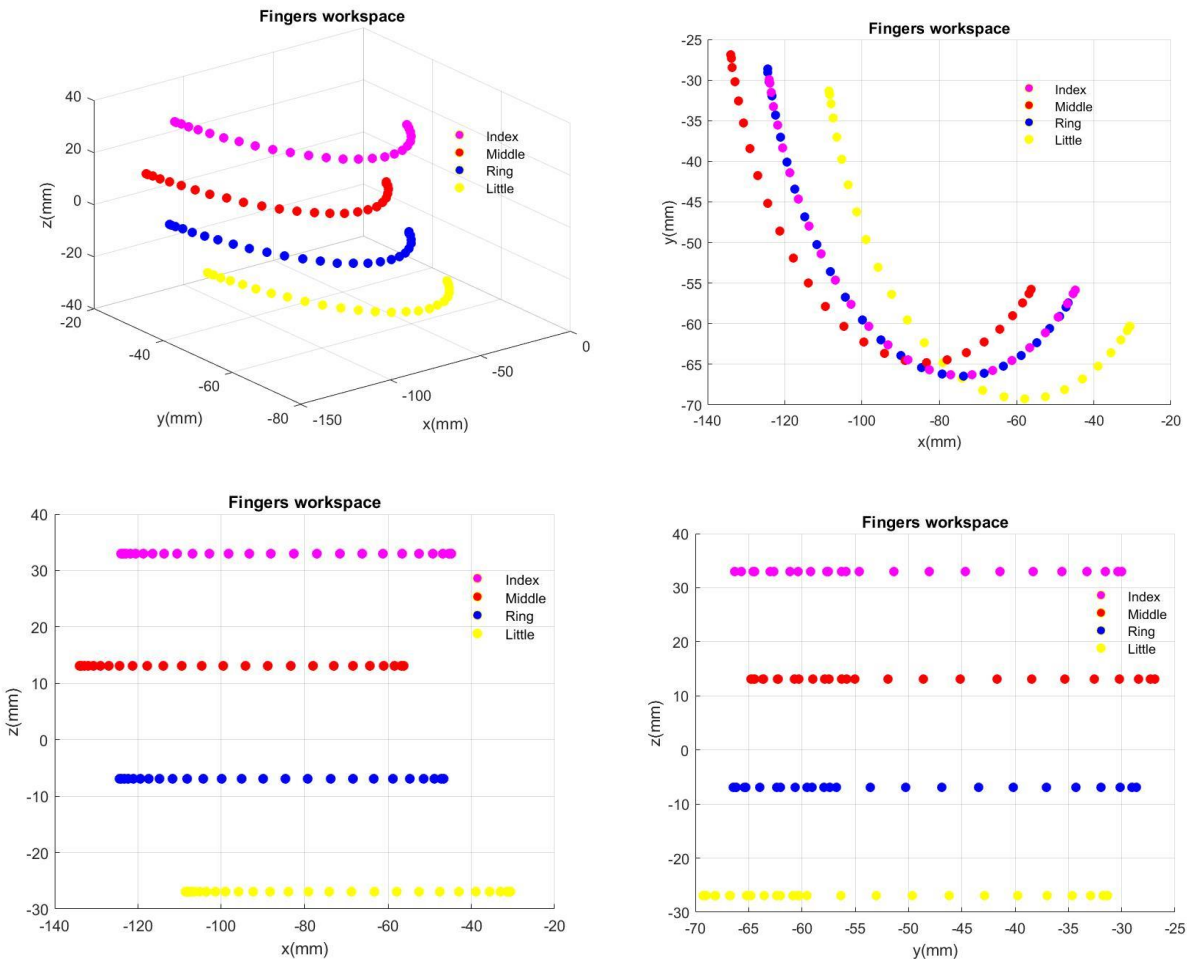


Figure 75: Fingers (index, middle, ring and small) simulation values visualized in the three-dimensional space and on the different planes .

The origin of coordinates is placed in the centre of the hand and the values for the entire hand have been plotted in the three-dimensional space (Figure 74) using the scatter3d function. And the four fingers and the thumb have been plotted in the 3D space and in the planes xy, yz and zx in the Figures 75 and 76 respectively.

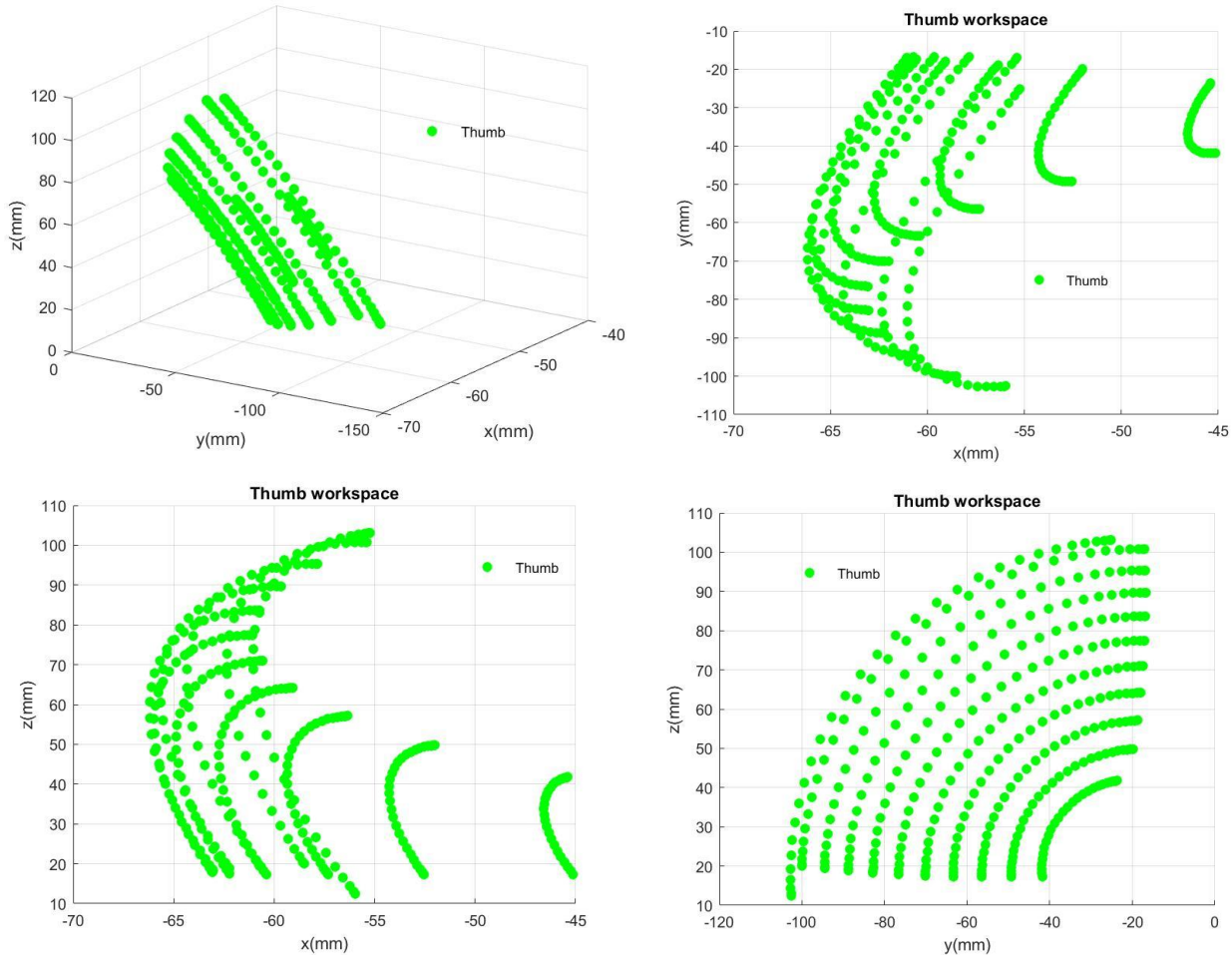


Figure 76: Thumb simulation values visualized in the three-dimensional space and on the different planes.

FINGER FLEXION-EXTENSION SPEED

For this study the Solidworks simulation package have been used (Appendix M) and from that simulation is known the sampling frequency (F_s), the recording time (T) and the full displacement of the actuator which is 15 mm:

$$T = 1\text{ s}$$

$$F_s = 25 \text{ Hz}$$

$$T_s = \frac{1}{F_s} = \frac{1}{25} = 0,04\text{ s}$$

The actuator displacement increases every 0,04 seconds as follows:

$$\text{Actuator displacement} = \frac{15 \text{ mm}}{25 \text{ samples}} = 0.6 \text{ mm}$$

From that data I can approximate the derivative of the x and y coordinates in discrete time as follows:

$$v_x = \frac{\Delta x}{\Delta t} = \frac{x_f - x_0}{t_f - t_0} \quad t \in [0,1] \text{ [mm/s]}$$

$$v_y = \frac{\Delta x}{\Delta t} = \frac{y_f - y_0}{t_f - t_0} \quad t \in [0,1] \text{ [mm/s]}$$

After these calculations the plots of the speed in each axis can be done (Figure 77).

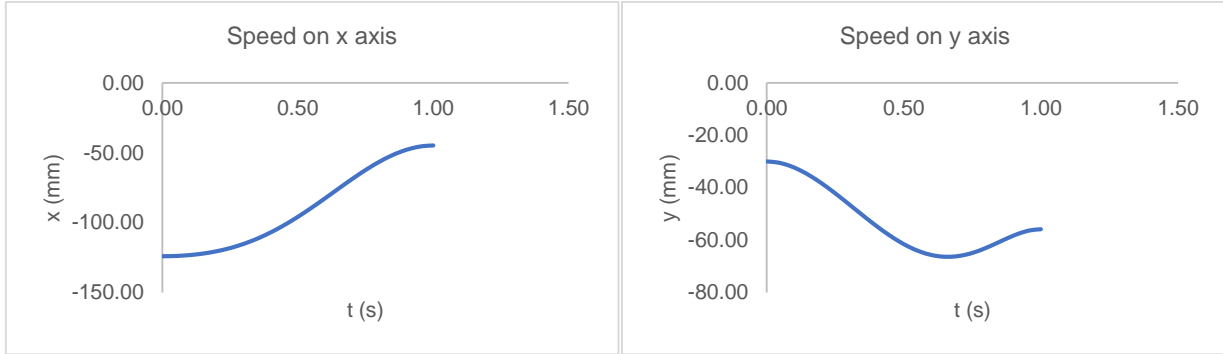


Figure 77: Speed of the index finger in the x (left) and y (right) axis.

$$\tan \alpha = \frac{\Delta y}{\Delta x} = \frac{y_f - y_0}{x_f - x_0}$$

$$\alpha = \tan^{-1} \left(\frac{\Delta y}{\Delta x} \right)$$

$$|\Delta \alpha| = |\alpha_f - \alpha_0|$$

$$|\Delta \alpha| = |38.71 - 161.72| = 123^\circ$$

The result of the virtual simulation can be used a prediction to find the angular velocity of flexion-extension of the finger using the Actuonix linear servo with the 63:1 gear ratio at maximum speed without external loads applied. Once known the angle travelled the angular velocity is directly known as:

$$\omega = \frac{|\Delta \alpha|}{t}$$

$$\omega = \frac{123^\circ}{1 \text{ s}} = 123 \frac{\circ}{\text{s}}$$

The angular velocity of the thumb is directly 600 °/s the rotation speed of the rotary servo motor extracted from the datasheet.

Mechanical static study

FINGER STATIC STUDY

The main objective with this study is to find which function set the relationship between the weight applied in one finger in the extended position, and predict the maximum load that the linear servo Actuonix PQ12R can hold in this extreme position. The system is solved as a machine system where the forces applied can generate bending moment in the segments [47]. In this study I have considered the weight of the phalanges as negligible because the masses of the phalanges range between 1-5 grams and that is 3 orders of magnitude under the actuator force. The six nodes have been considered as follows (A, B, C, D, E, F) and the load applied W. The dimensions of the finger have been extracted from the drawings of the finger assembly (Figure 78).

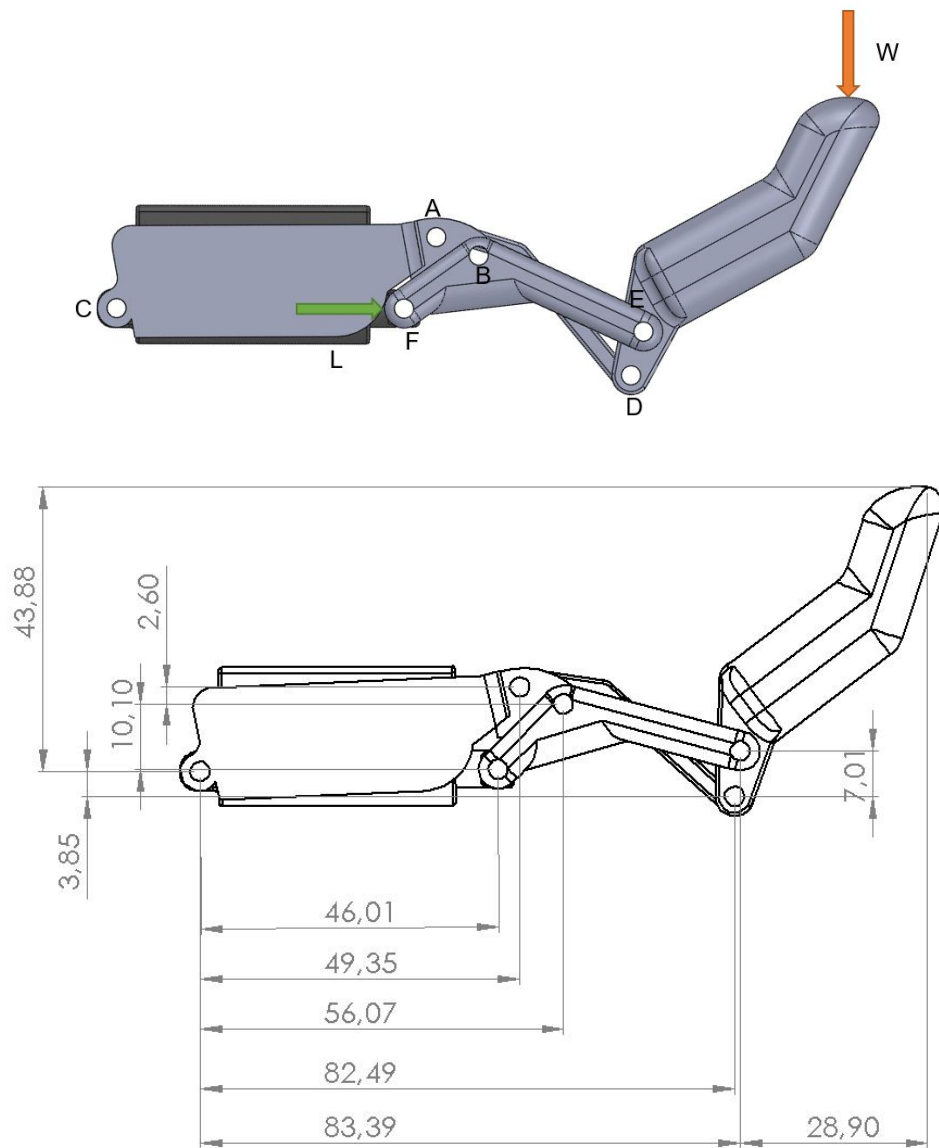


Figure 78: The finger forces diagram with the nodes from A to F and the external load applied W (above). The distances x and y between the nodes (below).

Free solid diagram

In this system there are four elements actuated by the linear servo which apply the internal forces of the system and an external weight applied on the most remote part of the finger system and generating torque, here the linear actuator is considered as a rigid body (Figure 79):

- Base (C-A-B)
- Proximal Phalanx (B-F-E)
- Distal Phalanx (E-D)
- Union (A-D)
- Linear actuator (C-F)

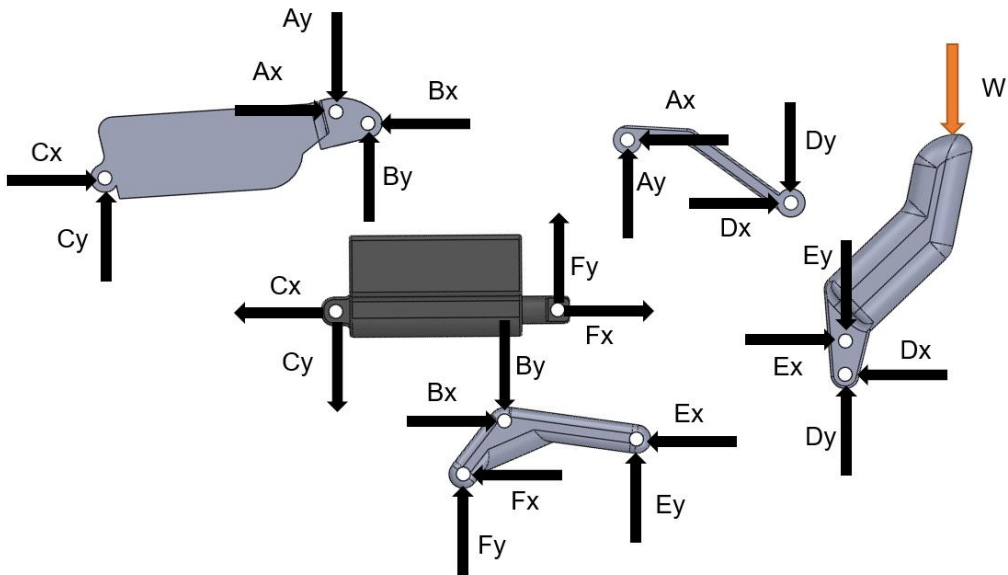


Figure 79: Reaction forces on the nodes in the initial hypothesis.

The general static conditions applied are:

$$\begin{array}{l}
 \sum F_x = 0 \\
 \sum F_y = 0 \\
 \sum M_z = 0
 \end{array}$$

For the base the equations are:

$$\sum F_x = 0 \Rightarrow C_x + A_x - B_x = 0$$

$$\sum F_y = 0 \Rightarrow B_y - A_y + C_y = 0$$

$$\sum M_c = 0 \Rightarrow -A_x \left(\frac{13.03}{1000} \right) - A_y \left(\frac{49.35}{1000} \right) + B_y \left(\frac{56.07}{1000} \right) + B_x \left(\frac{10.43}{1000} \right) = 0$$

For the Proximal Phalange the equations are:

$$\sum F_x = 0 \Rightarrow B_x - F_x - E_x = 0$$

$$\sum F_y = 0 \Rightarrow E_y - B_y + F_y = 0$$

$$\sum M_F = 0 \Rightarrow -B_x \left(\frac{10.10}{1000} \right) - B_y \left(\frac{10.07}{1000} \right) + E_y \left(\frac{37.39}{1000} \right) + E_x \left(\frac{2.83}{1000} \right) = 0$$

For the Distal Phalange the equations are:

$$\sum F_x = 0 \Rightarrow E_x - D_x = 0$$

$$\sum F_y = 0 \Rightarrow W + D_y - E_y = 0$$

$$\sum M_D = 0 \Rightarrow -E_x \left(\frac{7.01}{1000} \right) - E_y \left(\frac{0.90}{1000} \right) + W \left(\frac{29.80}{1000} \right) = 0$$

For the Union the equations are:

$$\sum F_x = 0 \Rightarrow D_x - A_x = 0$$

$$\sum F_y = 0 \Rightarrow A_y - D_y = 0$$

$$\sum M_A = 0 \Rightarrow D_x \left(\frac{16.89}{1000} \right) - D_y \left(\frac{33.14}{1000} \right) = 0$$

Results

The problem has been solved using a Matlab script created for this purpose. The scrip solves the system of equations inside a for loop increasing the applied load in every iteration, after that, the polyfit function is used to approximate the function (Appendix D1). The result can be seen in Figure 80.

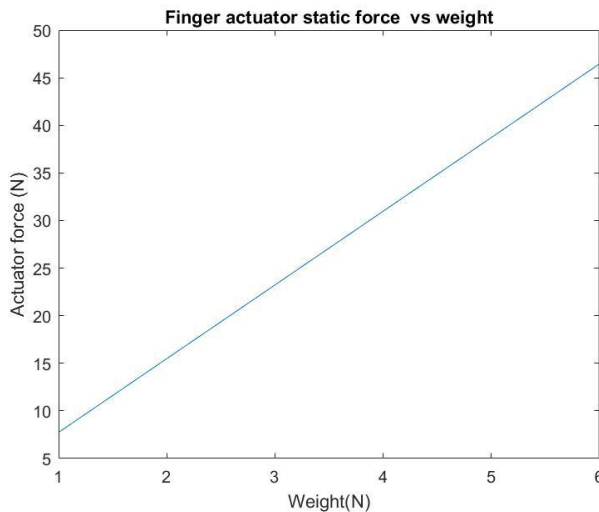


Figure 80: Finger equation weight vs actuator force.

The equation extracted from the polyfit command is:

$$F_{actuator} = 7.74 * W [N]$$

By the datasheet specifications, the maximum force that the actuator can lift is 45 N, this data can be used to predict the maximum lift that the linear servo is capable to hold with the finger in the extended position:

$$W = \frac{F_{maxactuator}}{7.74} [N]$$

$$W = \frac{45}{7.74} = 5.81 N$$

The reaction forces in the nodes for $W = 5.81 N$ are:

$$Ax = 23.22 N$$

$$Dx = 23.22 N$$

$$Ay = 11.83 N$$

$$Dy = 11.83 N$$

$$Bx = 69.68 N$$

$$Ex = 23.22 N$$

$$By = 2.85 N$$

$$Ey = 17.83 N$$

$$Cx = 46.47 N$$

$$Fx = 46.47 N$$

$$Cy = 8.98 N$$

$$Fy = -14.98 N$$

This values have been used to increase the material in the nodes where the reaction forces are higher. And the maximum value of W is the used to predict the maximum fingertip force of each finger.

THUMB STATIC STUDY

The procedure with the thumb was the same as previous with the finger. Figure 81 shows the forces diagram and the dimensions needed to solve the problem.

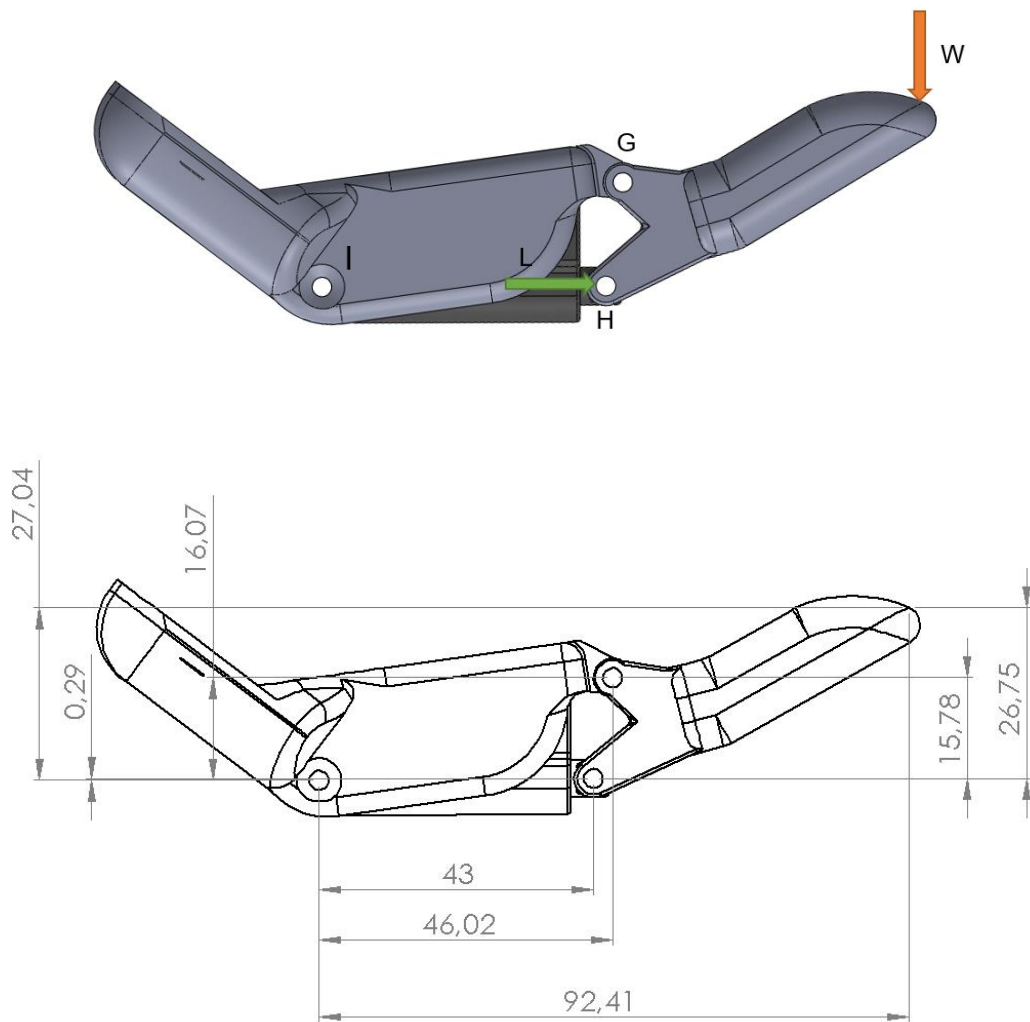


Figure 81: The thumb forces diagram with the nodes from G to I and the external load applied W(above). The distances x and y between the nodes (below).

Free solid diagram

For the thumb, the different segments are shown in Figure 82:

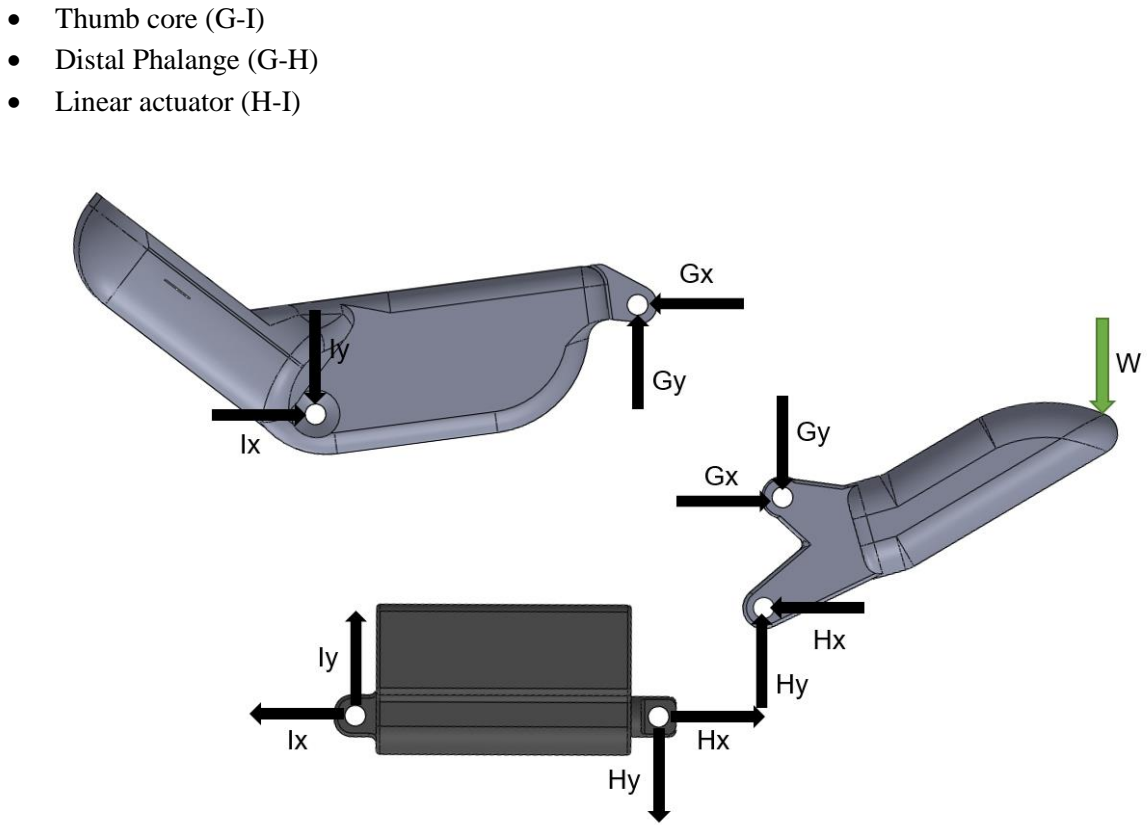


Figure 82: Reaction forces on the nodes in the initial hypothesis.

Again the general static conditions applied are the same:

$$\begin{array}{l} \sum F_x = 0 \\ \sum F_y = 0 \\ \sum M_z = 0 \end{array}$$

For the thumb core the equations are:

$$\begin{aligned} \sum F_x &= 0 \Rightarrow I_x + G_x = 0 \\ \sum F_y &= 0 \Rightarrow G_y - I_y = 0 \\ \sum M_I &= 0 \Rightarrow G_y \left(\frac{46.2}{1000} \right) + G_x \left(\frac{16.07}{1000} \right) = 0 \end{aligned}$$

For the distal phalanx the equations are:

$$\begin{aligned}\sum F_x &= 0 \Rightarrow G_x - H_x = 0 \\ \sum F_y &= 0 \Rightarrow H_y - G_y + W = 0 \\ \sum M_H &= 0 \Rightarrow -G_y \left(\frac{3.02}{1000} \right) - G_x \left(\frac{15.78}{1000} \right) + W \left(\frac{46.39}{1000} \right) = 0\end{aligned}$$

Results

The problem has been solved adapting the previous Matlab script (Appendix D2). The results are shown in Figure 83.

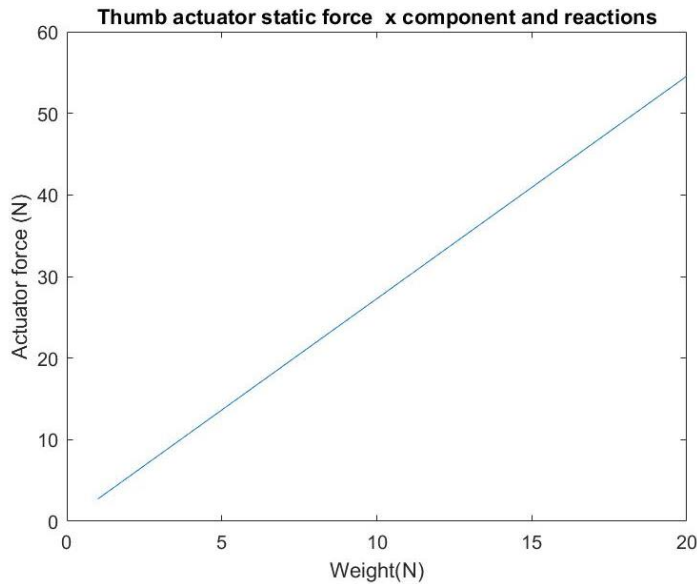


Figure 83: Thumb actuator fingertip force.

The equation extracted from the polyfit command is:

$$F_{actuator} = 2.73 * W [N]$$

With this result we can conclude that the maximum weight that the system can lift in this extreme position is 16.49 N and the reaction forces in the nodes can be predicted.

$$W = \frac{F_{maxactuator}}{2.73} [N]$$

$$W = \frac{45}{2.73} = 16.49 N$$

$$Gx = 46.38 N$$

$$Hy = -16.22 N$$

$$Gy = 0.78 N$$

$$Ix = 46.38 N$$

$$Hx = 46.38 N$$

$$Iy = 0.78$$

Stress study

THE FINITE ELEMENT METHOD

The aim of this study is to use the Finite Element Method (FEM) as a way to improve the geometry of the design reducing the concentration of stress points using fillets with higher radius or adding new ones, for example. The segments of the fingers are defined as an isotropic and homogeneous material. The 3D printed parts cannot be conceived in this definition, so the following results of the study are not able to predict the loads that would cause deformation or fracture in our real fingers. However, it is very useful to improve the geometry of the design in the way to make it capable to resist higher efforts. The software used for the FEM analysis is the package of simulations of Solidworks [46]. The thumb model for the study was simplified in order to study the stresses on the distal joint, where there is less material.

MATERIAL MECHANICAL PROPERTIES

The material used for the simulation is a custom material created in the software that has the properties of the regular Poly Lactic Acid (PLA) as a generic 3D printable polymer and this have been found at the technical datasheet of Ultimaker [48] but for the goal of this study, the material is the least important fact because it is focused in the geometry.

Elastic modulus: $E = 2.34 \text{ GPa}$

Yield strength: $\sigma_y = 37 \text{ Mpa}$

Poisson's Ratio: $\nu = 0.36$

Density: $\rho = 1240 \frac{\text{kg}}{\text{m}^3}$

STRONG FORM

Our main unknowns are the displacements:

$$u = u(x, y, z, t)$$

The equilibrium general equation is the following one, were the acceleration of force, depends on time:

$$\rho b + \nabla \cdot \sigma = \rho \frac{\partial u^2}{\partial t^2}$$

The problem can be simplified considering the final displacements without the mass of the bodies where the force is applied:

$$-\nabla \cdot \sigma = 0$$

BOUNDARY CONDITIONS

In the mechanical FEM stress problem, the boundary conditions relative to the function which is the displacement are the Dirichlet boundary conditions and force boundary conditions, relative to the derivative of the function are the accelerations or forces applied. The Dirichlet boundary conditions in the present systems are fixtures in the base of each finger type and the Neumann boundary conditions are the loads applied in the distal phalanges and homogeneous Neuman boundary conditions in the other domains (Figure 84).

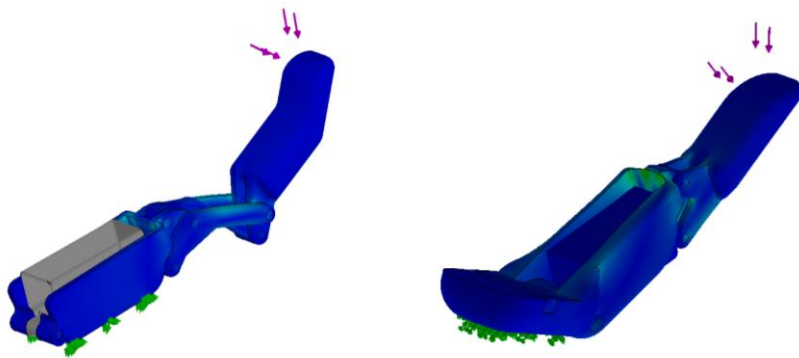


Figure 84: Boundary conditions applied in both systems.

LOAD-STRESS RELATIONSHIP STUDY

In this virtual experiment the external load applied to the distal phalanx has been increased from 10 N to 50 N in order to find the linear equation for each finger that describes the von Mises maximum stress (Figures 85 and 86).

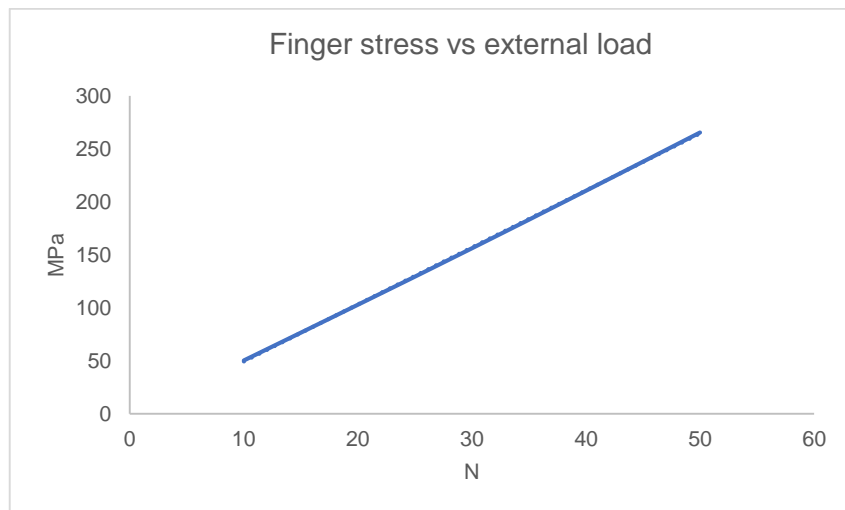


Figure 85: Finger function of von Mises stresses under applied load.

The stress-force equation resultant from the Finger study:

$$\sigma_{\text{von Mises(max)}} = 5.38F - 4.34 \text{ [MPa]}$$

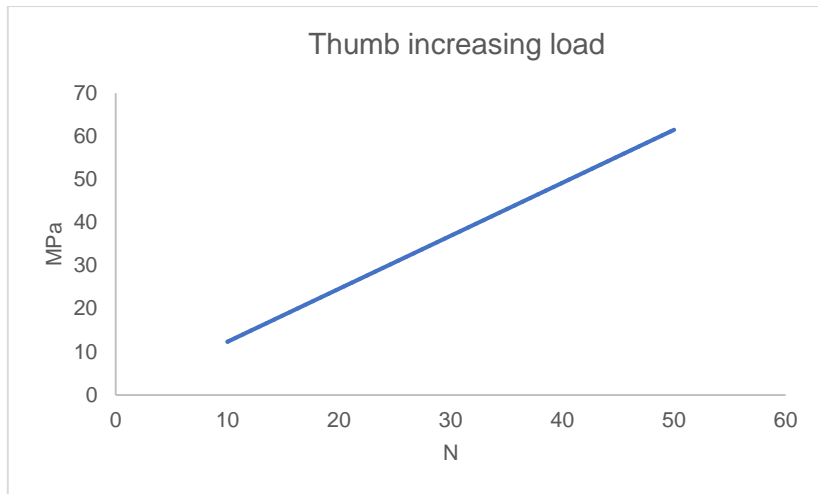


Figure 86: Thumb function of von Mises stresses under applied load.

The stress-force equation resultant from the Thumb study:

$$\sigma_{\text{von Mises}(\text{max})} = 1.23F \text{ [MPa]}$$

CONVERGENCE STUDY

Otherwise in the convergence study the number of nodes has been increased five times from approximately, from 10000 nodes to 100000 nodes (Figure 87) to see if the von Mises stress maximum value converges. That is a way to verify that there is no concentration stress point in the design. The mesh used has been the standard one without any refinement.



Figure 87: Finger (above) and thumb (below) initial and final mesh.

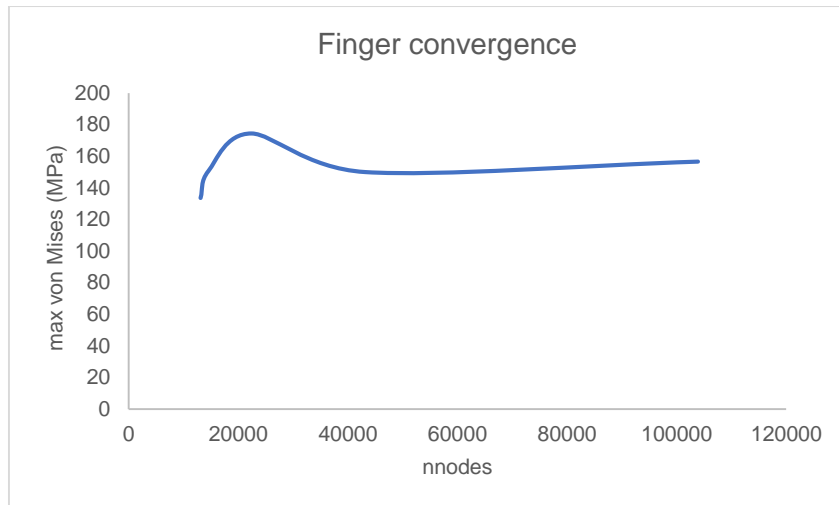


Figure 88: Finger convergence maximum value of von Mises stress increasing the number of nodes.

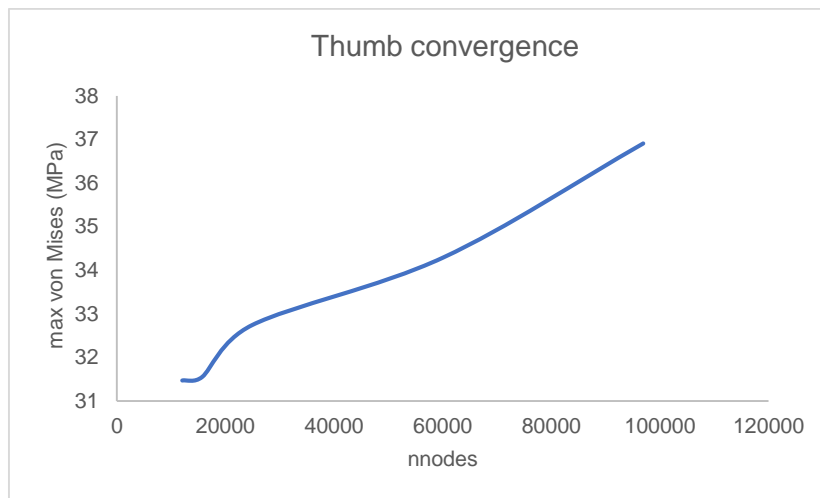


Figure 89: Thumb increasing value of von Mises stress maximum value while increase the number of nodes.

The results have been used in the design process to increase the fillets in the places where we have been found a stress concentration point non previously seen. The finger convergence can be seen in the Figure 88. In the case of the Thumb this stress concentration point has been found in the thumb core node 47818, the one of the two joints with the thumb distal phalanx, and then the fillets have been improved in this part (Figure 89).

Validation

GRIP TYPE TEST

After the assembly of the first prototype, the grasp type test has been performed catching different objects that are representative for each type of grip. For the precision grasps the lateral grasp have been showed catching a coin, the palmar grasp a pen and the tip grasp a piece of paper. For the power types a handle for the hook grasp, a tennis ball for the spherical and a bottle for the cylindrical have been the objects taken (Figure 90). This is one of the most important goals of this 6 DOF bionic hand in the way to be able to perform the most important activities of daily living.

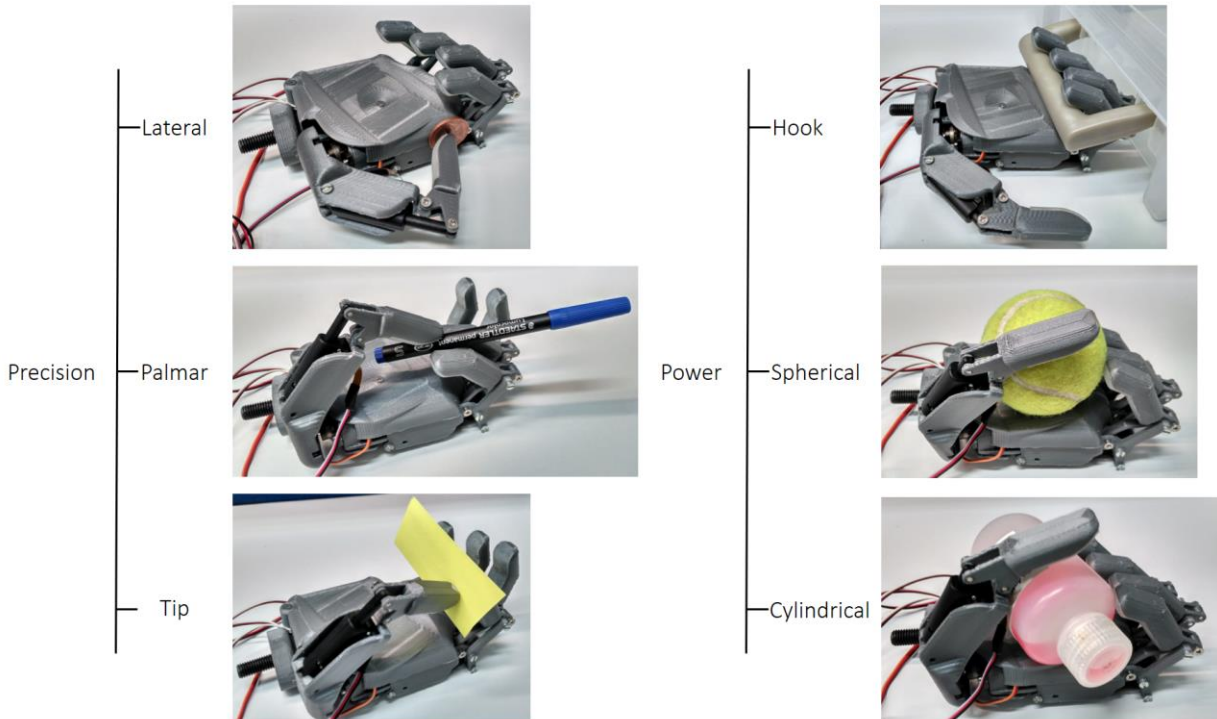


Figure 90: Different types of grasps validated.

REAL TESTS WITH LIMBLESS SUBJECTS

During the process of validation, the hands of the project have been tested with limbless subjects to see if the firmware and the hardware are functional and useful and if that can be improved, how these changes can be done. All the information collected in these trials have been used to improve the design of the last Grasp model (Figure 91).

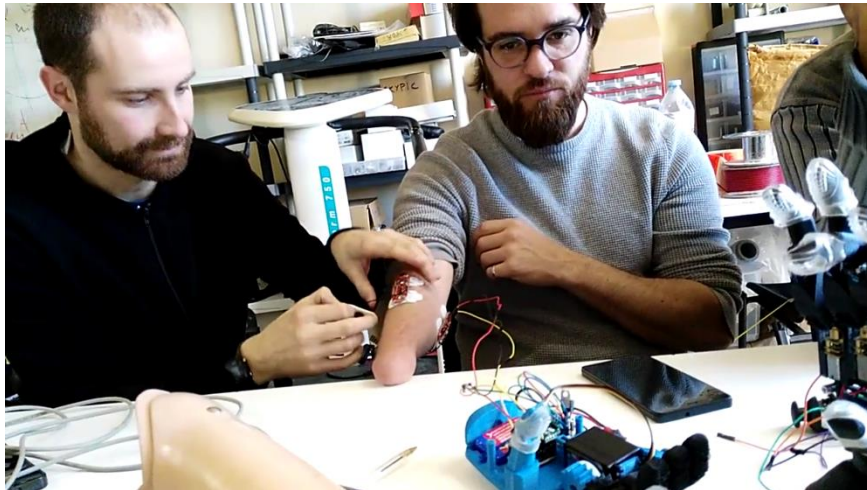


Figure 91: Myoware electrode skin placement.

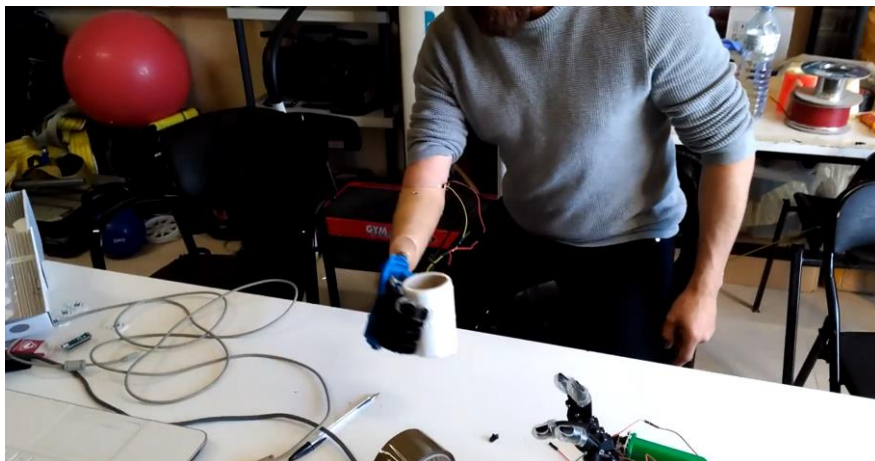


Figure 92: Myoelectric control of the prosthetic device using an old socket.

An important knowledge learned during this tests is applied on the control algorithm are the necessary force to bend the fingers because if it is too high, the subject will soon develop fatigue (Figure 92). Other facts like for example, the placement of the electrodes on the skin of an amputee that can change a lot between different subjects. And the experience of using different hands to catch different objects.

FINGERTIP FORCE EXPERIMENTAL DATA

With the aim to find the real fingertip force values of both types of fingers an experiment has been taken using a single model of each finger and the circuit using a resistive force sensor. The sensor used for this experiment is the FSR 402 (13mm circle x 56 mm) from the manufacturer Interlink Electronics [49] (Figure 93).



Figure 93: FSR 402 sensor [49].

As can be seen in the schematic, the Resistor used in the setup is a $10\text{k}\Omega$ for the voltage divider (Figure 94).

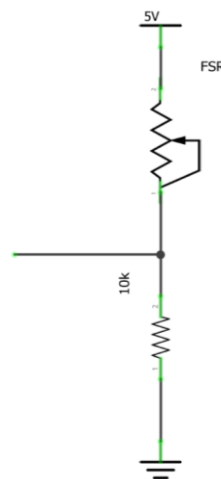


Figure 94: The voltage divider circuit.

The first step in the experiment procedure is to calibrate the sensor's curve by applying different force values (Figure 95) and record the analog inputs observed in the serial monitor of the Arduino Uno using a data rate of 9600 baud/s.

Another important step is to consider the resolution of the Arduino nano analog inputs with a maximum resolution of 10 bits for a maximum operating voltage of 5V that means 5V for 1024 (0-1023) levels of the analog to digital converted signal.

$$Resolution = \frac{5V}{2^n - 1} [\text{V}/\text{bit}]$$

$$Resolution = \frac{5V}{1023} = 4,89 \cdot 10^{-3} \frac{\text{V}}{\text{level}}$$

With the resolution the value of the output voltage of the force resistive sensor can be obtained in the range between 0 and 5V:

$$V_{out} = 4,89 \cdot 10^{-3} \frac{\text{V}}{\text{level}} \cdot N \text{ levels}$$

The results of the experiment can be seen on the Table (Appendix F).

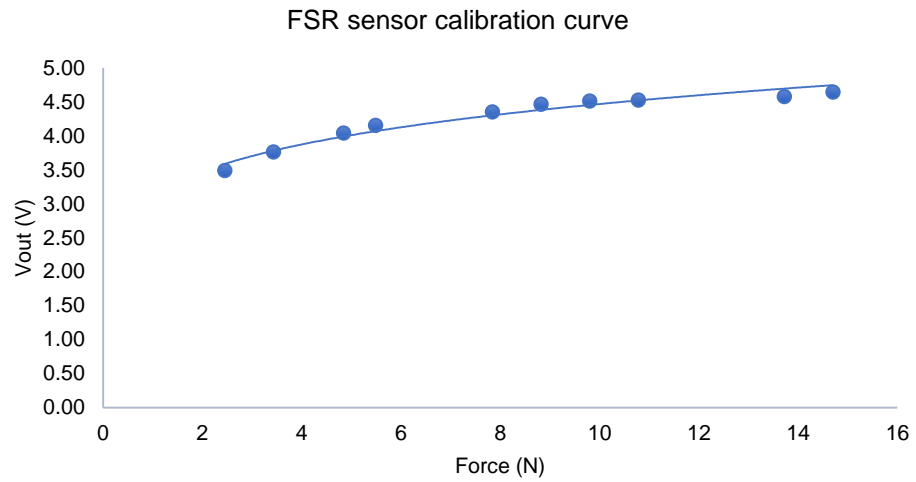


Figure 95: Sensor calibration curve.

The experimental procedure starts with the setup of the circuit to measure the force applied over the force sensor by the finger. Also a multimeter is used to measure the current output of the power supply and the potentiometer is used to control the movement of the finger and the force applied, the schematics are designed using the Frizzing software [50] (Figures 96 and 97).

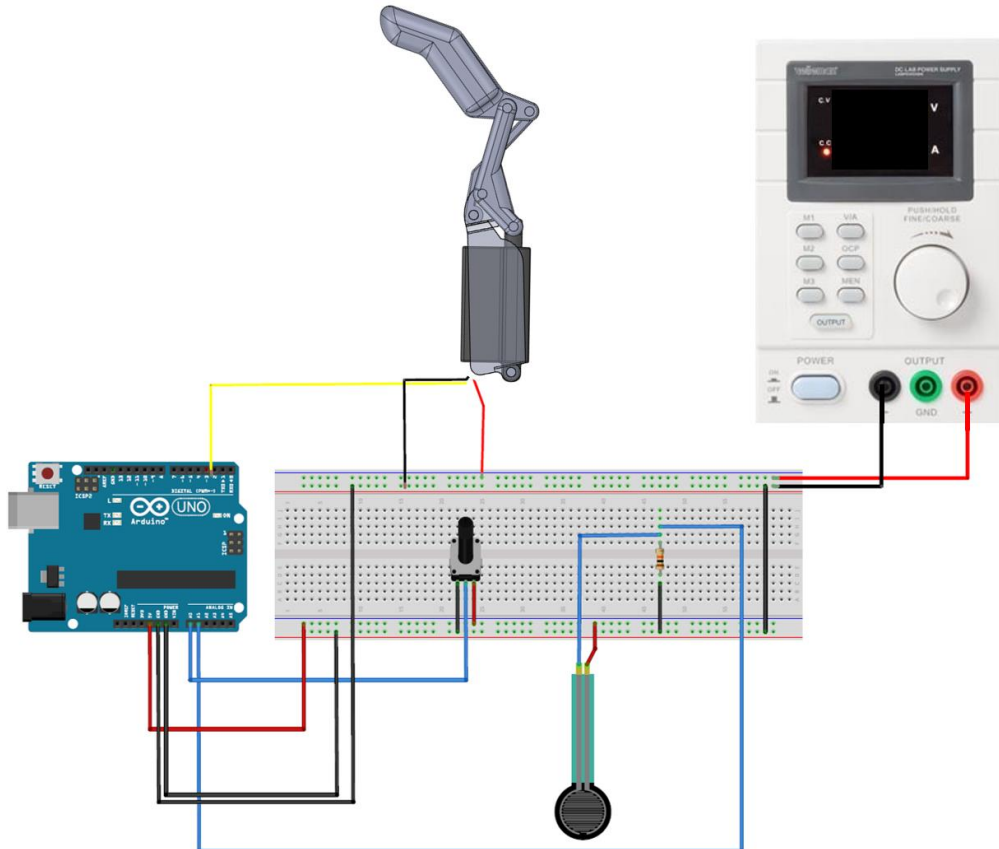


Figure 96: Breadboard schematic of the fingertip force experiment setup.

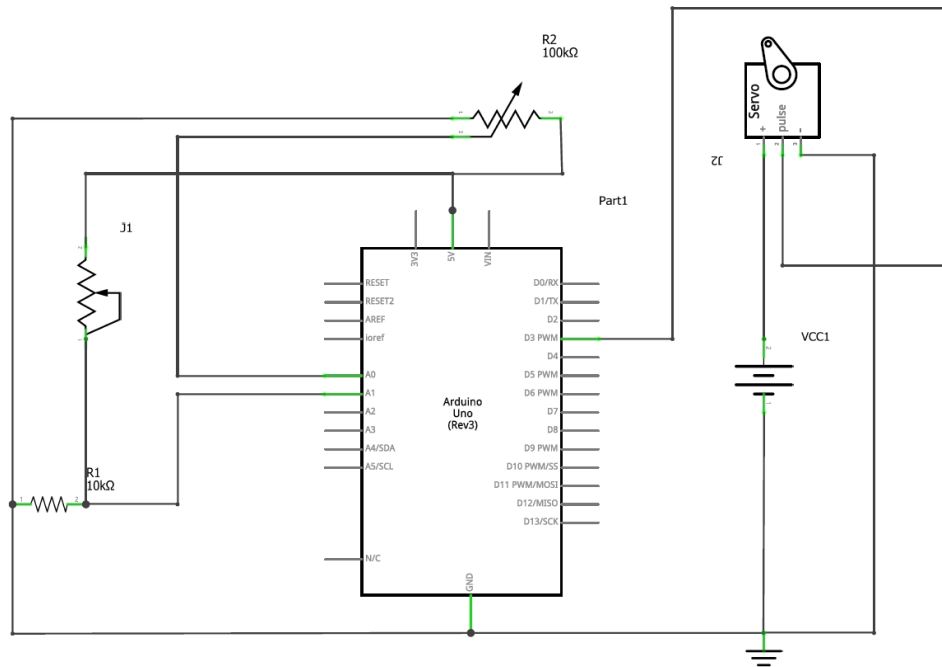


Figure 97: Schematic of the fingertip force experiment setup.

Setup for the experiment (Figure 98):

- Power supply at 6V.
- Multimeter to measure the output current of the power supply and motor consumption.
- FSR sensor Analog output to the A1 (Arduino analog input) using a $10\text{k}\Omega$ for the constant value of the voltage divider.
- Potentiometer signal to A0 (Arduino analog input)
- The potentiometer and the FSR sensor to 5V of the Arduino.
- The motor is connected to the 6 V of the power supply.
- The Arduino Nano is connected to the

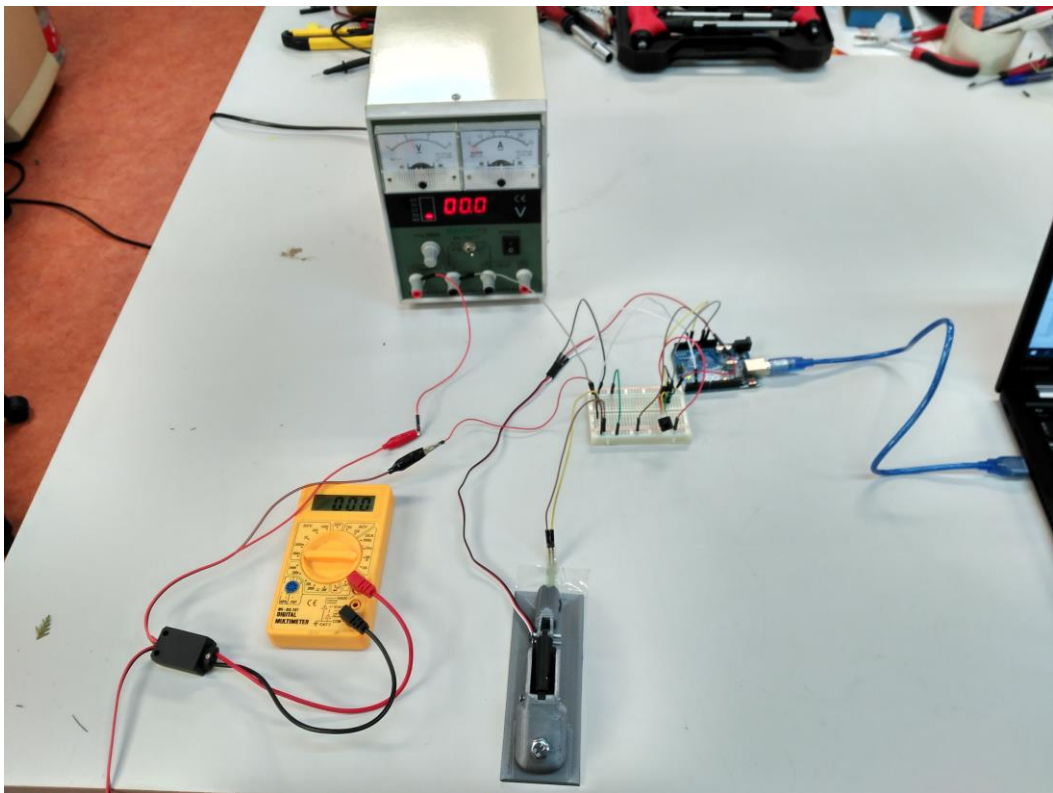


Figure 98: Experimental setup.

Two benches have been designed to hold the finger and the thumb models in an isometric position. This setup can be used to measure the stall force of the motor in the extended position of the finger (Figure 99).

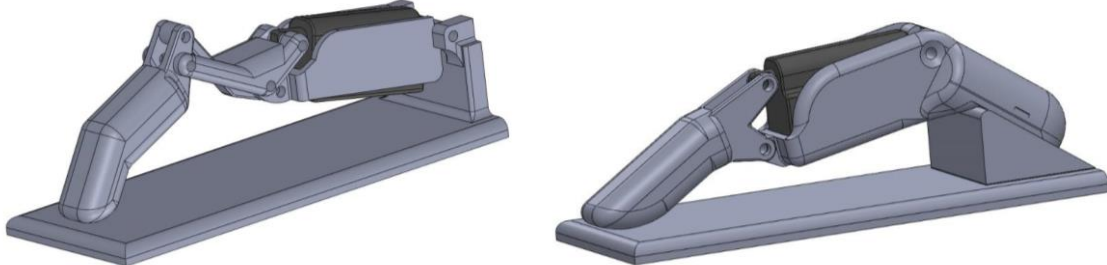


Figure 99: Finger and Thumb CAD benches models respectively.

The result after holding the two assemblies in the benches is the presented in Figure 100.

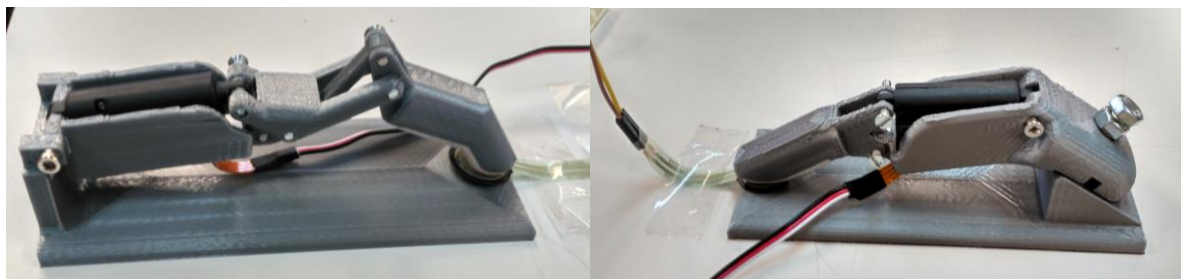


Figure 100: Finger and Thumb assembled in their respective benches.

The movement of the finger and the thumb is applied using a potentiometer which send the value of its position to the microcontroller and this one send this value to the linear servo motor. Once the equation is obtained, the value of the Force (N) must be obtained isolating the function variable:

$$V = 3.12F^{0.156} [V]$$

$$F = \left(\frac{V}{3.12}\right)^{\frac{1}{0.156}} [N]$$

The experiment has been done acquiring 5 independent samples of each fingers and the mean and the standard deviation are obtained using the following expressions:

$$\bar{F} = \sum_{k=1}^N F_k [N]$$

$$s(F) = \sqrt{\frac{1}{N-1} \sum_{k=1}^n (F_k - \bar{F})} [N]$$

For the finger model the experimental values obtained are (Appendix G):

$$\bar{F} = 6.82 N$$

$$s(F) = 0.14 N$$

For the thumb model the experimental values obtained are (Appendix H):

$$\bar{F} = 14.50 N$$

$$s(F) = 0.21 N$$

In conclusion, the values for the fingertip force are:

$$F_{thumb} = 14.50 \pm 0.21 N$$

$$F_{finger} = 6.82 \pm 0.14 N$$

FINGER FLEXION-EXTENSION SPEED

The flexion-extension speed of the finger and the opposition-retroposition speed of the thumb are important experimental data to compare the performance of the Grasp bionic hand with the best in the market, for this reason the experiment to find this values have been done using video analysis techniques with the open source software Kinovea [51] and tracking the finger and thumb trajectories in the movement of each finger against the gravity. Three trials for each finger have been analysed by following the path of one pixel and exporting the data in xls file. The full angle of the trajectory has been measured using the measuring angle tool and then finding the first and last frame when there are no changes in space position and the initial and final time values. The angular velocity is using the common expression:

$$\omega = \frac{\theta}{t} \text{ [}^{\circ} \cdot s^{-1}\text{]}$$

In order to avoid movements of the hand, it has been fixed by the M10 screw of the wrist and for that reason the fingers are isolated from any contact with other bodies (Figure 101).

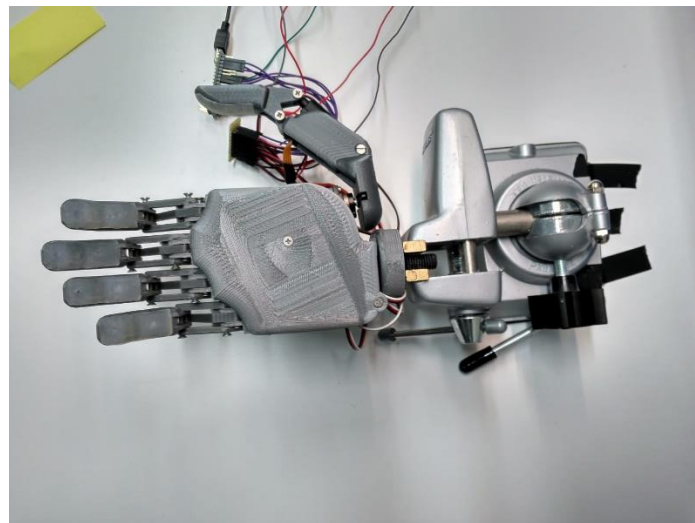


Figure 101: Experimental setup.



Figure 102: Opposition trajectory and angle.

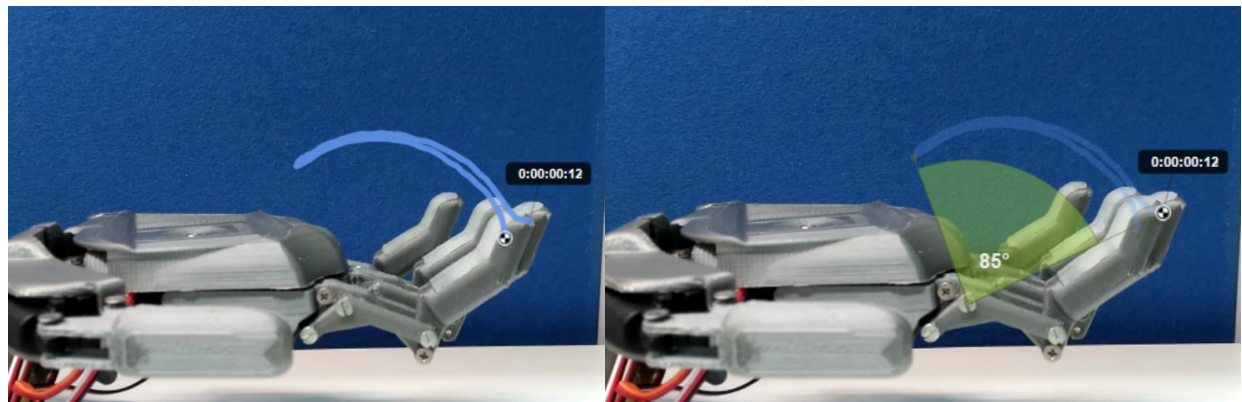


Figure 103: Flexion trajectory and angle.

The results obtained from the experimental data (Figures 102 and 103) can be found in the table of the Appendix O. And the values of the two angular velocities are:

$$\omega_{finger} = 72 \pm 16 \text{ } {}^{\circ} \cdot s^{-1}$$

$$\omega_{thumb} = 196 \pm 60 \text{ } {}^{\circ} \cdot s^{-1}$$

MAXIMUM RESISTANCE EXPERIMENTAL DATA

One model of each type of finger have been printed to perform a destructive test until fracture applying an increasing load, the materials used in this trials for the two types of fingers is (Figure 104):

- Dynamometer Colemeter WH-C300.
 - o Weight limit is 300 Kg / 600 LBS, accuracy will up to 100 g, minimum weight measure is 0.2 kg.
- Plastic chain
- Weight to fix the chain on the ground.
- Chain tensor.
- Clamp
- Flange

The 3D printed parts have been printed using the following settings:

- 3D printer: BQ Hepstero 2 [37].
- Material PLA 3D850 [36].
- Wall thickness: 1.2 mm.
- Filling percentage: 20 %.
- Filling pattern: Lines.



Figure 104: Experimental setup for the destructive essay.

In the experiment, the load has been increased by screwing the chain tensor until fracture (Figure 106).



Figure 105: Finger (left) and thumb (right) positioning.

First of all, the dynamometer is weighted to obtain the offset weight, this is 368 g.

- For the finger model the maximum experimental fracture force is 19.30 N.
- For the thumb model the maximum experimental fracture force is 107.60 N.

This test ideally should be performed more than once in order to give a statistic value because is a stochastic process but, being a destructive essay, it has been performed once during this project. The results of any of this tests are highly dependent on the filling pattern and density, for that reason the toughness of the hand can be increased using different patterns and the maximum density.



Figure 106: Fracture of the finger model.

Control

EMG MORPHOLOGY OF DIFERENT TYPES OF GRASPS

The initial approach was to find different patterns in the EMG signal and study the morphologic differences between different types of grips and use cross correlation or other signal processing techniques to compare between the signals recorded previously as a pattern and the real time recorded. Arduino Nano was used for a recording with Matlab using the scripts and functions (Appendices I, J adapted from [52] and K).

The result of this experiment was interesting, huge differences between the EMG signals from power, palm and tripod grasps but no significantly different values for the precision grasps (Figure 107). For that reason, this method was discarded. Also the differences of signal morphology if there is a disease, and the fact that the muscles of an amputee are not used to trained to be contracted.

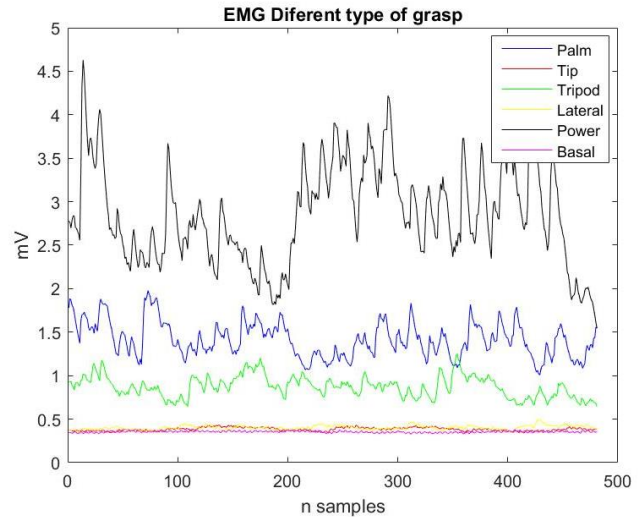


Figure 107: Amplitude of the different types of grasps.



Figure 108: Flexion contraction muscles of the hand send the EMG signal to the microcontroller.

For an automatic control is necessary a previous training and the aim of this project is to provide an easy tool to be used without training easily configured by the user or someone without experience.

The current solution is to use one EMG sensor, to send the signal of the flexor muscles of the forearm as an analog signal to the Arduino AO analog input in order to control the flexion movement of the bionic hand (Figure 108). Also the change between types of grasps is changed using a pushbutton which select one type or the other inside a switch structure in the main program.

The type of control that have been used starts with the research of a calibration function, the first step is to generate this function with a common analog input signal that actuates in the whole range of 0 to 5 volts and then see the singularities of the EMG signal and adapt this function at that particular case.

ANALOG SENSOR INPUT – LINEAR SERVO OUTPUT SYSTEM CALIBRATION

The calibration starts with a single finger control process, in this first step, a potentiometer (Figure 110) has been used to generate an analog input signal from 0 to 5 volts and find the function that connect this two ranges, the input signal range from 0 to 1023 which is the voltage converted in to a 10 bit variable and the output that is a range defined inside the servo.write() Arduino [19] function in the case of the finger that range is from 38 to 145 degrees (Figure 109).

The equations for the linear and rotary servos are described in the Figure 111.

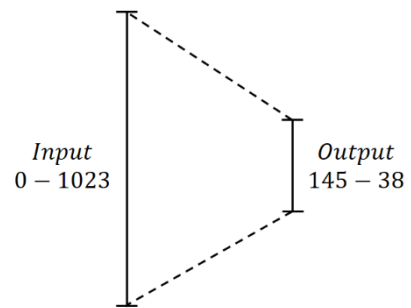


Figure 109: Two different ranges in the input and the output signals.

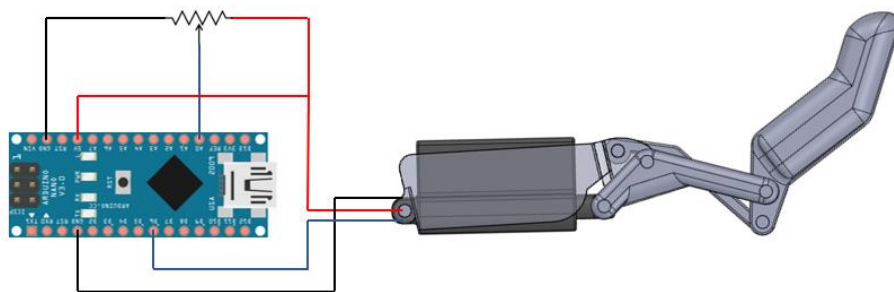


Figure 110: PQ12R linear servo calibration schematic with a 10KΩ resistor.

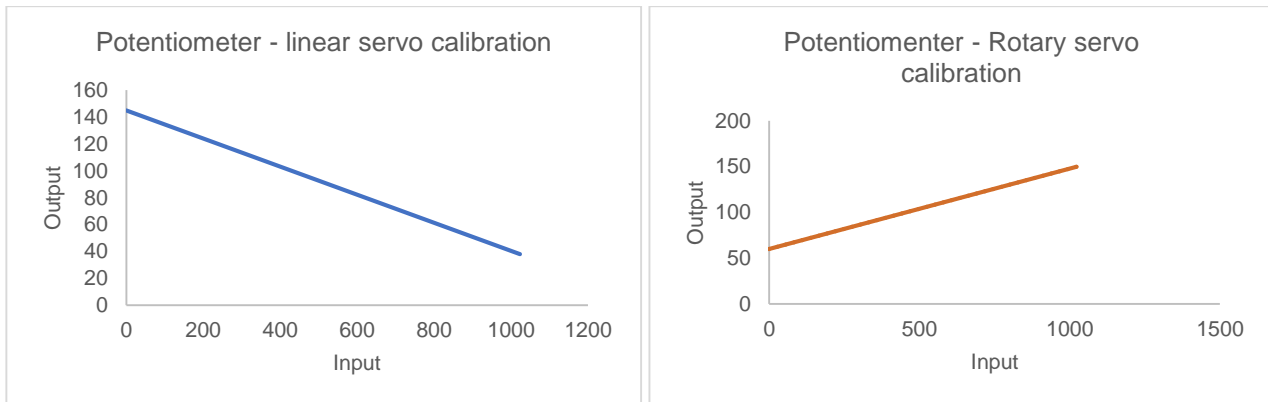


Figure 111: PQ12R linear servo and MG90S rotary servo calibration equations for the potentiometer range.

$$y_{potentiometer_linear\ servo} = -0,1046x + 145$$

$$y_{potentiometer_rotary\ servo} = 0,088x + 60$$

EMG ANALOG SENSOR CALIBRATION

In the case of using an EMG sensor (Figure 112) the maximum value amplified by the signal conditioning circuit will change from one subject to other, so the maximum value of 1023 for a 5V input will change to other random value between different subjects (max_subject). For that reason, the two steps previously described must be generalized as follows:

$$EMG3 = \frac{38 - 145}{\text{max_subject} - 0} \cdot EMG2 + 145$$

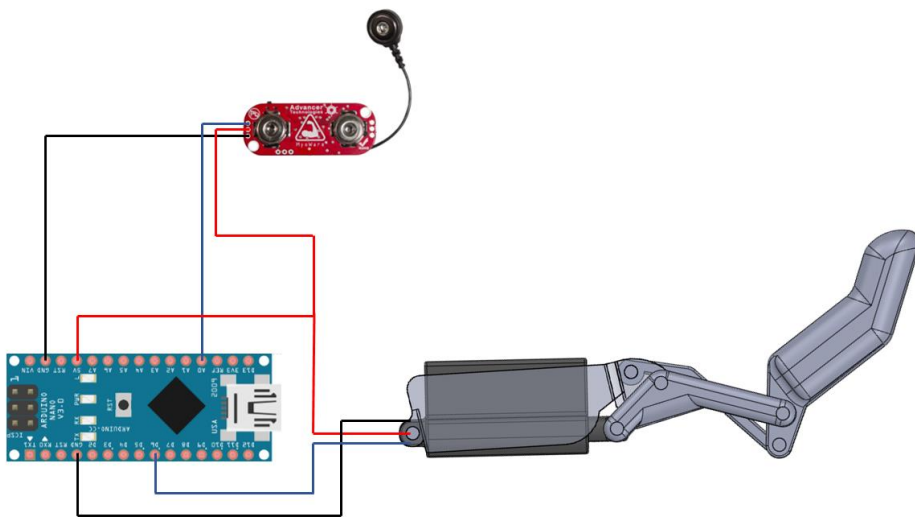
$$EMG_{Flexion} = \frac{-107}{\text{max_subject}} \cdot EMG2 + 145$$

And the same for the opposition movement:

$$EMG_{Opposition} = \frac{150 - 60}{\text{max_subject} - 0} \cdot EMG2 + 60$$

$$EMG_{Opposition} = \frac{90}{\text{max_subject}} \cdot EMG2 + 60$$

Using these two equations a linear proportional control can be made. As can be seen in the electronics design and components chapters, there is a push button, once the control over the different types of grasps is achieved the push button makes the hand able to change from one type of grasp to the other. A Switch based structure let the user change across the tip, tripod, palm, hook, spherical or cylindrical grasp. The different types of grasps are defined in functions outside of the main loop program.



FUNCTIONS OF THE MAIN PROGRAM

The main loop function has an initial conditional structure to change from type of grip if the pushbutton is pressed and then the EMG calibration linear function is used to set the input and output ranges and each case of the switch structure send the parameters of degrees of rotation to the actuators (Figure 113).

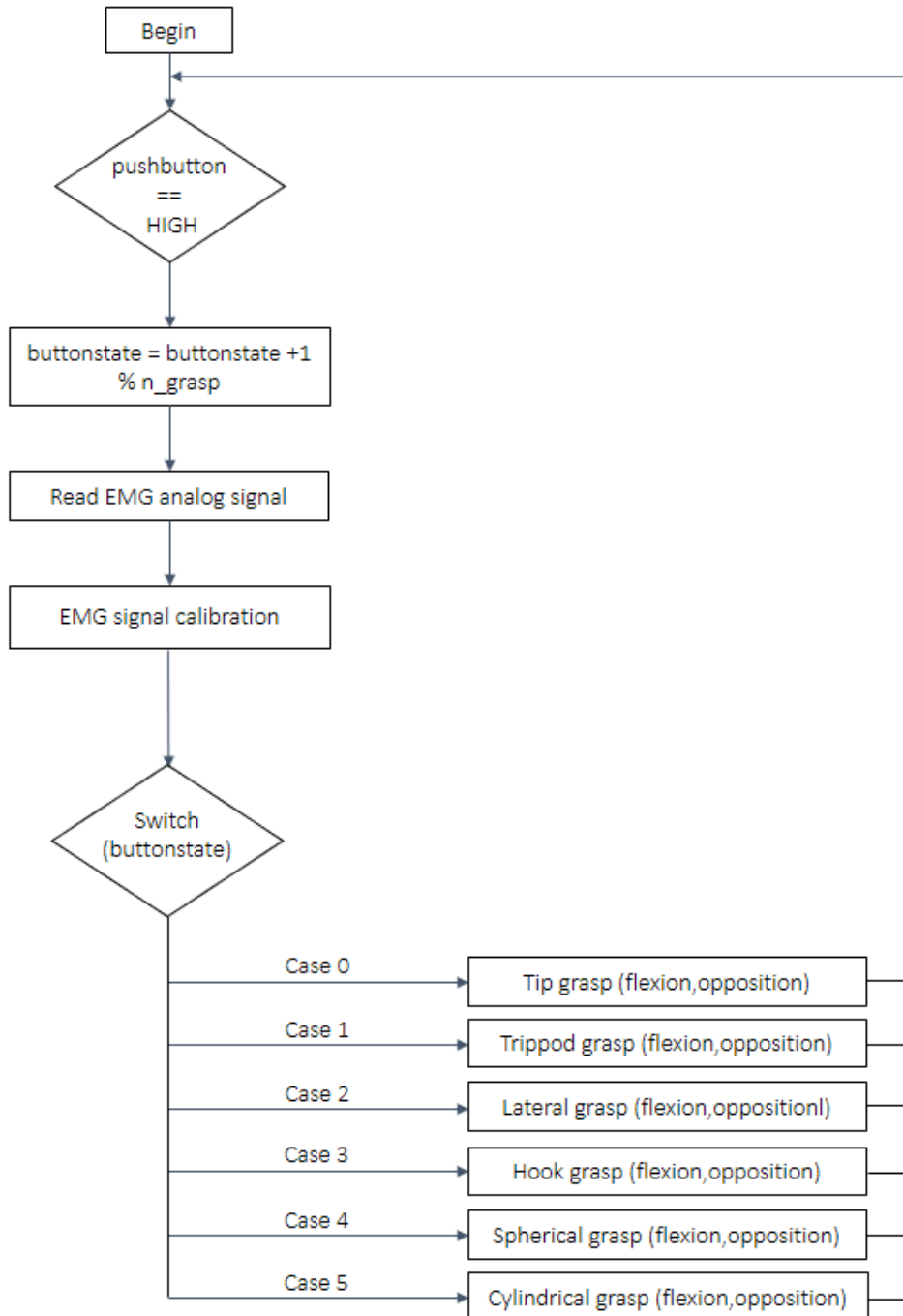


Figure 113: Main loop function of the Grasp hand.

The values recorded for the EMG input sensor and calibrated using the calibration equations are sent to the type of grasp function selected by the user through the pushbutton. The type of grasp function use the Arduino servo library function [19] servo.write() to send to the actuators the position coming from the EMG sensors as can be seen in the Figure 114. The result of all this process is a final control test with EMG signal and the assembled hand (Figure 115).

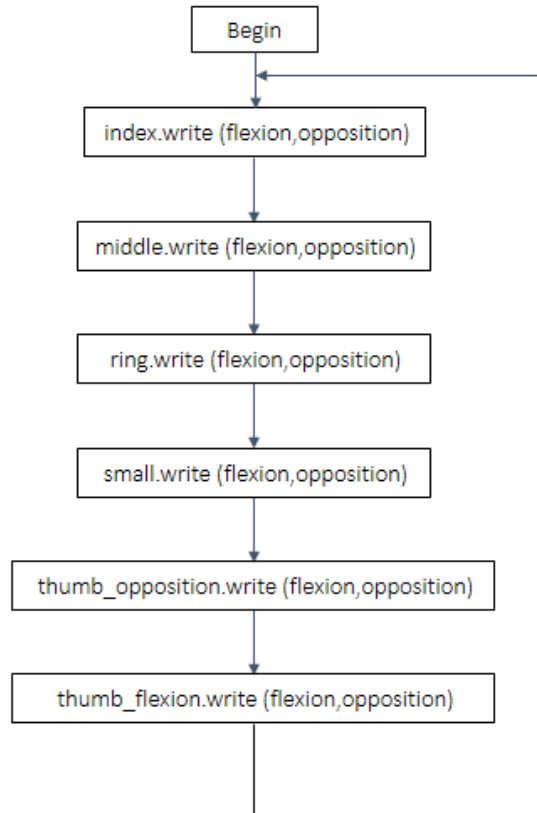


Figure 114: Grasp type function structure.

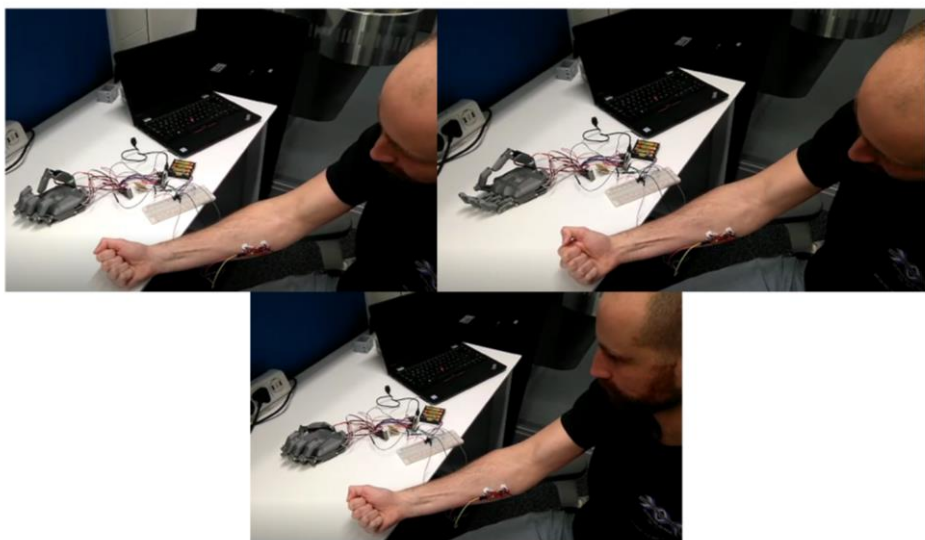


Figure 115: Grasp EMG calibration test changing the type of grip with the pushbutton and controlling the flexion-extension movement of the fingers with the EMG linear function.

Graphical user interface

GRAPHICAL USER INTERFACE

The last step of the project is the creation of a graphical user interface (GUI) to facilitate the configuration of the maximum EMG signal value. The application has been designed to be able to communicate with the Arduino board, once the user selects a window of time for the EMG recording introducing the time (Figure 116), the “EMG signal” button is pressed, the function starts recording and the graph window starts showing the analog input where the EMG sensor is connected during the time introduced by the user (Figure 117).

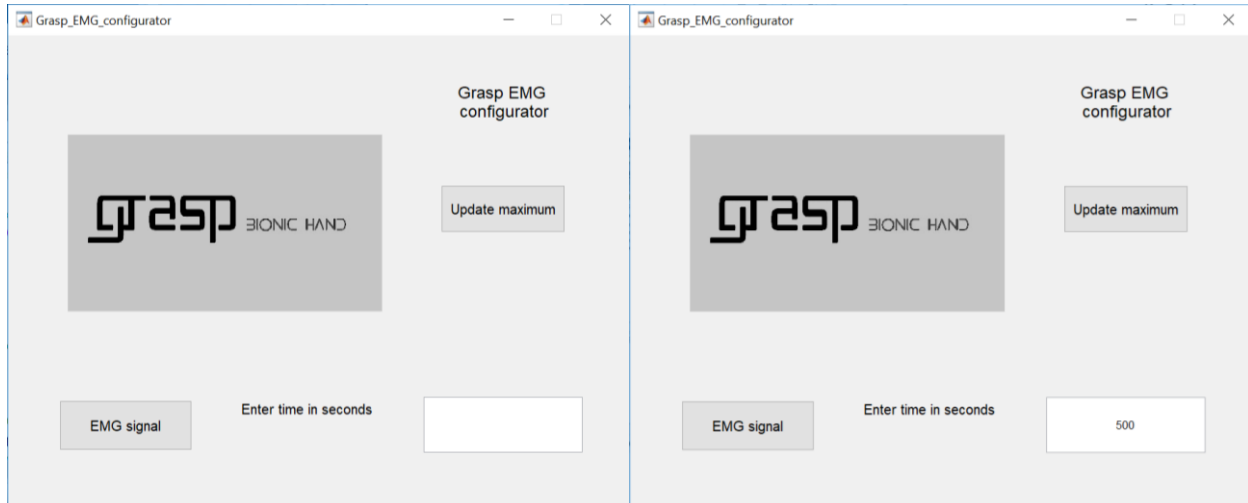


Figure 116: Step one (left) first appearance of the GUI and step two, the value of time is introduced by the user (right).

Once the “EMG signal” button is clicked, the Grasp bionic hand logo disappears and the plot starts showing the EMG signal. During the recording, the user can make several forearm’s muscles contraction-relaxation cycles depending on the chosen time.

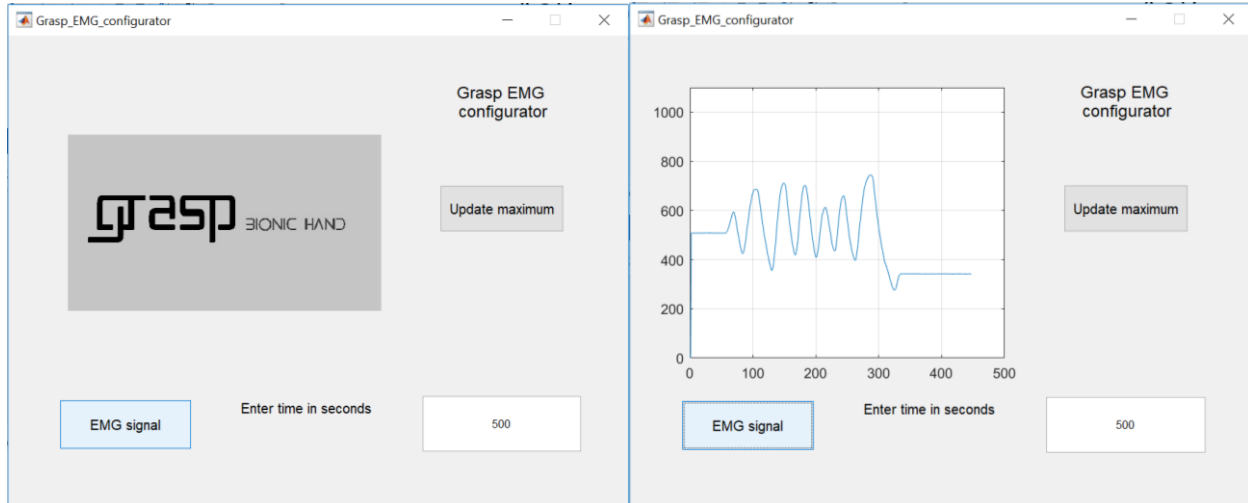


Figure 117: The “EMG signal button is pressed” (left) and the plot starts showing the values of the signal (right).

In the end of the recording window the user can press the button “Update maximum” and the static text below the button will show the maximum EMG value between 0 and 1023 values that has been registered on the analog input (Figure 118).

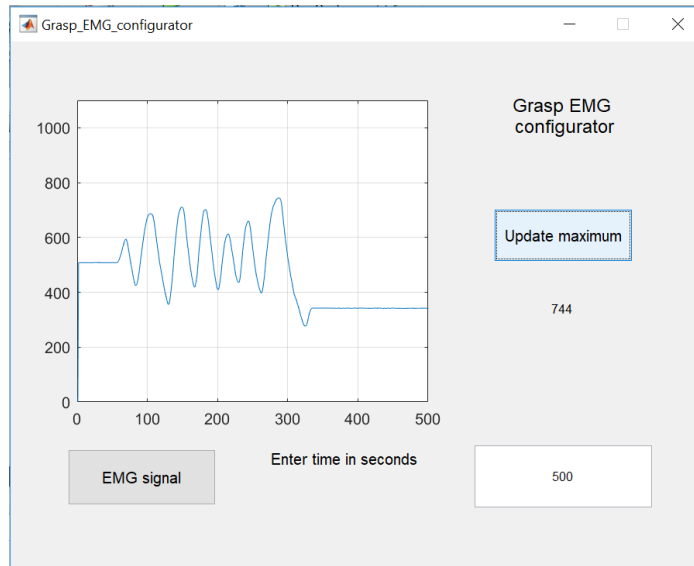


Figure 118: The “Update maximum” button is pressed and the static text shows the maximum value of the EMG signal recorded.

The graphic user interface has been created using the Matlab GUI toolbox. First of all, the figure has been created, a file with the extension fig. is the frame where the widgets are placed: buttons, plots, sliders, etc. The components used in this interface are: the graph plot, the button, the static text and the dynamic text. An example of the figure editor can be seen in the Appendix Q.

Regulatory framework

DEVICE CLASSIFICATION ACCORDING TO THE DIRECTIVE

In the current state of development, the hand is only recommended for Research, robotics or educational purposes. Following the Annex VIII of the Directive 2017/75 EU Grasp Bionic Hand would be classified as medical device under the essential concepts:

- Active device
- Long term device
- Non-implantable device

According to the rule 13, that include all active devices that are not devices intended to: therapeutic methods that administer or exchange energy, diagnosis devices and devices that administer or remove drugs and any substance to or from the body, our medical device is classified as Class I. The device does not either have measuring function. The conformity assessment procedure for a class I medical device without a measuring function can be followed in the Figure 119.

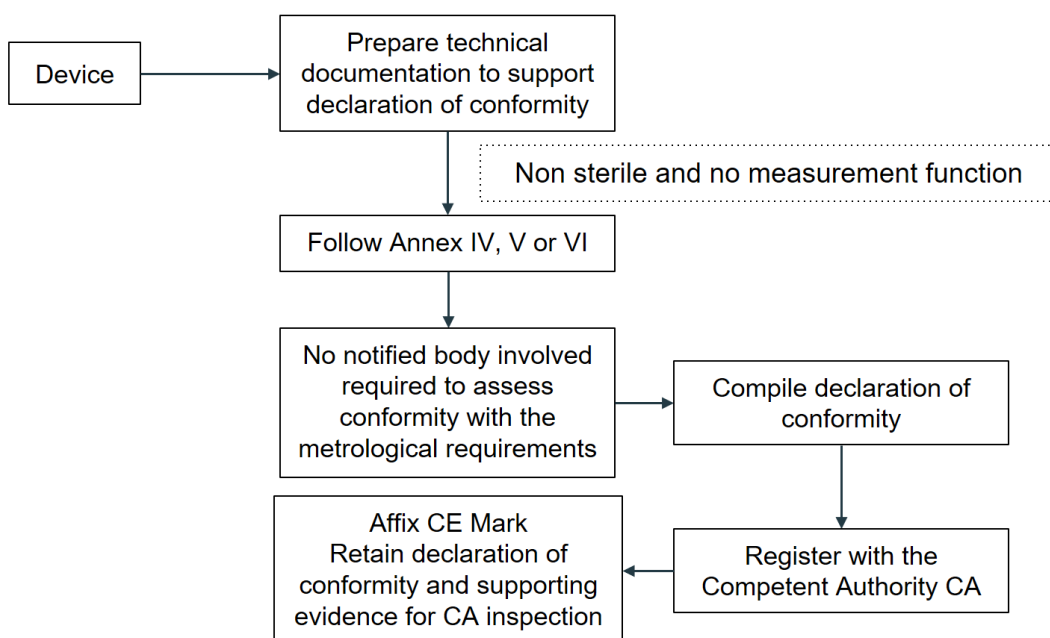


Figure 119: Conformity assessment procedure for a class I medical device.

DECLARATION OF CONFORMITY

The hand should be compliant with the Medical Devices EC Directive 2017/75 EU in the European regulatory framework. Grasp Bionic Hand should declare that they meet appropriate European standards for design, manufacture and supply of prosthetic products and user software. Would be mandatory a continued compliance with the standard is monitored by a programme of internal and external audits. The CE mark should be applied on packaging and the product should be accompanied with the declaration of conformity where Grasp Bionic Hand declares that conforms with:

- Directive 2011/65/EU on the restriction of the use of certain hazardous substances in electrical and electronic equipment.
- Directive 2017/75 EU on medical devices.

And also would be applicable the following standards in order to be compliant with the directives.

- EN 60601-1: Medical Electrical Equipment.
- EN 60601-1-2: Compliance against EMI/EMC.
- EN 60601-1-6: General requirements for basic safety and essential performance – Collateral standard: Usability.
- ISO 14971: Risk management for medical devices.

The list of symbols that should appear in the labelling of the medical device (Figure 120):

- CE mark: This mark indicates the product conforms with the essential requirements and provisions of Council Directive 2017/75 EU.
- Type B applied part: This mark indicates the product is a Class B medical electrical device.
- Refer to operating instructions: This mark indicates the user should read the operating instructions before use.
- Manufacturer (adjacent to company name): This mark indicates the manufacturer.
- Wheelie bin (WEEE) mark: This mark indicates that the product falls under the WEEE Directive (2012/19/EU).
- Protect from water: This symbol indicates the product should be protected from water.
- Temperature range: This symbol indicates the products temperature range.
- The recycling symbol for the mechanical parts of made of plastic.

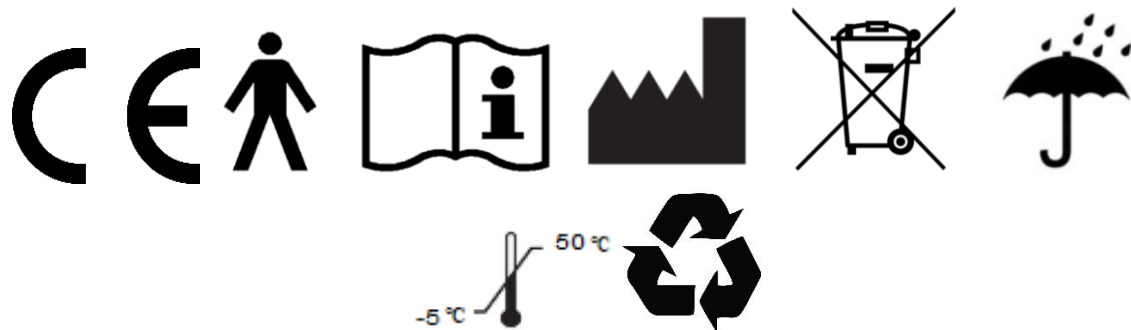


Figure 120: Symbols of the label organized in the order of the previous description from left to right [16].

Sustainability

ENVIRONMENTAL COST COMPARING 3D PRINTING AND MOLDING INJECTION

The scope of this chapter is to compare the traditional way of manufacturing (Table 29) with the option chosen for the present work taking into account that the 3D printed product is produced at home or closer than the other option (Table 30).

In order to make an approximation of the impact of producing one Grasp hand, some considerations have been taken using data extracted from different user's experience and the literature. The first consideration is that the hand can be produced by 3D printing in the user's house or in some proximity digital fabrication place (fab-cafe, fab-lab...) and the environmental cost of this transport is the cost of the transport in the same area.

The average of a desktop 3D printer energy consumption is set at 12.7 kWh/kg [53] and it is more than 1 order of magnitude under the injection molding which can be 1850 kWh/kg [46]. Otherwise, as a conclusion of the study of Song and Telenko [54], the 34% of the plastic is wasted during a 3D printing process.

Table 29: Environmental Impact of Mold injection in Asia.

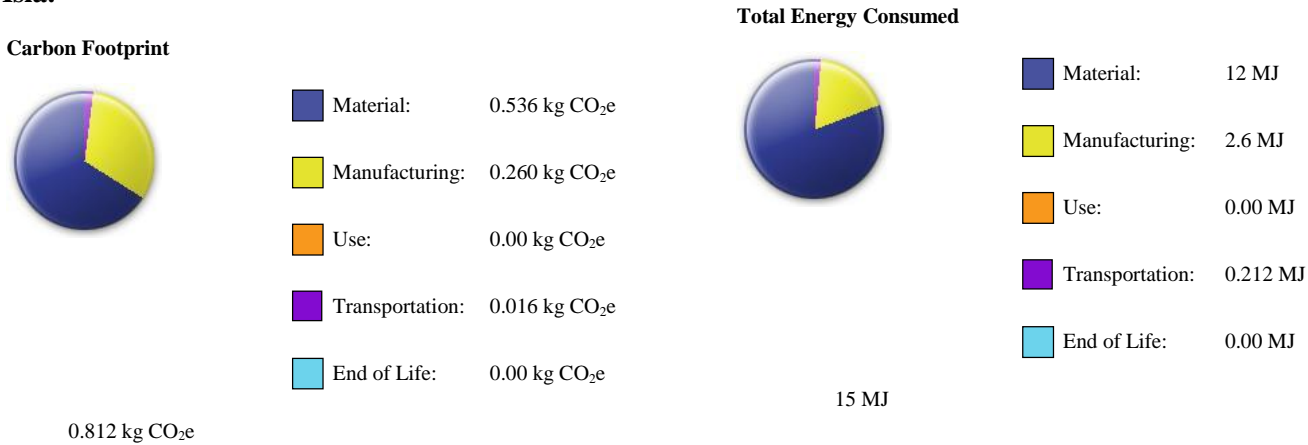
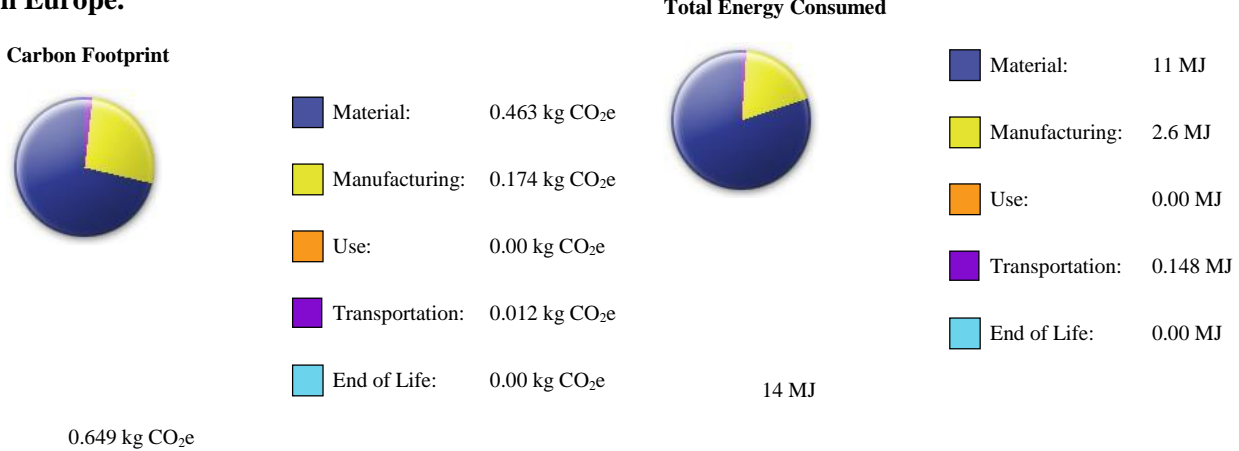


Table 30: Environmental Impact of 3D printing in Europe.



The energy required in the case of the 3D printing is 9.3% less than the molding injection and the Carbon footprint is 20% more for the molding injection. The selected type of medical ABS for the hand is 100% recyclable and the electronic board and electronic components can be recycled on the proper places. In the case of the PCB production, in both cases is an industrial procedure.

Budget

DEVICE CONSTRUCTION BUDGET

In the device construction budget are included the costs of all the components and 3D printable parts. The cost of each gram of ABS medical grade is 0.6 g approximately [55].

Table 31: 3D printed components budget.

Component	Unit cost (€)	Units	Total cost (€)
Finger proximal Phalanx	0.24	4	0.96
Finger distal phalanx	0.32	4	1.29
Thumb distal phalanx	0.24	1	0.24
Thumb core	0.88	1	0.88
Palm	3.46	1	3.46
Joint	0.08	4	0.32
Top cover	0.32	1	0.32
Bottom cover	0.24	1	0.24
Finger distal phalanx silicone cover	0.13	4	0.5
Thump phalanx silicone cover	0.28	1	0.28
Finger mold 1	0.28	1	0.28
Finger mold 2	0.28	1	0.28
Thumb mold 1	0.28	1	0.28
Thumb mold 2	0.28	1	0.28
TOTAL			9.61

Considering that there is an extra cost for the plastic needed to make the construction beds and it is 34% extra. The cost of the 3D printing increases up to **13.90 €**.

Table 32: Electric components budget.

Component	Unit cost (€)	Units	Total cost (€)
Linear Actuators Actuonix PQ12R	60	5	300
Micro servo motor MG90S	3.9	1	3.9
Arduino Nano	19.9	1	19.9
Pololu step down voltage regulator D24V25F6	10.15	1	10.15
Wires	0.5	1	0.5
Mioware / DFR robot muscle sensor	37.5	1	37.5
Battery charger	15.96	1	15.96
Battery 7.4 V Li-po	22	1	22
USB micro cable	2	1	2
PCB	6	1	6
TOTAL			417.91

Table 33: Other components budget.

Component	Unit cost (€)	Units	Total cost (€)
M3 screw cap	0.25	12	3
M3 screw cap	0.25	8	1
M4 screw	0.18	2	0.36
M2 screw	0.12	4	0.48
M10 screw cap	0.5	1	0.5
IP67 briefcase	37.5	1	37.5
		TOTAL	42.84

The total cost of the hand components is **474.65 €**.

ENERGY CONSUMPTION BUDGET

In terms of energy the electrical consumption of the production process with the 3D printer must be included in the final budget. To calculate the total mass needed for each part, each mass has been multiplied by 1.34 because the 34 % of the plastic in the FDM printer is used to create the supports [54]. In order to find the electrical energy, the constant applied was mentioned in the sustainability chapter, 0.0127 kWh/g.

Table 34: Energy consumption budget.

Component	Weight (g)	Quantity	Total mass (g)	Mass with wasted plastic (g)	Electrical energy (kWh)
Proximal Phalanx	3	4	12	16.08	0.20
Distal phalanx	4	4	16	21.44	0.27
Thumb distal phalanx	3	1	3	4.02	0.05
Thumb core	11	1	11	14.74	0.19
Palm	43	1	43	57.62	0.73
Joint	1	4	4	5.36	0.07
Top cover	4	1	4	5.36	0.07
Bottom cover	3	1	3	4.02	0.05
Mold 1	12	1	12	16.08	0.20
Mold 2	10	1	10	13.4	0.17
				TOTAL	2.01

Now the total energy cost can be calculated applying the constant value of the current price of the electricity, 0.11989 €/kWh [56] and the total energy cost will be 0.24 €. As has been done before, the extra cost of 34 % of energy to print the plastic must be included and it makes an increase to 2.70. So, the final cost of the hand in this conditions is 477.35 €.

Publications and divulgation

PUBLICATIONS

As how it has been started to say the present project has his own website, has been published in several Object libraries and social networks with the aim to be shared and accessible for any user in the world interested in using for any application. The website [57] was created to update information about the trajectory of the project and where are the files and information to build it (Figure 121). Also a Youtube channel is used to publish the videos and media on the social networks [58]. The hand has been published under a Creative Commons-Attribution-Non-Commercial license.

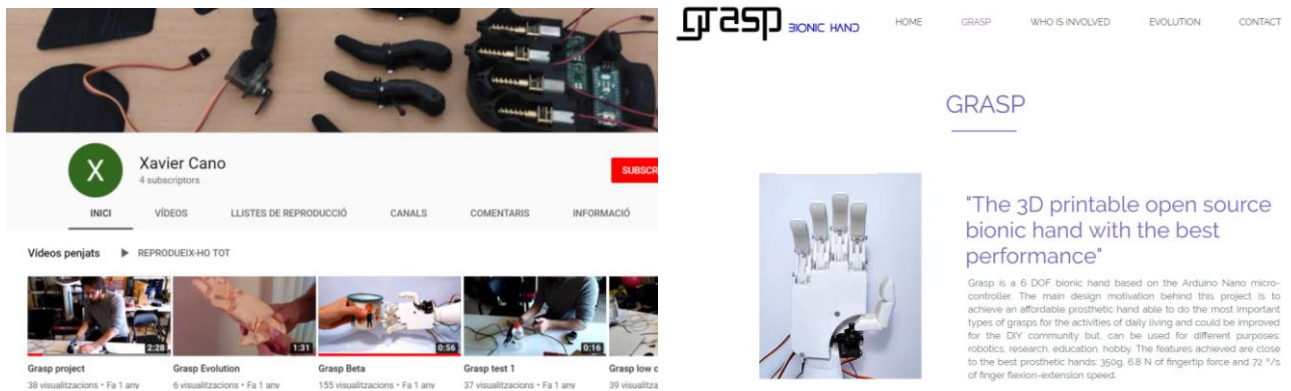


Figure 121: Image from the website [57] and Youtube channel.

Otherwise, the documentation and files that are necessary to build the hand are located in different object libraries when other open source projects are also sheared. All the designs mentioned previously in the evolution point of the present work are available at Thingiverse [59] and Hackaday [60] where all the files can be downloaded and the other elements of the bill of materials can be found as well (Figure 122). The most important open source projects all over the world are publish in these communities and this shared information creates an inspirational environment to keep improving and creating new projects related to each field. Nowadays the different Grasp designs downloads are more than 1000.

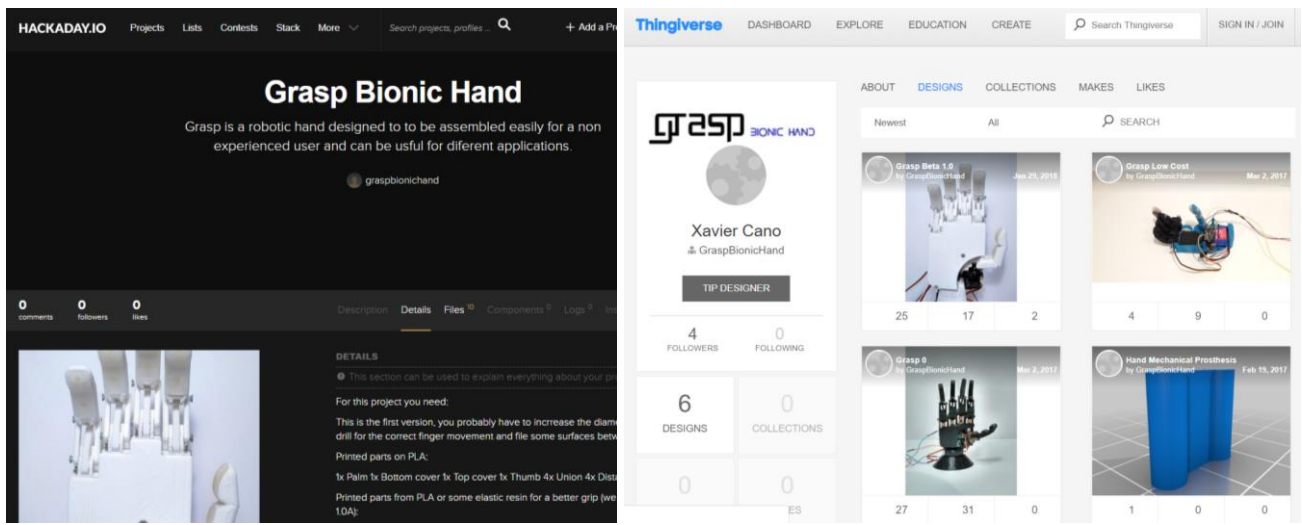


Figure 122: The project published in Hackaday [60] on the left and Thingiverse [59] on the right.

Assembly instructions

GRASP 1.0 ASSEMBLY INSTRUCTIONS

Introduction

This is a step by step guide to make the Grasp 1.0 from the Grasp Bionic Hand project. To be able to build the hand it is necessary to have the files downloaded from Thingiverse or Hackaday and acquire the bill of materials: screws, actuators, PCB circuit, sensors and the other electric components.

Downloading the files

The first thing to do is downloading the files in Thingiverse and Hackaday in any of the following links:

<https://www.thingiverse.com/GraspBionicHand/designs>

<https://hackaday.io/project/163935-grasp-bionic-hand>

Assembly steps

- 1- Printing and removing support material
- 2- Fingers assembly
- 3- Thumb assembly
- 4- Inserting the motors on the palm
- 5- Inserting the motor on the thumb
- 6- Fingers and palm assembly
- 7- Casting silicone in the molds
- 8- Gluing the silicone “skin” in the fingers
- 9- Mounting the electronics and electrical components in the palm
- 10- Electric connections
- 11- Assembling the covers
- 12- Connect the hand to your body
- 13- Grasp EMG configuration
- 14- Upload the firmware
- 15- Start exploring!

Tools

- 1- Micro USB cable
- 2- M3 Allen key
- 3- Little flat blade screwdriver
- 4- Phillips (star) screwdriver
- 5- Super glue

Bill of materials

- 1- 5 x Micro linear servos motor Actuonix PQ12R
- 2- 1 x Rotary servo motor Tower pro MG90S
- 3- 1 x Arduino/Genuino Nano
- 4- 2 x DFRobot OYMotion SKU:SEN0240 EMG analog sensor or Mioware EMG analog sensor
- 5- 1 x Pololu DV2425F6 Voltage regulator
- 6- 1 x Pololu Switch ON/OFF
- 7- 1 x Grasp PCB board (optional)
- 8- 1 x Tournigy Nano-tech 6000 mAh or other Li-po 7.4 V power supply
- 9- 1 x Li-po battery charger
- 10- 1 x DFRobot 0029-B Pushbutton module

- 11- 10 x M3 allen screws 10 mm long
- 12- 12 x M3 allen screw 16 mm long
- 13- 1 x M3 allen screw 20 mm long
- 14- 4 x M2 blade screw 8 mm long
- 15- 2 x M4 star screw
- 16- 1 x M10 allens screw 30 mm long
- 17- 1 x MG90S servo screw

3D printed parts

- 1- 4 x Finger distal phalanx
- 2- 4 x Finger proximal phalanx
- 3- 4 x Joint
- 4- 1 x Palm
- 5- 1 x Thumb core
- 6- 1 x Thumb distal phalanx
- 7- 1 x Top cover
- 8- 1 x Bottom cover
- 9- 1 x Finger grip mold
- 10- 1 x Thumb grip mold

1- Printing and removing support material

Once you have the downloaded files you can use any SLS or FDM printer to print the parts in PLA, ABS or resin. The project has been tested using an FDM machine and the dimensions of the holes can change with and SLS printer.

As an example the hand can be printed in a FDM printer (BQ Hepstero 2) using the following settings:

- Material: PLA 3D850.
- Wall thickness: 1.2 mm.
- Filling percentage: 20 %.
- Filling pattern: Lines.
- Printing temperature: 230 °C
- Printing speed: 60 mm/s

2- Fingers assembly

Two M3 Allen screws for each finger are needed to make the assembly of the finger distal phalanx, the joint and the finger proximal phalanx.

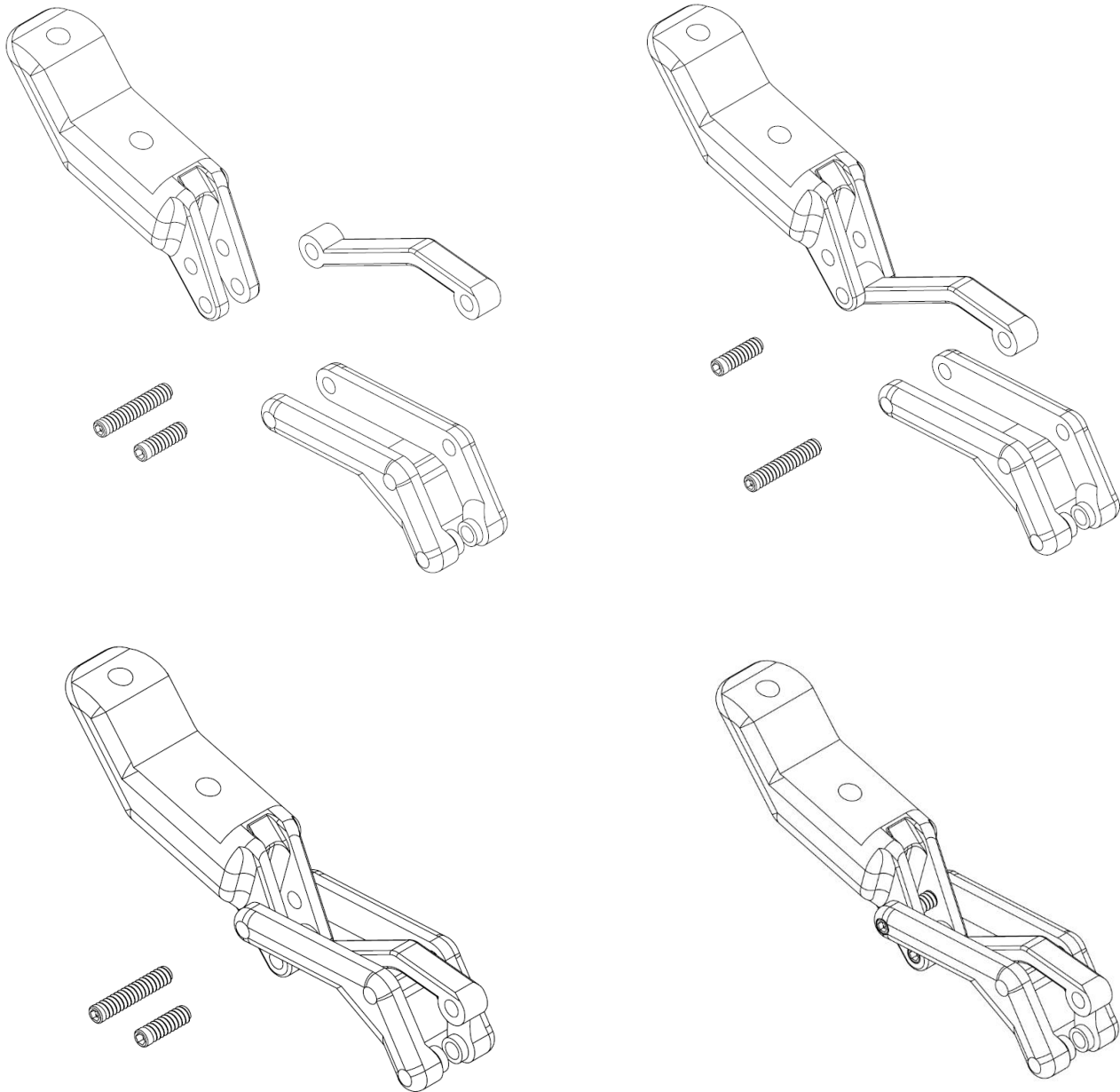


Figure 123: Regular finger assembly of four steps.

3- Thumb assembly

Use an M3 Allen screw for the joint between the thumb core and the thumb distal phalanx.

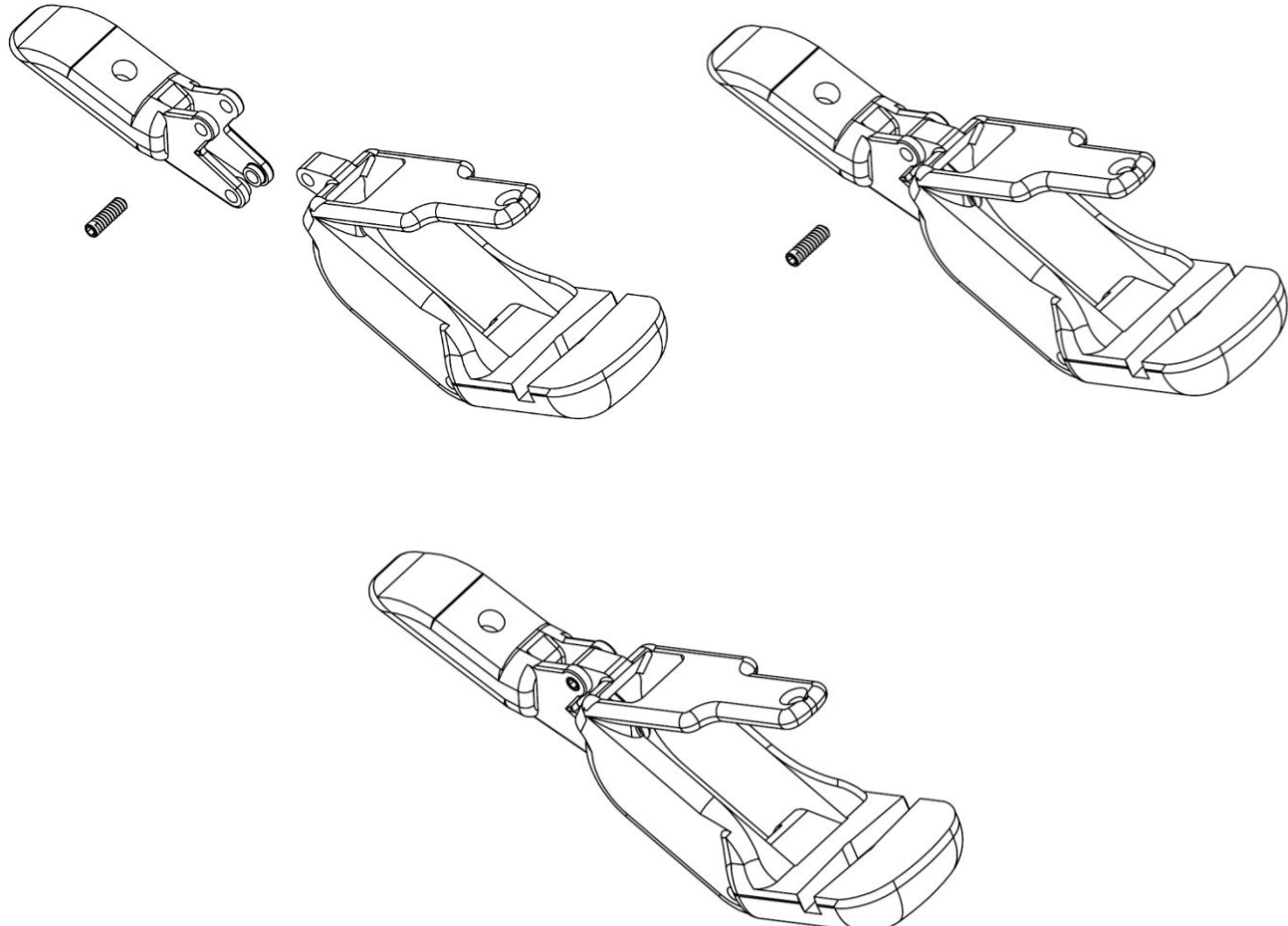
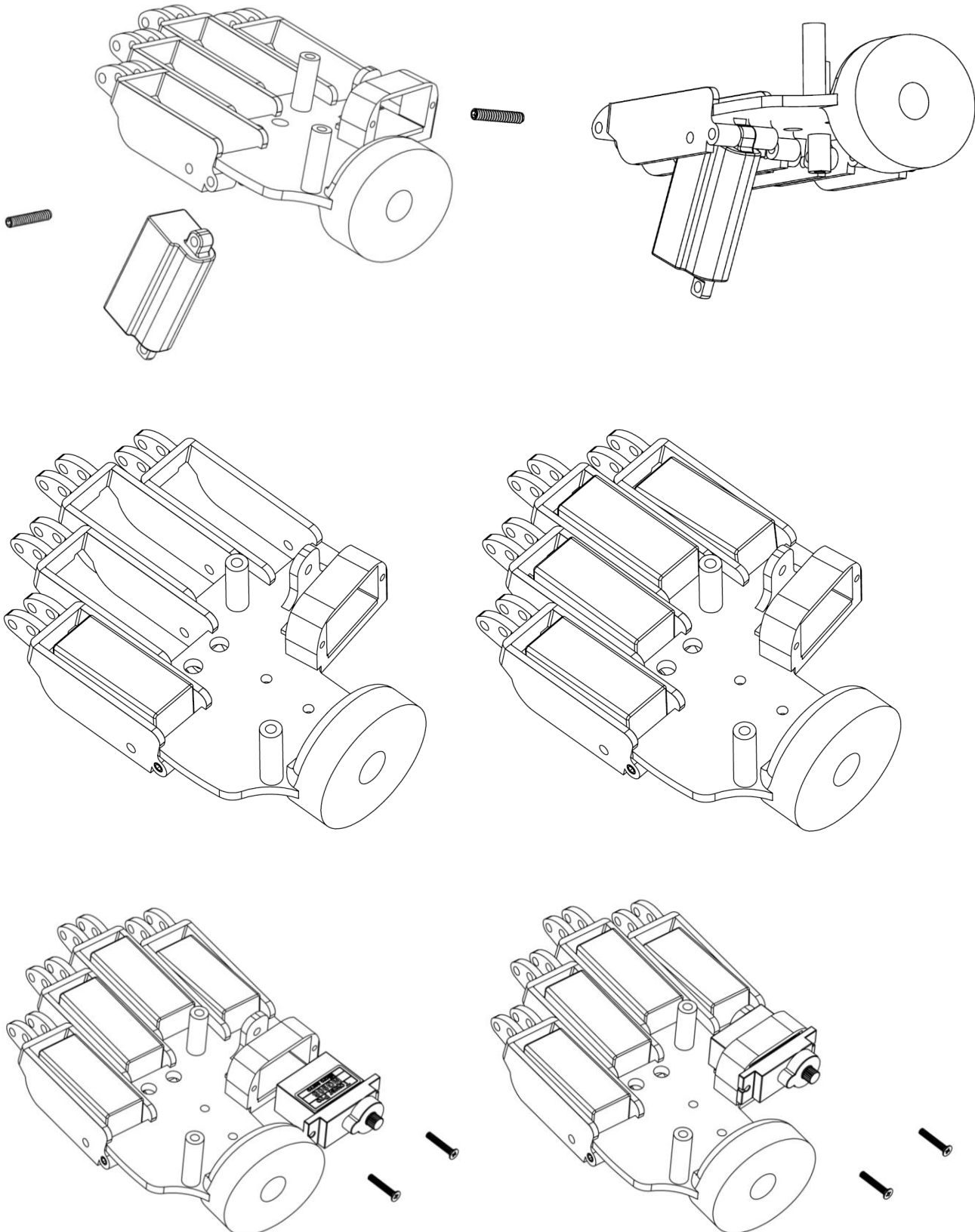


Figure 124: Thumb assembly of three steps.

4- Inserting the linear actuators on the palm

Insert all the actuators with four Allen 16 mm M3 screws and the rotary servo with two M2 screws.



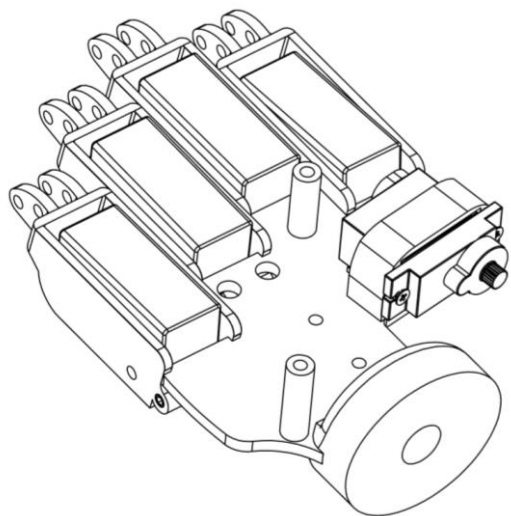
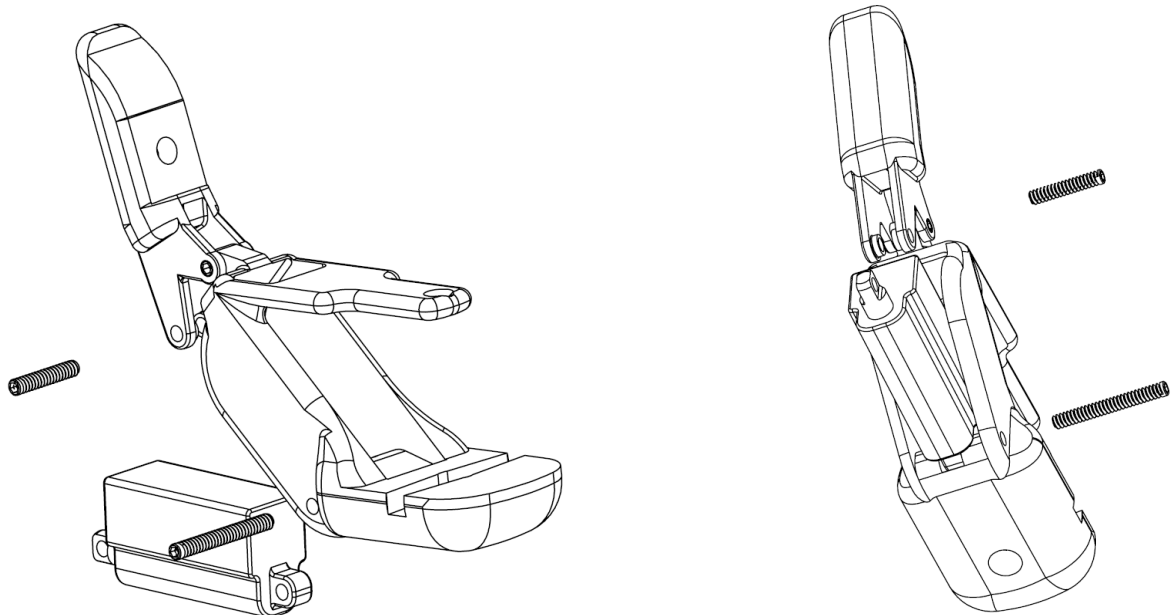


Figure 125: Linear and rotary servos assembly with the palm.

5- Inserting the linear actuators on the thumb

Use the 20mm M3 screw and one 10mm screw to insert the linear actuator in the thumb.



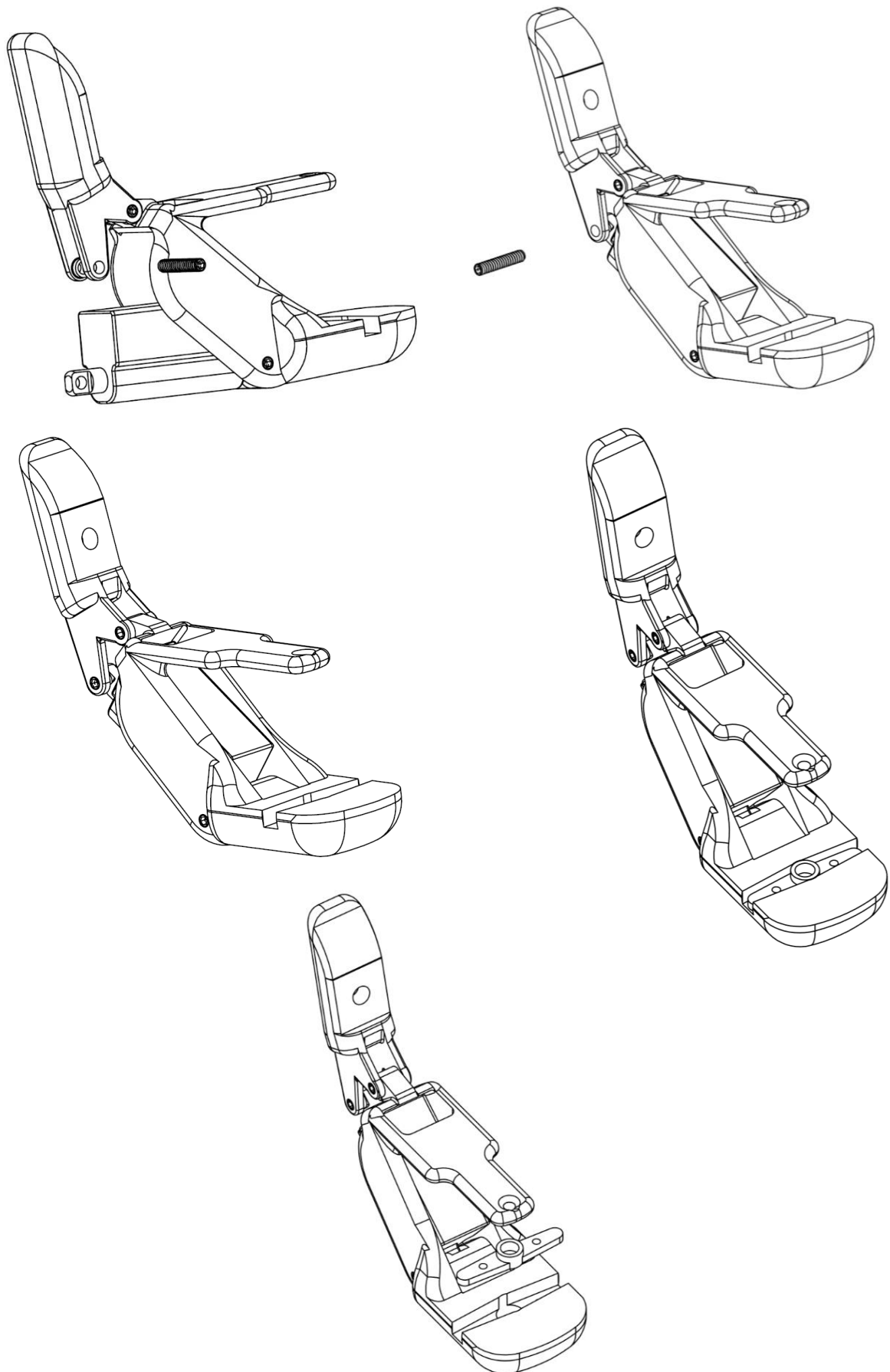


Figure 126: Linear actuators and thumb assembly.

6- Fingers and palm assembly

Now use two of 16mm and one of 10mm M3 Allen screws to make the assembly of each finger with the palm.

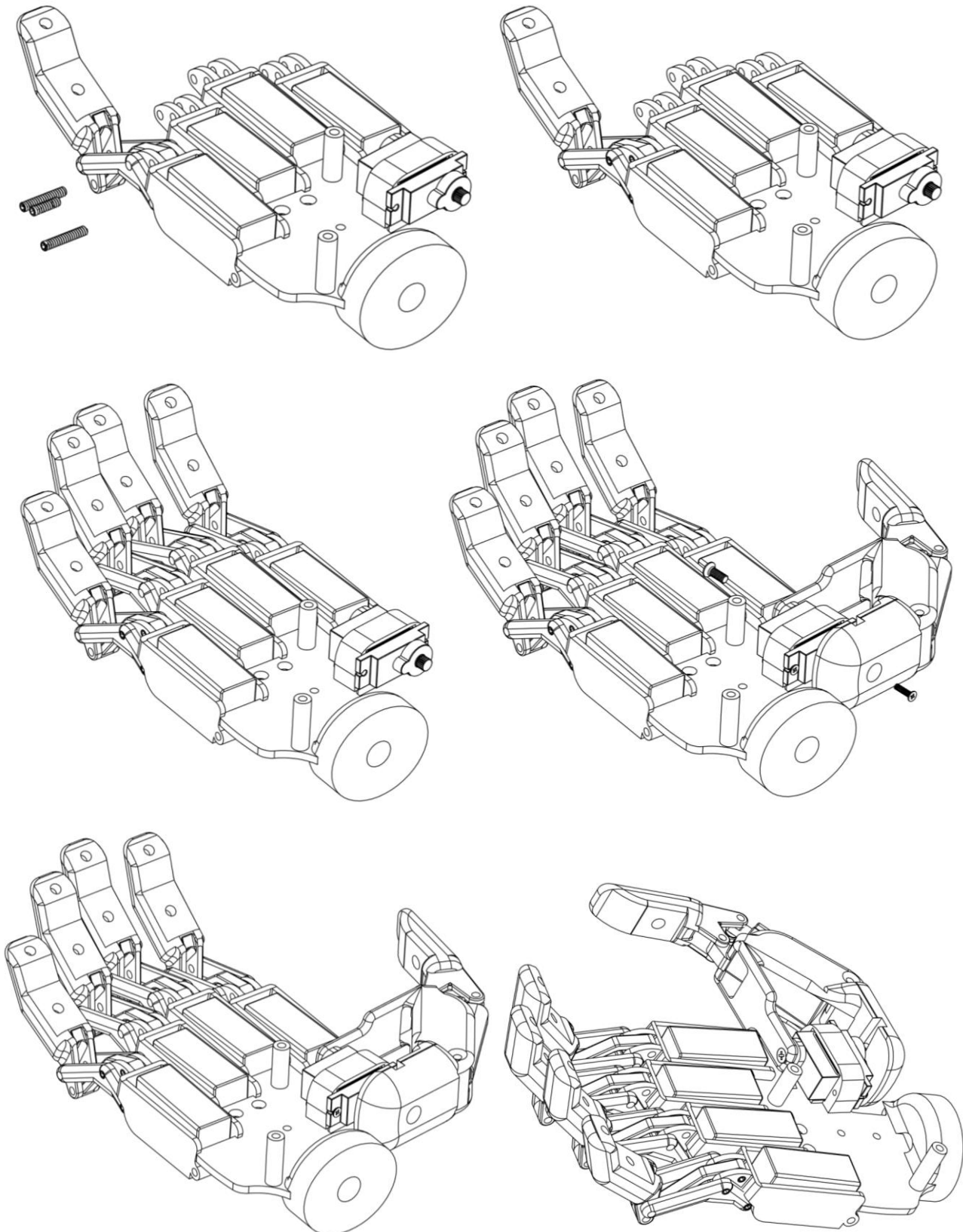


Figure 127: Fingers and palm assembly.

7- Casting the silicone in the molds

Now put silicone between the two parts of the finger and thumb mold and close the mold, with the pressure of the silicone is enough.

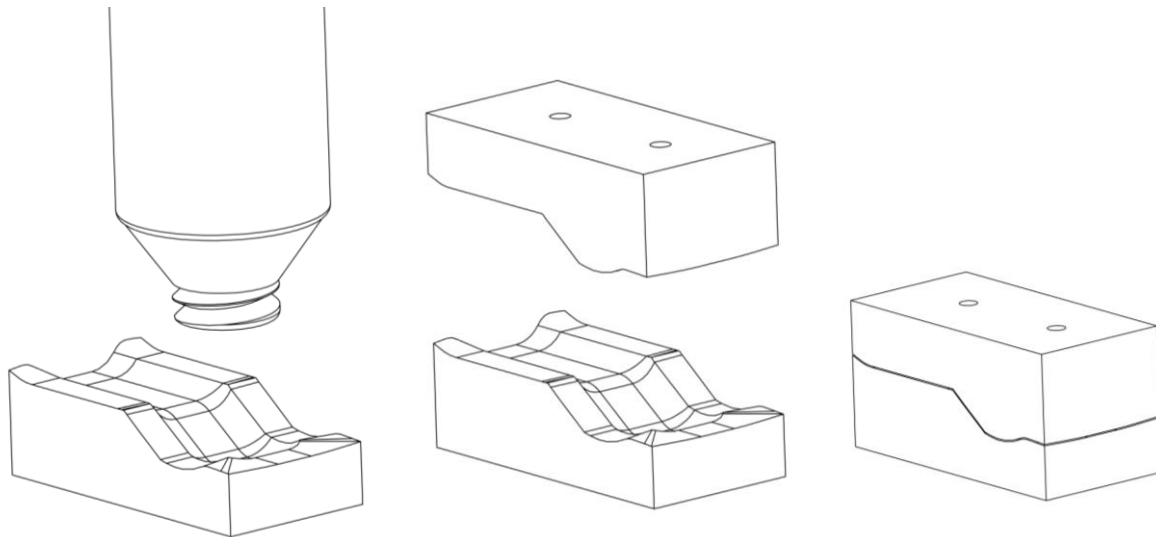


Figure 128: The silicone is applied between the two parts of the finger mold.

This step must be reproduced four times, one for each finger.

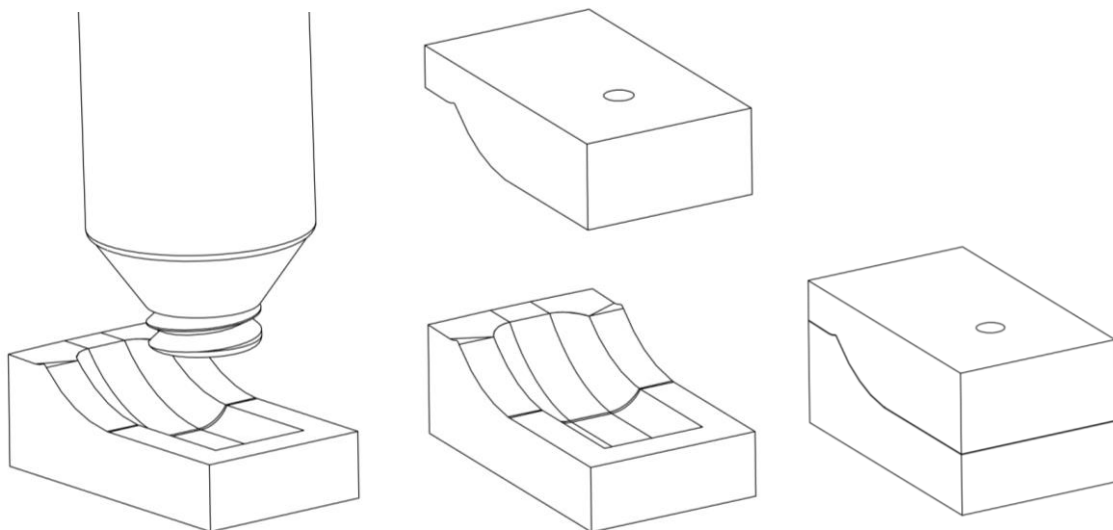


Figure 129: The silicone is applied between the two parts of the thumb mold.

Wait for 72 hours and the silicone will be ready for the next step.

8- Gluing the silicone “skins” on the distal phalanx

Now is the time of the super glue that is used to glue the silicone covers for each finger.

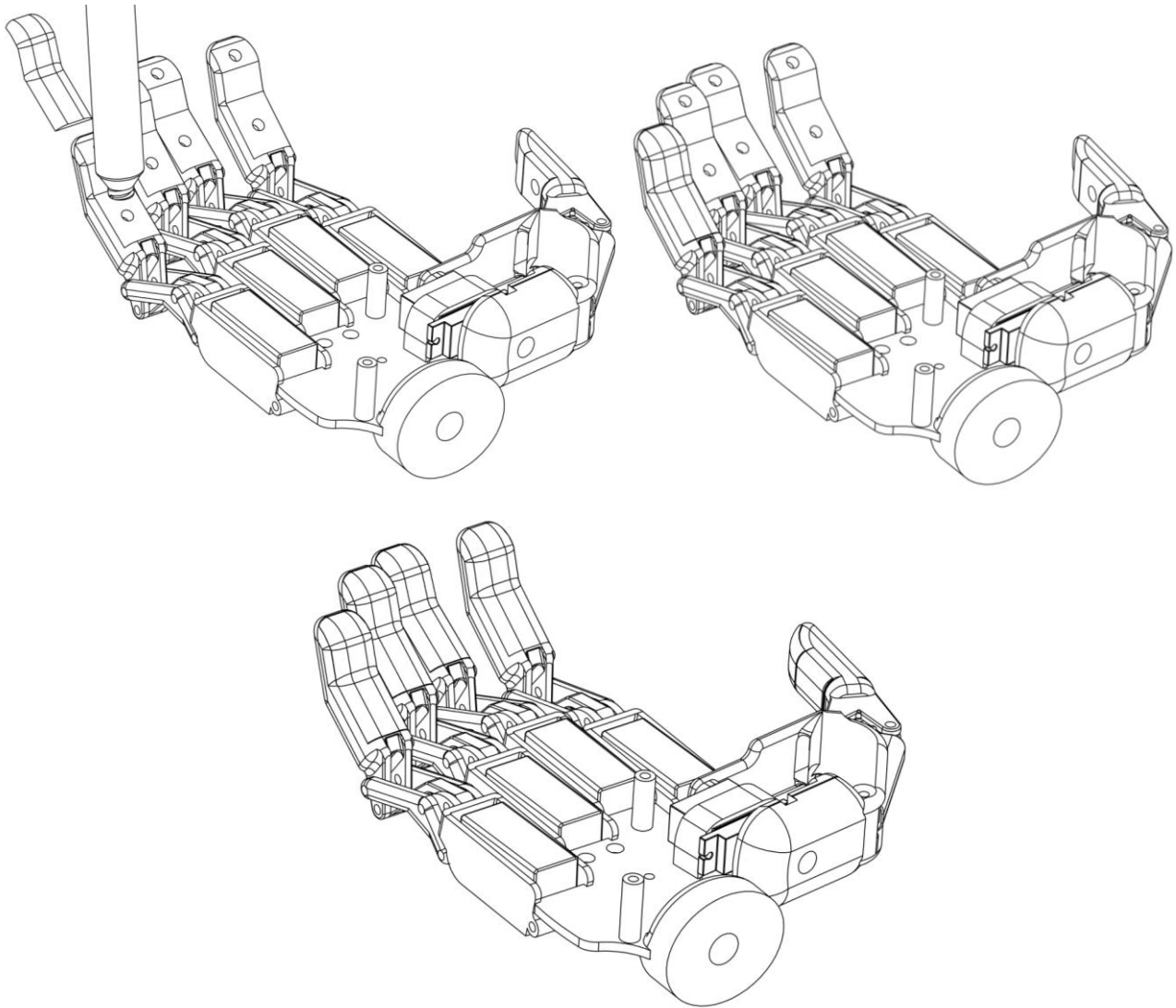


Figure 130: The fingertip covers are glued with super gule.

9- Mounting the electronics and electrical components in the palm

Use screws to attach the PCB with the palm. Configuration with the DFRobot EMG sensor. The configuration with the Myoware EMG sensor is without the electronics in the left figure because the electronic board of the sensor goes outside of the hand.

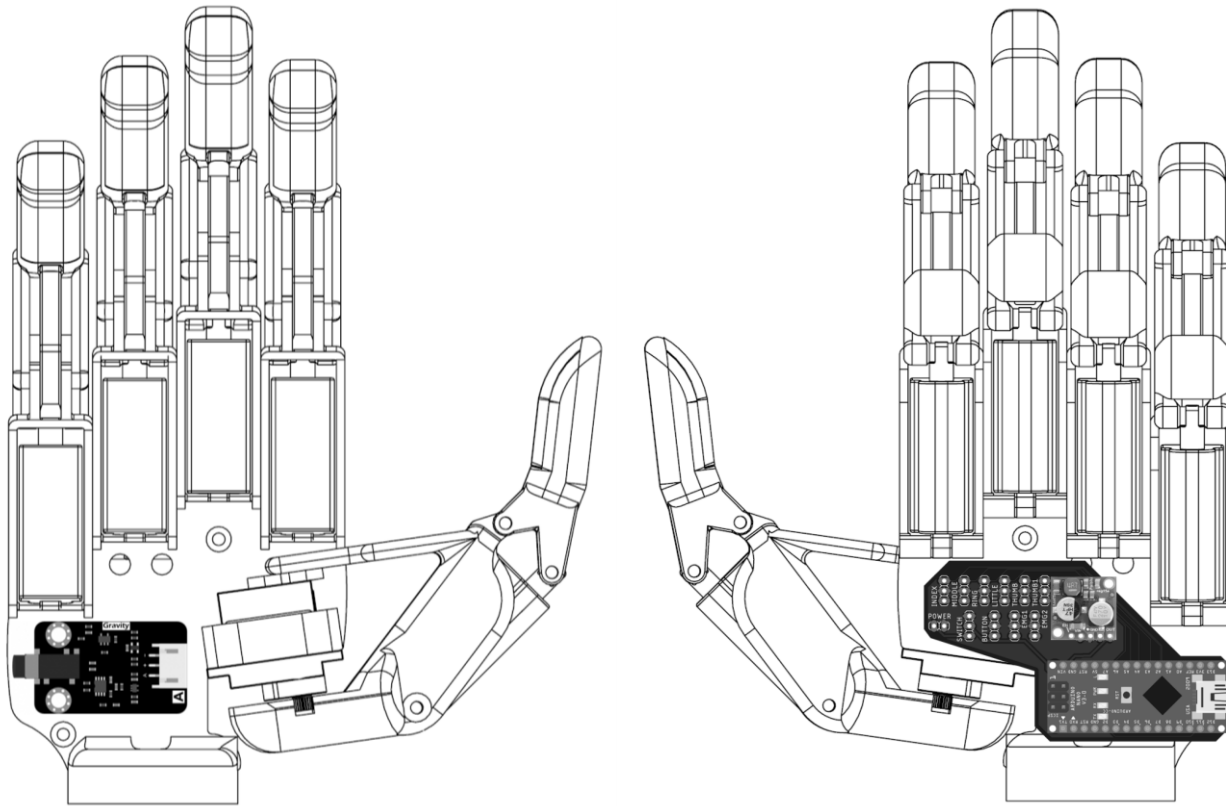
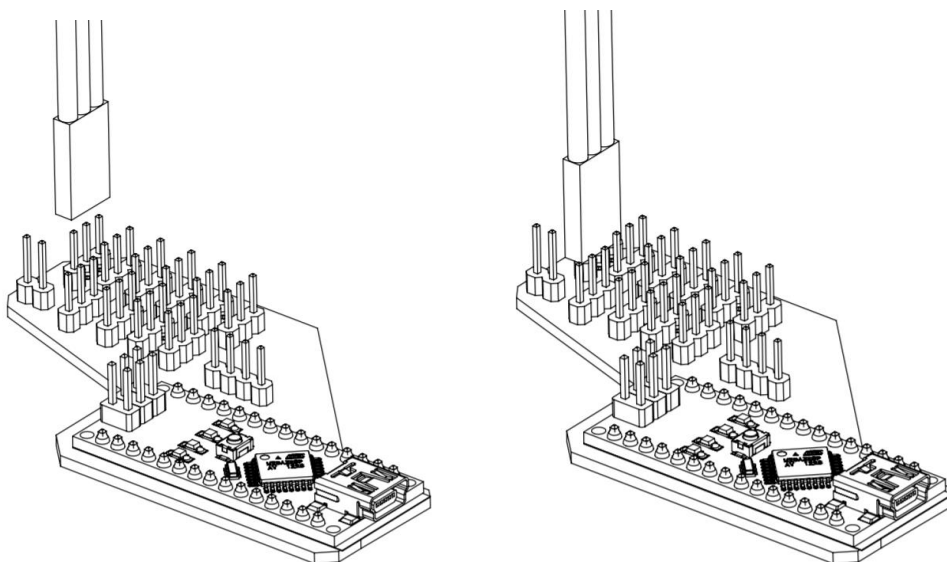


Figure 131: PCB assembly for the two sensors: Myoware and DFRobot.

10-Electric connections

Now use the names of each connection to link the actuators and sensors with the PCB.



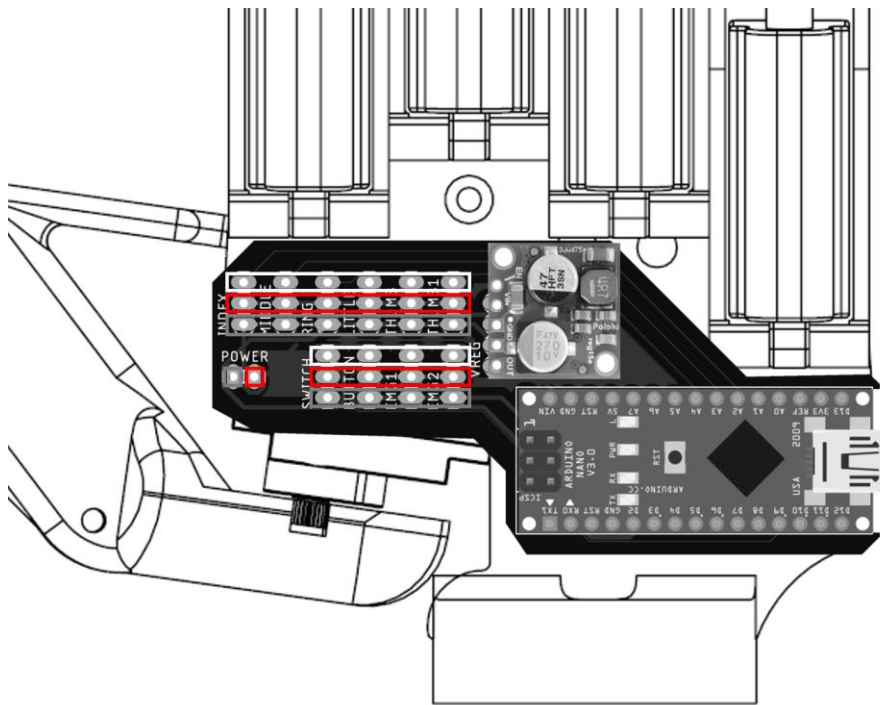


Figure 132: Connector and pin connection (bottom) PCB connections GND (grey) Vcc (red) and signal (white) on top.

WARNING/Safety: This configuration is designed to be used as the manufacturer Myoware recommends, you never must use the hand connected to your body by the EMG sensor, and the PC connection via USB at the same time if the PC is connected to the grid, the PC must be disconnected to the grid!

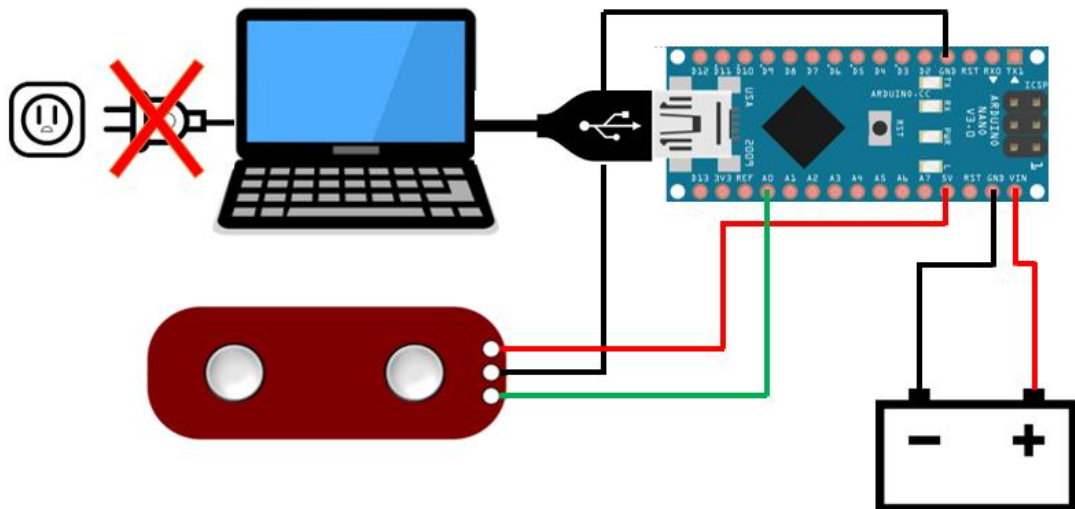


Figure 133: Schematic for safety recommendations.

11-Assembling the covers

Four 10 mm M3 screws are used to attach the two covers with the hand.

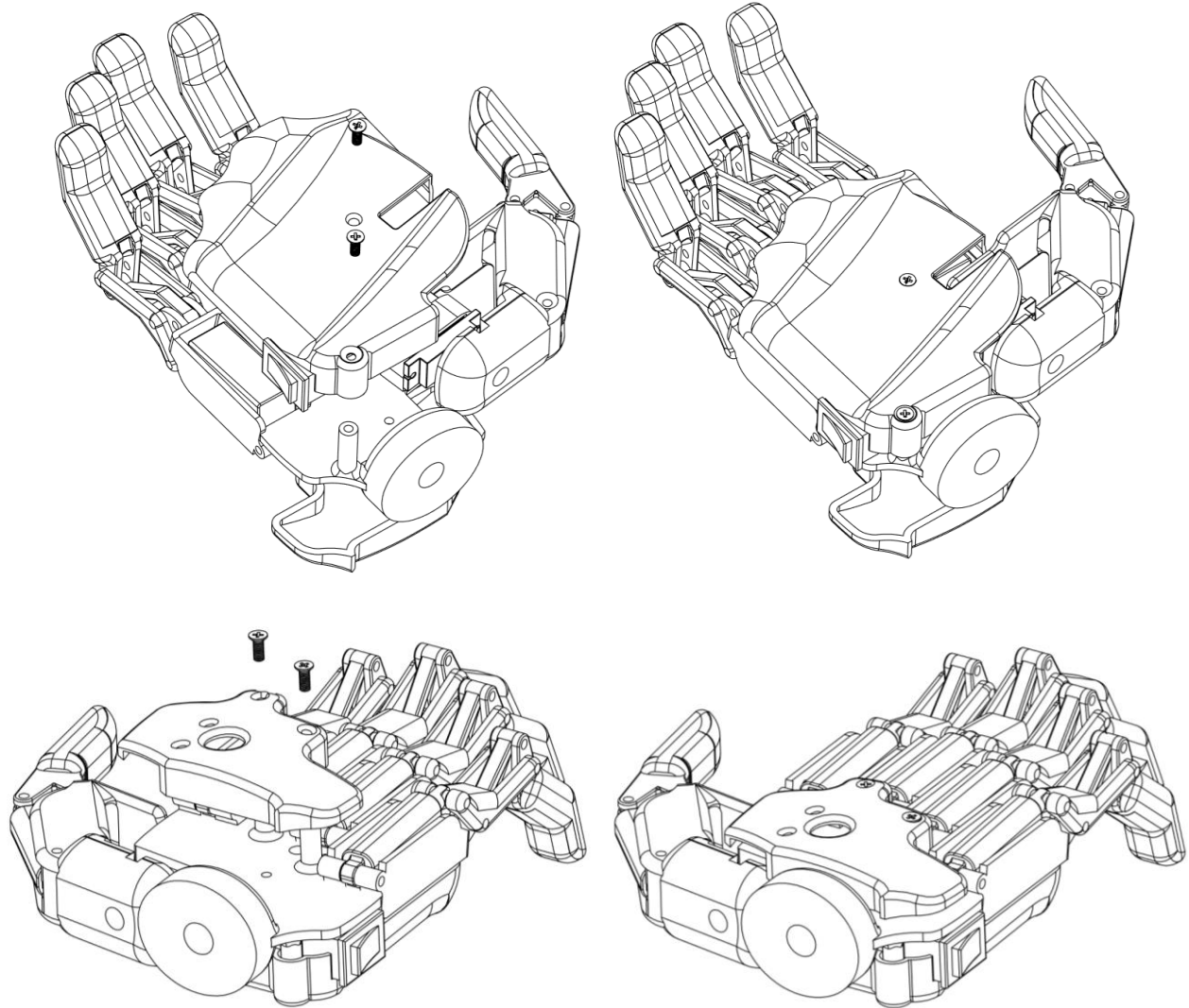


Figure 134: Assembly of the top and bottom covers.

12-Connect the hand to your body.

Switch off the hand.

Use disposable electrodes to attach the Myoware EMG sensor in your forearm with the hand disconnected. In the case of the DFR robot EMG sensor, the sensor goes directly in contact with the skin.

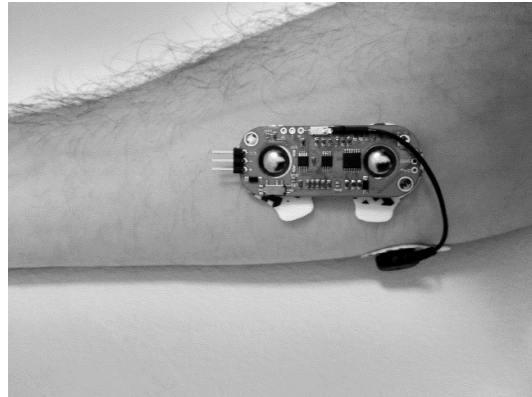


Figure 135: Forearm-EMG sensor example connection.

13-Grasp_EMG_configuration

Open the Grasp_EMG_configurator.exe:

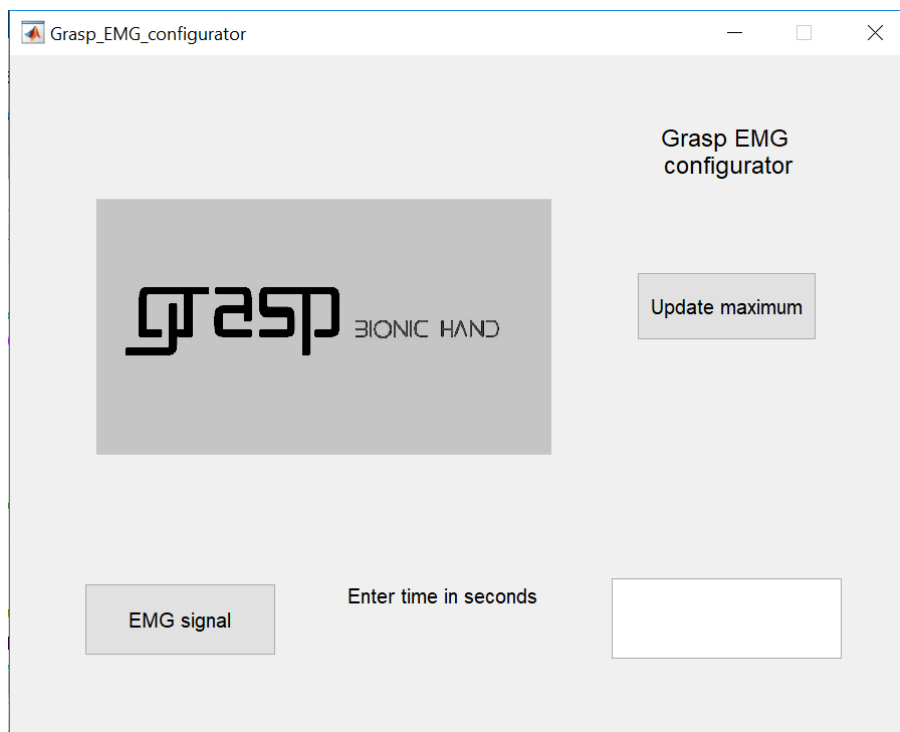


Figure 136: First view of the graphical user interface.

Introduce a time value in the window on the right of the “EMG signal” button:

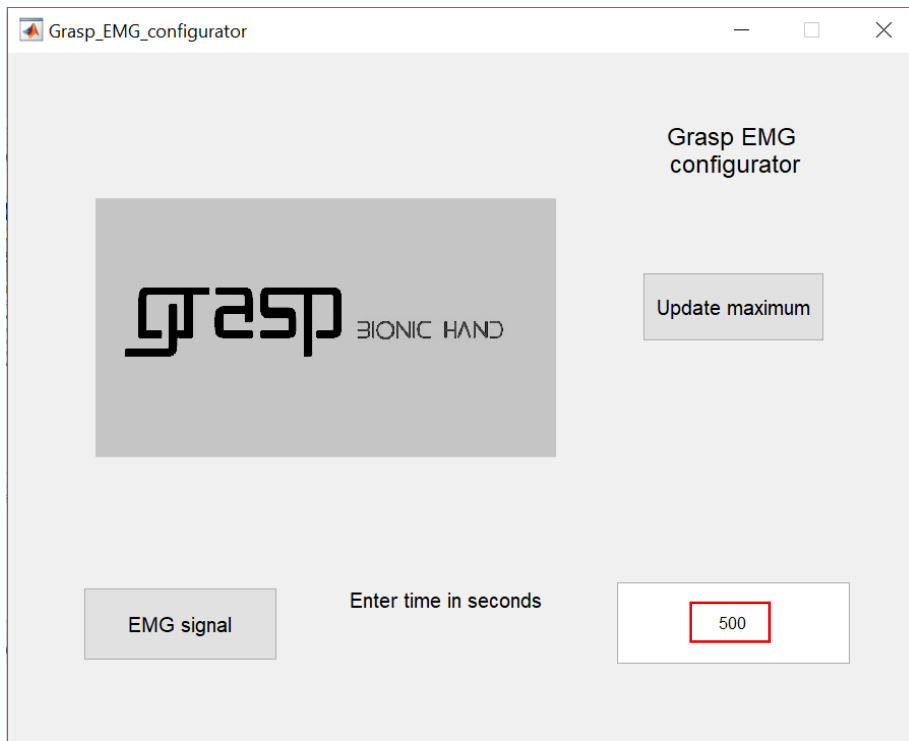


Figure 137: Time window introduced by the user.

Click on the EMG signal button and contract and relax your muscles naturally (without making so much force) as many times as you want during the recording time, the signal will appear on the graph:

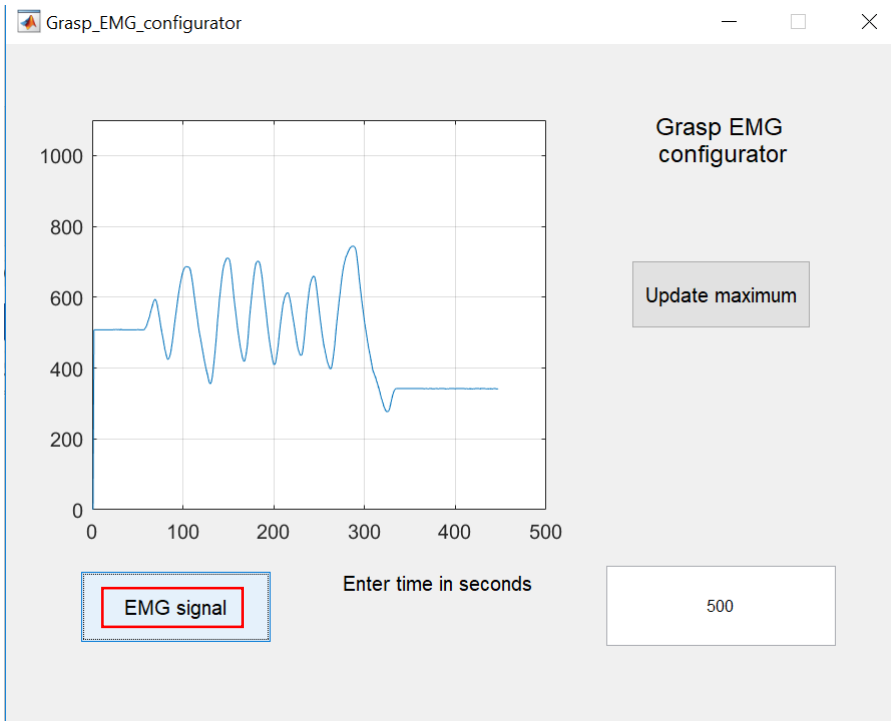


Figure 138: EMG signal displayed in the graph window.

Once the recording is finished press the button “update maximum”, under the button, your maximum will appear:



Figure 139: Maximum of the EMG signal showed in the end of the recording.

This value will be used to calibrate your hand and set the range of values in between your hand will work for a comfortable control.

14-Upload the firmware

The code can be downloaded from Hackaday:

<https://hackaday.io/project/164989-grasp-bionic-hand>

Open the code with the Arduino IDE:

The figure shows a screenshot of the Arduino IDE. The title bar says 'Grasp_control_3 | Arduino 1.8.3'. The main area contains the following C++ code:

```

Grasp_control_3 | Arduino 1.8.3
Fitxer Edits Esbós Ajuda
Grasp_control_3.h
// Include the Servo.h library
#include <Servo.h>

const float max_EMG = 200;

// Declare the digital pin D2 for the pushbutton
const int pushbutton = 2;

// Declare the servos
Servo index;
Servo middle;
Servo ring;
Servo small;
Servo thumb_flexion;
Servo thumb_opposition;

// Declare the buttonstate variable
int buttonstate = 0;

void setup()
{
    // Set the serial communication at 9600 bauds
    Serial.begin(9600);
}

```

Figure 140: Grasp code open in the Arduino IDE.

Change the constant float named “max_EMG” placed in the beginning of the program to set your maximum EMG value and put the value displayed on the window of the application: Grasp_EMG_configurator:

```
const float max_EMG = 744;
```

Figure 141: EMG maximum value introduced in the constant variable of the program.

Connect the Arduino to a USB port.

Compile the code using the  button.

Upload the code to the Arduino board using the  button.

Once the code upload is successful disconnect the Arduino from the USB port.

15-Start exploring!

Switch on the hand.

The pushbutton will let you change from one type of grasp to the other and with the contraction of your forearm muscles you will be able to control the opening and closing action of the fingers.

Discussion

GRASP PERFORMANCE

The main objectives of the project were: an affordable cost, enclose the electronics and actuators in the palm of the hand, ease of assembly, weight under the average of the human hand, equivalent features of the commercial models and be able to perform the most important grasps for the ADL's. The cost under 500 € has been achieved including all components, and is exactly 477.35 € (Table 42). With the mechanical design and components selection, the actuators have been included in the palm and PCB design has been fitted in the space left. The assembly steps are included in the present work in the assembly instructions document.

Table 35: Grasp 1.0 features.

Summary of Grasp 1.0 features	
Flexion-extension speed (°/s)	71.96
Opposition speed (°/s)	196.10
Finger fingertip force (N)	6.82
Thumb fingertip force (N)	16.50
Mass (g)	335
DOF	6
Size (mm)	190 x 141 x 53
Cost (€)	477.35

The dimensions of the hand are close to the average in the global population and the mass of the device has been set under 400g. During the hand validation (Figure 142), the more important six types of grasps for the ADL's have been performed catching several objects.

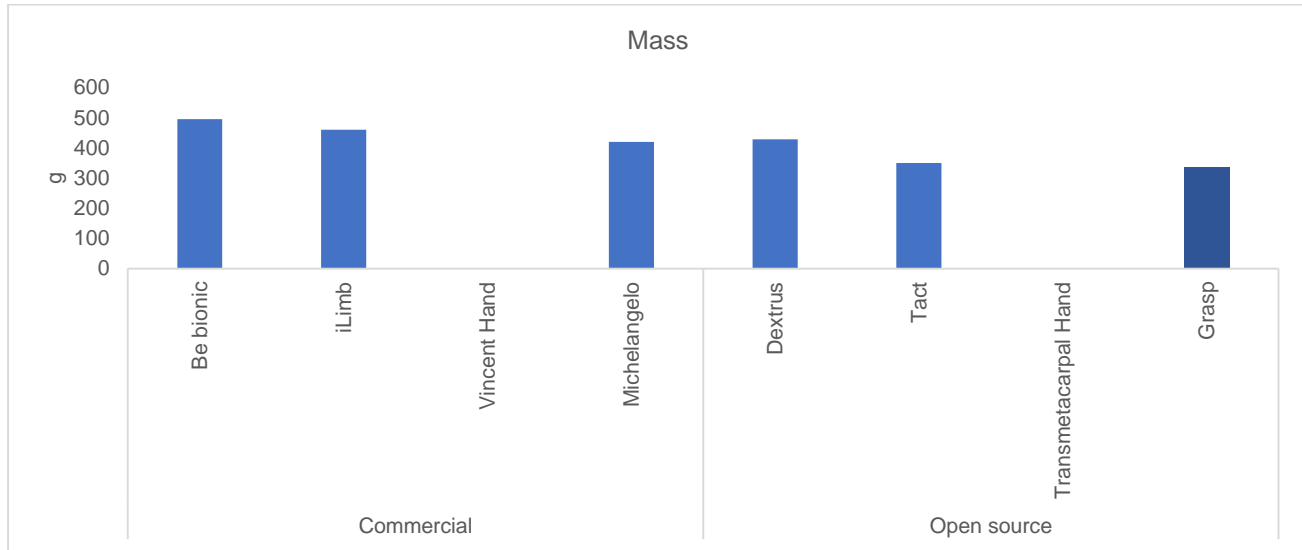


Figure 142: Mass comparison between Grasp and the other projects.

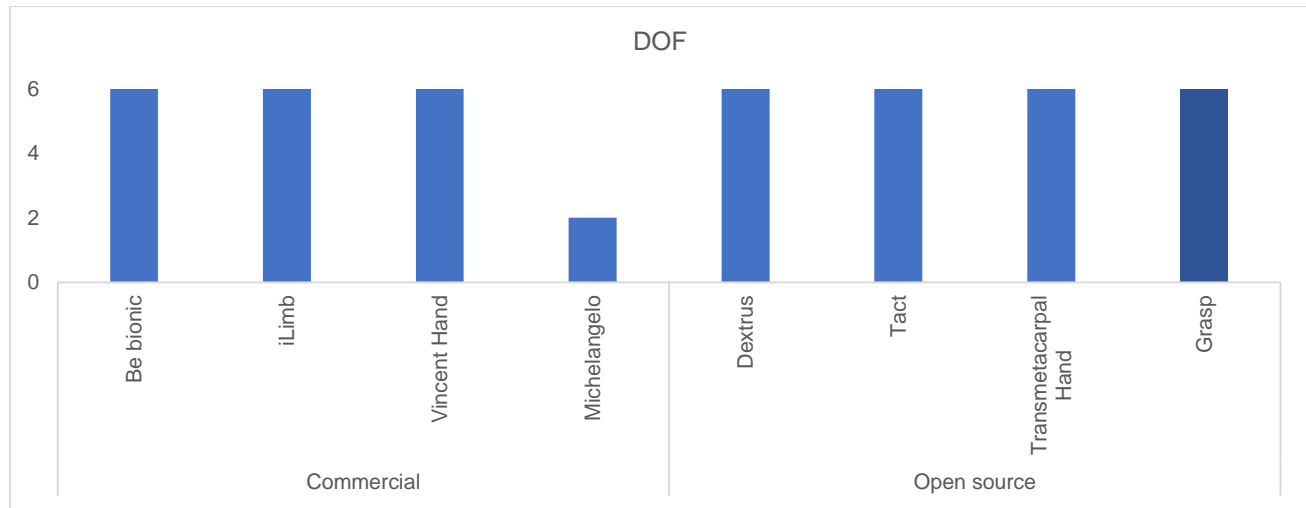


Figure 143: DOF comparison between Grasp and the other projects.

The most two representative features of a good performance compared with the commercial and other open source hands available are also the most challenging goals of this project: to get a good relation between the fingertip force and the flexion-extension speed of the fingers. Both are satisfactory results of the project achieving 6.82 and 16.5 N of fingertip force (Figure 144) in the finger and the thumb respectively and a flexion-extension speed of 71.96 and 196.10 °/s (Figure 145) performed by the finger and the thumb respectively.

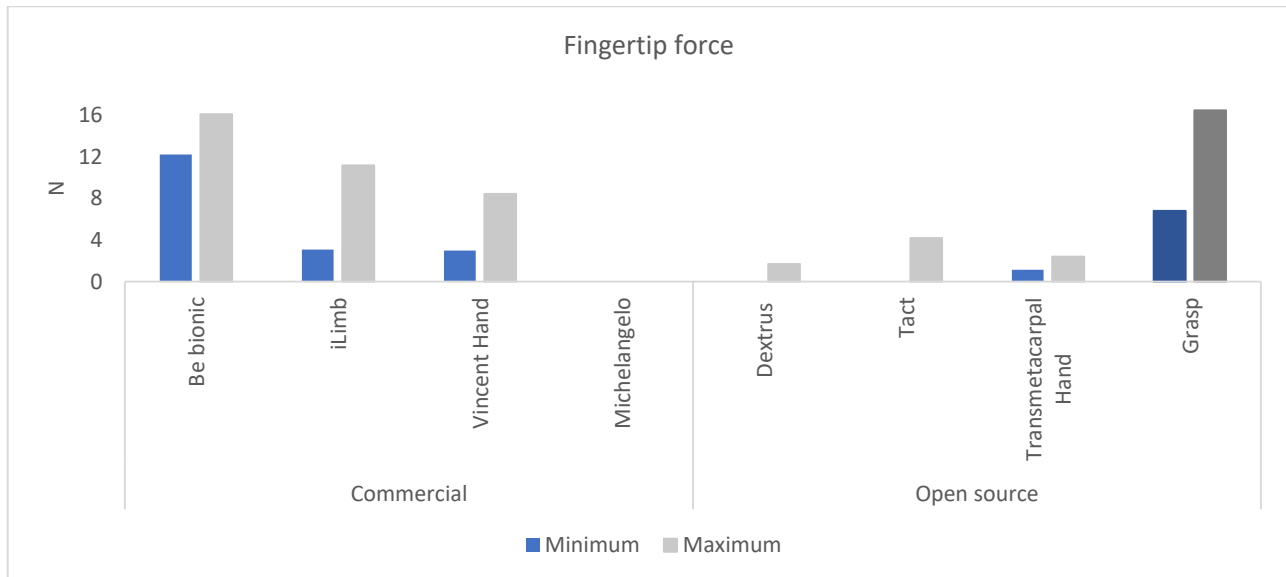


Figure 144: Fingertip force comparison between Grasp and the other projects.

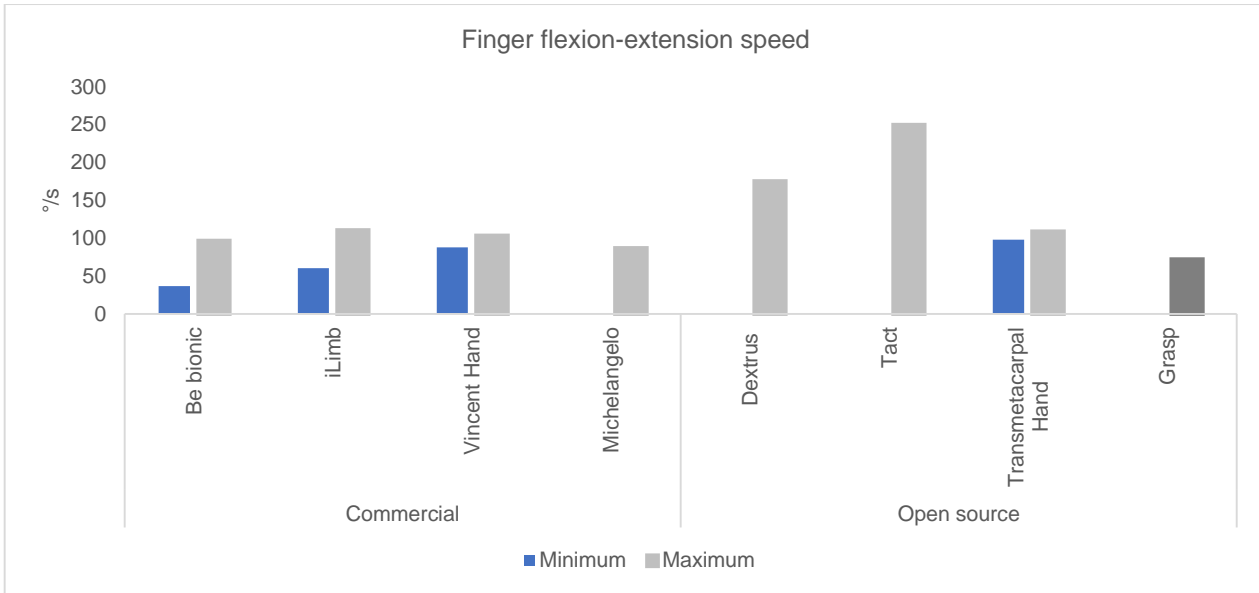


Figure 145: Finger flexion-extension speed comparison between Grasp and the other projects.

However, as can be seen in the Figure 146, comparing the results of the Grasp finger trajectory against the model of the real human finger indicates there is a long way to achieve a fully functional bionic hand in terms of range of motion.

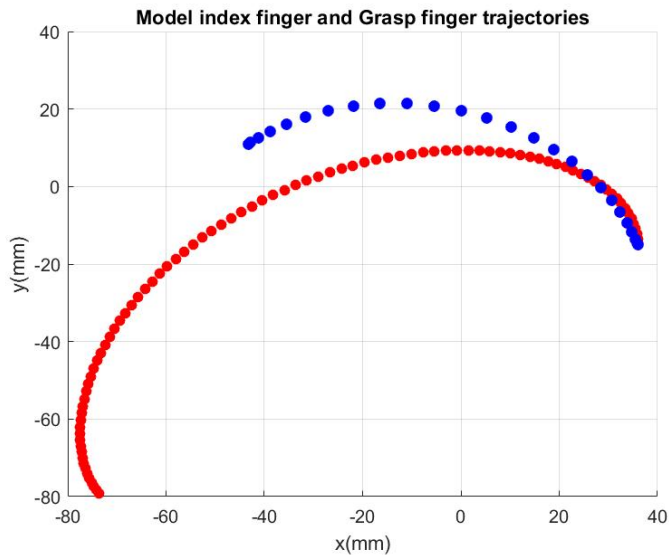


Figure 146: Comparison of the model hand index finger (red) and Grasp index finger (blue).

The trajectories of the fingers in the Solidworks kinematics simulation and the real flexion-extension test can be normalized and compared to see that are almost identical (Figure 147). The small deviations are caused by the differences in dimensions in the real holes against the simulation holes but, the result can be considered as a good approximation.

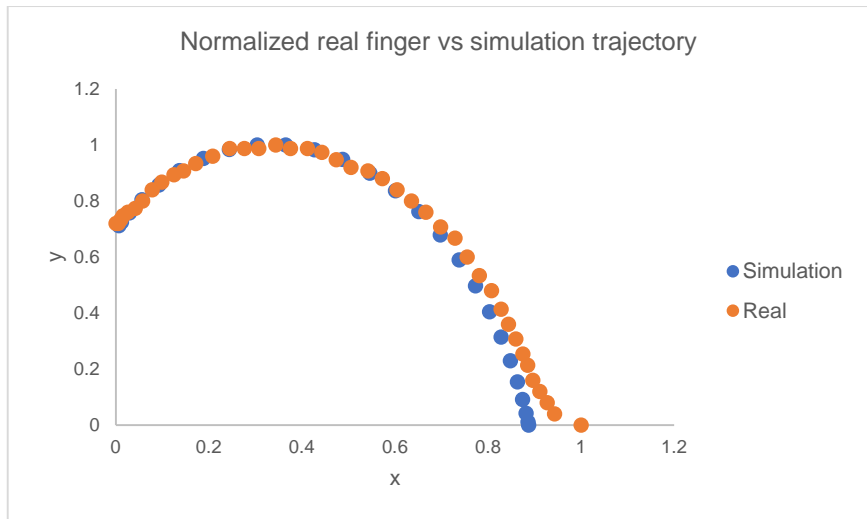


Figure 147: Comparison of the Solidworks simulation finger (blue) and the real Grasp index finger analysed using Kinovea (red) normalized.

Even with big improvements in the hand performance, the obtained values of 6.82 and 16.5 N of fingertip force are far away from the real human hand values of fingertip forces, which are 412 ± 93 N for men and 235 ± 50 N for women [25] and flexion-extension speed of $384^{\circ}/s$ [30].

Conclusions

CONCLUSIONS

- The hand has all the electronics and actuators included inside the palm, which makes it suitable for the three type of upper limb amputations: wrist disarticulation, trans humeral and trans radial amputations.
- The device can be 3D printed using FDM printers and it has been printed and assembled in the present work.
- Grasp 1.0 can be easily assembled and programmed by following the instructions created for that purpose.
- Grasp 1.0 files can be currently downloaded from the platforms Thingiverse and Hackaday. They have more than 1000 downloads if all the models of the design process are considered.
- The current cost of a single Grasp 1.0 is 477.35 € including all components and therefore, under 500 €.
- Grasp has achieved the 6 DOF and is able to perform the six most important grips (spherical grip, hook grip, lateral grip, tip grip, tripod or palmar grip and cylindrical grip) to perform the activities of daily living.
- The hand is controlled by surface EMG signals from the forearm using the sensor Myoware, the cheapest sensor in the market.
- The hand weight is 335 g, 65 g below the estimated value uncomfortable for the amputee.
- With Grasp 1.0 the range of flexion-extension speed and fingertip forces that have been achieved are competitive compared with the best commercial hands.
- The state of art of bionic hands is still in an early stage and there are huge differences between the current options and the human hand.
- The way of manufacturing the hand using 3D printing is more sustainable in terms of energy waste and carbon footprint than manufacturing them with plastic injection.
- This project has contributed to the field of bionic hands with a novel device that has good performance in absolute terms, with all components and parts easily acquirable with a low cost.
- The methods selected for the verification have become a good approximation to predict the real behaviour of the hand.

Future work

WHAT IS NEXT

The natural evolution of this kind of robotic project is to increase the range of movements by increasing the number of actuators. But previously, using the same number of DOF and actuators, the range of motion can be especially improved and that will be probably the first step to take in the future. The flexion-extension speed values should be increased up to 100 °/s to get the standards of the best hands in the market, and the fingertip forces up to 12 N. The efficiency probably using actuators with a 12V voltage supply in order to reduce the current values and increase the time of use. A challenging work for the future will be the control of the hand using auto-correlation or other signal processing tool to discriminate between the morphology of the different EMG signals and actuate the device without using the pushbutton.

The graphical user interface will be improved exporting the value of the maximum of EMG signal recorded and writing this value in to the Arduino Code without opening the Arduino IDE. Another important step to take is to have more experience with different amputees and different needs. And try to find new ways to control the bionic maintaining the principles of easy configuration and usability.

In terms of safety, another step to make soon will be the inclusion of an isolation amplifier (Figure 148) between the Arduino board and the EMG sensor body connection in order to avoid leakage current from the electrical grid while the USB is connected simultaneously with the EMG recording using the graphical user interface to make the device calibration.

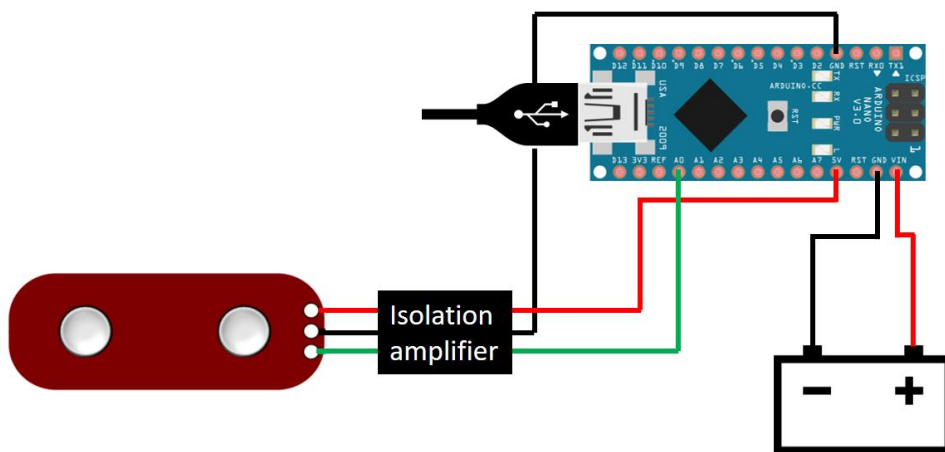


Figure 148: EMG Myoware sensor with simultaneous connection with the grid safety recommendations.

References

REFERENCES

- [1] M. L. Blanc, “"Give Hope - Give a Hand" - The LN-4,” 2008.
- [2] G. Matías Clavero, J. L. López Galiacho, M. Delgado Acedo and J. Martínez Marqués, Libro blanco de la prestación ortoprotésica, Madrid, 2012.
- [3] J. t. Kate, G. Smith and P. Breedveld, “3D printed upper limb prostheses: a review.,” *Disability and rehabilitation: Assistive technology*, vol. 12, no. 3, pp. 300-314, 2017.
- [4] “<https://stanfordhealthcare.org/medical-conditions/bones-joints-and-muscles/amputation/causes.html>,” [Online].
- [5] “<http://www.cpousa.com/prosthetics/upper-extremity/>,” [Online].
- [6] C. Anderson, Makers. The New Industrial Revolution, New York: Crown Business, 2013.
- [7] “<http://www.openhandproject.org/>,” [Online].
- [8] P. Slade, A. Akhtar, M. Nguyen and T. Bretl, “Tact: Design and Performance of an Open-Source, Affordable, Myoelectric Prosthetic Hand,” 2015.
- [9] A. Akhtar, K. Yun Choi, M. Fatina, J. Cornman, E. Wu, J. Sombeck, C. Yim, P. Slade, J. Lee, J. Moore, D. Gonzales, A. Wu, G. Anderson, D. Rotter, C. Shin and T. Bretl, “A Low Cost, Open-Source, Compliant Hand for Enabling Sensorimotor Control for People with Transradial Amputations,” 2017.
- [10] P. Wattanasiri, P. Tangpornprasert and V. Chanyaphan, “Design of Multi-Grip Patterns Prosthetic Hand with Single Actuator,” *IEEE Transactions on Neural Systems and Rehabilitation Engineering*, vol. 26, no. 7, pp. 1188 - 1198, 2018.
- [11] “<https://www.youbionic.com/>,” [Online].
- [12] R. Mio, B. Villegas, L. Ccorimanya, K. M. Flores, G. Salazar and D. Elías, “Development and Assessment of a Powered 3D-printed Prosthetic Hand for Transmetacarpal Amputees,” in *International Conference on Control, Automation and Robotics*, 2017.
- [13] “<http://exiii-hackberry.com/>,” [Online].
- [14] J. T. Belter, J. L. Segil, A. M. Dollar and R. F. Weir, “Mechanical design and performance specifications of anthropometric prosthetic hands: A review,” *Journal of Rehabilitation Research & Development (JRRD)*, vol. 50, no. 5, pp. 599-618, 2013.
- [15] “<http://www.taskaprosthetics.com/>,” [Online].
- [16] “<https://openbionics.com/>,” [Online].
- [17] “<https://www.pololu.com/>,” [Online].
- [18] “<https://hitecrcd.com/>,” [Online].
- [19] “<https://www.arduino.cc>,” [Online].
- [20] “<https://www.actuonix.com>,” [Online].

- [21] “<http://www.advancertechnologies.com/p/myoware.html>,” [Online].
- [22] “www.jameco.com,” [Online].
- [23] “<http://www.mootio-components.com/>,” [Online].
- [24] L. Mosquera Camelo and V. Guedez, “Estudio biomecánico de la mano durante el agarre de herramientas manualesÑ Datos antropométricos preliminares.,” in *3rd International Conference on Occupational Risk and Prevention*, 2004.
- [25] L. Muñoz Jashimoto, E. de la Vega Bustillos, F. O. Lopez Millan, B. A. Ortiz Navar and K. Lucero Duarte, “Fuerza máxima de agarre con mano dominante y no dominante,” in *XV CONGRESO INTERNACIONAL DE ERGONOMÍA SEMAC*, 2009.
- [26] K. Shima, Y. Tamura, T. Tsuji, A. Kandori, M. Yokoe and S. Sakoda, “Estimation of Human Finger Tapping Forces Based on a Fingerpad-Stiffness Model,” in *31st Annual International Conference of the IEEE EMBS*, Minneapolis, 2009.
- [27] M. Lloret, *Anatomía aplicada a la actividad física y deportiva*, Padotribo, 2008.
- [28] E. Peña-Pitarch, N. Ticó Farguera and J. (. Yang, “Virtual human hand: model and kinematics,” *Computer Methods in Biomechanics and Biomedical Engineering*, pp. 1-12, 2012.
- [29] “<https://www.kinovea.org/>,” [Online].
- [30] D. van der Riet, R. Stopforth, G. Bright and O. Diegel, “THE LOW COST DESIGN OF A 3D PRINTED MULTI-FINGERED MYOELECTRIC PROSTHETIC HAND,” in *Mechatronics: Principles, Technologies and Applications*, Nova Science Publishers, 2015, pp. 86-116.
- [31] L. Jaworski and R. Karpinski, “Biomechanics of the human hand,” *Journal of Technology and Exploitation in Mechanical Engineering*, vol. 3, no. 1, pp. 28-33, 2017.
- [32] A. Barrientos, “Capítulo 4 Cinemática del robot,” in *Fundamentos de robótica*, Madrid, Mc Graw-Hill, 2007, pp. 93-123.
- [33] “https://www.trossenrobotics.com/mightyZAP_7v12n,” [Online].
- [34] “<https://www.towerpro.com>,” [Online].
- [35] “<https://grabcad.com/library/arduino-nano--1>,” [Online].
- [36] “<https://filament2print.com>,” [Online].
- [37] “www.bq.com,” [Online].
- [38] “<https://www.pcbgogo.com>,” [Online].
- [39] “<https://www.dfrobot.com>,” [Online].
- [40] “<https://www.hobbyking.com>,” [Online].
- [41] S. S. M. 3D, “Smartfil Medical”.
- [42] I. Factor II, “SAFETY DATA SHEET A-103 Base MEDICAL GRADE ELASTOMER BASE,” 2015.

- [43] “<https://www.mathworks.com>,” [Online].
- [44] “<https://www.autodesk.com/products/eagle>,” [Online].
- [45] M. P. Aparicio, “Diseño y desarrollo de circuitos impresos con KICAD,” RC Libros, Madrid, 2010.
- [46] “<https://www.solidworks.com>”.
- [47] F. P. Beer, E. Russell Johnston and E. E. Eisenberg, Mecánica vectorial para ingenieros, McGraw-Hill, 2007.
- [48] Ultimaker, “Technical data sheet PLA,” 2018.
- [49] “<https://www.interlinkelectronics.com/fsr-402>,” [Online].
- [50] “www.frizzing.org,” [Online].
- [51] “<https://www.kinovea.org/>,” [Online].
- [52] “www.geeklectronica.blogspot.com,” [Online].
- [53] F. Cerdas, M. Juraschek, S. Thiede and C. Herrmann, “Life Cycle Assessment of 3D Printed Products in a Distributed Manufacturing System,” *Journal of Industrial Ecology*, vol. 21, no. S1, pp. 80-93, 2017.
- [54] R. Song and . C. Telenko , “MATERIAL WASTE OF COMMERCIAL FDM PRINTERS UNDER REALSTIC CONDITIONS,” in *Proceedings of the 26th Annual International Solid Freeform Fabrication Symposium – An Additive Manufacturing Conference*, Atlanta, 2016.
- [55] “<https://www.ldlc.com/es-es/ficha/PB00253260.html>,” [Online].
- [56] “<https://tarifasgasluz.com/comercializadoras/endesa/precio-kwh>,” [Online].
- [57] “<https://graspbionichand.wixsite.com/grasp/about>,” [Online].
- [58] “https://www.youtube.com/channel/UCM9uCBVx_Or2t6A4Se4PdUA/featured,” [Online].
- [59] “<https://www.thingiverse.com/thing:2736588>,” [Online].
- [60] “<https://hackaday.io/project/163935-grasp-bionic-hand>,” [Online].
- [61] “<https://vincentsystems.de/en/>,” [Online].
- [62] “<http://bebionic.com>,” [Online].
- [63] “<http://touchbionics.com>,” [Online].
- [64] “<https://www.ottobockus.com/prosthetics/upper-limb-prosthetics/solution-overview/michelangelo-prosthetic-hand/>,” [Online].
- [65] “<http://enablingthefuture.org/upper-limb-prosthetics/the-flexy-hand/>,” [Online].
- [66] “<https://www.active-robots.com>,” [Online].
- [67] “<https://www.openimpulse.com>,” [Online].

[68] “<https://www.ottobockus.com>,” [Online].

[69] J. Sobotta, Sobotta's Atlas and Text-book of Human Anatomy, Elsevier, 1909.

[70] H. Gray and W. Lewis, Anatomy of the Human Body, 1918.

[71] “<https://www.towerpro.com.tw/product/mg90s-3/>,” [Online].

Appendices

APPENDIX A: Finger model script

```
clc
clear all

% variables

xi = [];
yi = [];

l1 = 40;
l2 = 22;
l3 = 25;

q1 = [0:1:90];
q2 = [0:1:90];
q3 = [0:1:90];
q4 = [0:-1:-90];

cxi = 51,5;
cy = 15;
zi = ones(1,90).*0;
n = 90;

%index values

for i=1:n

xi(i) = cxi + l1* cosd(q1(i))+l2*cosd(q1(i)+q2(i))+l3*cosd(q1(i)+q2(i)+q3(i));
yi(i) = cy + l1* sind(q1(i))+l2*sind(q1(i)+q2(i))+l3*sind(q1(i)+q2(i)+q3(i));

end

scatter3(xi,yi,zi,'filled')
hold on

title('Model hand finger trajectory')
xlabel('x (mm)')
ylabel('y (mm)')
zlabel('z (mm)')
legend('boxoff')
```

APPENDIX B: Micro servo comparison table

Model	Dimensions (mm)	Weight (kg)	Operating voltage (V)	Rotation time (s/60°) at 6V	Stall torque (Kg-cm) at 6V	Cost (€)
MG-90S	22,5x12x35,5	13,4	6	0,08	2,2	3,57
TG9e	23x12.2x29	9	6	0,09	1,7	1,8
HXT500	1.3x11.5x22	6,2	6	0,07	0,8	1,92
SM-S2309S	22,2x11,6x21,5	9	6	0,1	1,2	7,57
HK15178	-	10	6	0,09	1,4	1,76
HKSCM9-6	-	10	6	0,07	1,6	2,3
D05010MG	-	5,7	6	0,07	0,6	5,93
TG9d	22.4x12.5x23	9	6	0,09	1,8	2,92
TSS-9	23.1x12.0x24.9	9	6	0,09	1,9	3,08
TG9z	23x12.1x21.4	9	6	0,12	1,7	1,8
TGY-50090M	23.1x12.0x25.9	9	6	0,07	2	3,84
HKSCM9-5	-	10	6	0,09	1,4	2,3
HK-CS928BB	22.5X11.5X24.6	9	6	0,13	1,8	2,29
DS-928B	22.5x11.5x24.6	9	6	0,12	1,8	5,51
DS-633BP	23.5x9.5x19.5	6,2	6	0,1	0,95	5,38
HKSCM12-5	-	12	6	0,18	1,5	2,91
EM_9g	-	9	6	-	1,5	2,3
HK15168	-	8	6	0,12	1,2	1,94
TGY-1800A	22x11.7x24.3	8	6	0,1	1,7	3,07
DS918MP	22.5X11.5X24.6	9	-	0,06	1,8	3,83
MX-D80E	23.6x11.6x24	8,5	-	0,1	2	2,9
D56LV	19.8x8.2x20	5,6	-	0,1	0,9	5,34
RS-2125MGC	22.8x12x25.6	14,2	6	0,09	2,6	13,71
9103MG	21 x 20 x 8.5	5,6	-	0,12	1	9,63
BMS-306DMAX	22 x 10 x 23	7,1	6	0,11	2	9,89
TSS-9S	23.1x12.0x24.8	9	6	2	1,2	3,16
BMS-306BB	22 x 10 x 23	6,6	-	0,1	1,1	10
DS928HV	22.5X11.5X24.6	9	6	0,09	1,7	5,38
BMS-306MAX	22 x 10 x 23	7,1	-	0,11	2	8,62
TGY-1550A	21x19.6x20.1	5,5	-	0,1	0,9	2,83
TGY-1600A	22x11.7x22.8	6	-	0,1	1,2	3,07
HD-1900A	23x12.2x29	9	6	0,08	1,7	3,07
MX-A801	23.6x11.6x24	8,5	6	0,1	1,8	2,65

BMS-308DB	24 x 10 x 23.5	6,2	-	0,1	1,2	8,97
CS-918MP	22.5X11.5X24.6	9	6	0,06	1,8	3,29
EM_8g	21x11x28	8	-	0,12	1,4	2,5
HKSCM8	-	6,8	-	0,09	0,9	2,26
BMS-371	24 x 11 x 24	8,4	-	0,12	1,5	6,47
DS65HB	20.8x11x20	6,5	-	0,09	1,5	4,54
HK15178L	-	9,8	-	1,6	0,8	2,83
VS-5M	22.94 x 12.2 x 24.2	10	-	0,17	1,2	7,7
Mean		8,44		0,18	1,48	4,51
SD		1,96		0,38	0,44	2,87

APPENDIX C: Matlab Code for the hand current simulation

```
t = simout.time;
I = simout.data;
T = length (t);
plot (t,I);
title('Current vs time')
xlabel('Time (s)');
ylabel('Current (mA)');
integral = trapz (I);
Im = integral/T;
Im2 = mean(I);
```

APPENDIX D1: Matlab Code for the finger static study

```
clc
clear all

%Variables

Ax=1;
Ay=1;
Bx=1;
By=1;
Cx=1;
Cy=1;
Dx=1;
Dy=1;
Ex=1;
Ey=1;
Fx=1;
Fy=1;

alpha = 13.03;
beta = 49.35;
gamma = 10.43;
epsilon = 56.07;
delta = 10.10;
sigma = 10.07;
rho = 2.83;
```

```

theta = 37.39;
lambda = 7.01;
zeta =0.9;
eta =16.89;
tau = 33.14;

%Weight initial value
W=0;

Weight=zeros(size(20));
Actuator_force=zeros(size(20));

%Matriu de Coeficients

C=[Ax , 0*Ay , -Bx , 0*By , Cx , 0*Cy , 0*Dx , 0*Dy , 0*Ex , 0*Ey , 0*Fx , 0*Fy;
    0*Ax , -Ay , 0*Bx , By , 0*Cx , Cy , 0*Dx , 0*Dy , 0*Ex , 0*Ey , 0*Fx , 0*Fy;
    -Ax*(alpha/1000) , -Ay*(beta/1000) , Bx*(gamma/1000) , By*(epsilon/1000) ,
    0*Cx , 0*Cy , 0*Dx , 0*Dy , 0*Ex , 0*Ey , 0*Fx , 0*Fy;
    0*Ax , 0*Ay , Bx , 0*By , 0*Cx , 0*Cy , 0*Dx , 0*Dy , -Ex , 0*Ey , -Fx ,
    0*Fy;
    0*Ax , 0*Ay , 0*Bx , -By , 0*Cx , 0*Cy , 0*Dx , 0*Dy , 0*Ex , Ey , 0*Fx ,
    Fy;
    0*Ax , 0*Ay , -Bx*(delta/1000) ,-By*(sigma/1000) , 0*Cx , 0*Cy , 0*Dx ,
    0*Dy , Ex*(rho/1000) , Ey*(theta/1000) , 0*Fx , 0*Fy;
    0*Ax , 0*Ay , 0*Bx , 0*By , 0*Cx , 0*Cy , -Dx , 0*Dy , Ex , 0*Ey , 0*Fx ,
    0*Fy;
    0*Ax , 0*Ay , 0*Bx , 0*By , 0*Cx , 0*Cy , 0*Dx , Dy , 0*Ex , -Ey , 0*Fx ,
    0*Fy;
    0*Ax , 0*Ay , 0*Bx , 0*By , 0*Cx , 0*Cy , 0*Dx , 0*Dy , -Ex*(lambda/1000) ,
    -Ey*(zeta/1000) , 0*Fx , 0*Fy;
    -Ax , 0*Ay , 0*Bx , 0*By , 0*Cx , 0*Cy , Dx , 0*Dy , 0*Ex , 0*Ey , 0*Fx ,
    0*Fy;
    0*Ax , Ay , 0*Bx , 0*By , 0*Cx , 0*Cy , 0*Dx , -Dy , 0*Ex , 0*Ey , 0*Fx ,
    0*Fy;
    0*Ax , 0*Ay , 0*Bx , 0*By , 0*Cx , 0*Cy , Dx*(eta/1000) , -Dy*(tau/1000) ,
    0*Ex , 0*Ey , 0*Fx , 0*Fy;
    ];

n=6;

for i=1:n
    W=W+1;
    A=[0;0;0;0;0;0;-W;(-29.80/1000)*W;0;0;0];
    S=inv(C)*A;
    Weight(i)=W;
    Actuator_force(i)= [S(11)];
end

%Representació gràfica dels vectors

plot(Weight,Actuator_force)
ylabel('Actuator force (N)')
xlabel('Weight(N)')
title('Finger actuator static force vs weight')
hold on

%Càcul de l'equació de la recta

Equacio=polyfit(Weight,Actuator_force,1);

```

APPENDIX D2: Matlab Code for the thumb static study

```

clc
clear all

%Variables

Gx=1;
Gy=1;
Ix=1;
Iy=1;
Hx=1;
Hy=1;

alphax = 43;
alphay = 0.29;
betax = 46.2;
rhox = 3.02;
rhoy = 15.78;
thetax = 92.41;

%Weight initial value

W=0;

Weight=zeros(size(20));
Actuator_force=zeros(size(20));

%Matrix coeficients

C =[-Gx, 0*GY , 0*Hx , 0*Hy , Ix , 0*Iy;
      0*Gx , Gy , 0*Hx , 0*Hy , 0*Ix , -Iy;
      Gx*((rhoy+alphay)/1000) , Gy*(betax/1000) , 0*Hx , 0*Hy , 0*Ix , -Iy;
      Gx , 0*Gy , -Hx , 0*Hy , 0*Ix , 0*Iy;
      0*Gx , -Gy , 0*Hx , Hy , 0*Ix , 0*Iy;
      -Gx*(rhoy/1000) , -Gy*(rhox/1000) , 0*Hx , 0*Hy , 0*Ix , 0*Iy
    ];

%for loop to calculate the reactions

n=17;

for i=1:n

  W=W+1;
  A=[0;0;0;0;-W;((thetax-betax-rhox)/1000)*-W];
  S=inv(C)*A;
  Weight(i)=W;
  Actuator_force(i)= [S(5)];

end

%Representació gràfica dels vectors

plot(Weight,Actuator_force)
ylabel('Actuator force (N)')
xlabel('Weight (N)')
title('Finger actuator static force vs weight')
hold on

%Càlcul de l'equació de la recta

```

```
Equacio=polyfit(Weight,Actuator_force,1);
```

APPENDIX E: FEM Solidworks simulation stress study results.

Thumb load vs stress			Finger load vs stress		
Load (N)	max von Mises (Mpa)	nnodes	Load (N)	max von Mises (Mpa)	nnodes
10	12.30	96939	10	50.28	103877
20	24.61	96939	20	102.90	103877
30	36.91	96939	30	156.20	103877
40	49.21	96939	40	210.50	103877
50	61.51	96939	50	265.50	103877

Thumb convergence study			Finger convergence study		
Load (N)	max von Mises (Mpa)	nnodes	Load (N)	max von Mises (Mpa)	nnodes
30	31.47	12047	30	133.60	13101
30	31.55	15706	30	150.60	14527
30	32.74	24891	30	174.40	22401
30	34.29	60063	30	150.00	43108
30	36.91	96939	30	156.60	103877

APPENDIX F: FSR calibration equation values using $g = 9.81 \text{ m/s}^2$.

Digital Input (A0)	Vout (V)	mass (g)	Force (N)
580	2.83	150	1.47
714	3.49	250	2.45
770	3.76	350	3.43
827	4.04	494	4.84
850	4.15	560	5.49
891	4.35	800	7.84
914	4.47	900	8.82
923	4.51	1000	9.80
926	4.53	1100	10.78
937	4.58	1400	13.72
950	4.64	1500	14.70

APPENDIX G: Fingertip force values from the finger model.

Sample	Digital input (A0)	Digital input (V)	Force (N)
1	864	4.22	6.96
2	863	4.22	6.91
3	857	4.19	6.61
4	862	4.21	6.86
5	860	4.20	6.76

APPENDIX H: Fingertip force values from the thumb model.

Sample	Digital Input (A0)	Digital input (V)	Force (N)
1	972	4.75	14.81
2	967	4.73	14.33
3	968	4.73	14.42
4	967	4.73	14.33
5	970	4.74	14.62

APPENDIX I: Arduino script for serial EMG data acquisition using Matlab and Arduino.

```
int valADC=0;

void setup()
{
Serial.begin(9600);
}

void loop()
{
valADC = analogRead(A0);
Serial.println(valADC);
delay(1);
}
```

APPENDIX J: Matlab Function for serial EMG data acquisition using Matlab and Arduino.

```
function voltage=ADC_Serial2(samples) %Function recieve the number of samples
from Arduino serial

clc;
voltage=0;
voltage1=0;

% Delete previous ports and open new ones
delete(instrfind({'port'},{'COM9'}));
port=serial('COM9');
port.BaudRate=9600;

% Open the new port to use
fopen(port);
count=1;

%Print

figure('Name','Grafica de EMG')
title('GRAFICA DE EMG');
xlabel('Numero de Muestras');
ylabel('Voltaje (V)');
grid on;
hold on;
```

```

while count<=samples
    valADC=fscanf(port, '%d%d');
    %8 Bit conversion
    voltage(count)=valADC(1)*5/1023;
    plot(voltage);
    drawnow
    count=count+1;
end

%Close the port
fclose(port);

end

```

APPENDIX K: Matlab script to plot the results of the EMG acquisition.

```

clc
clear all

muestras = 500;

%grasp 4 Palm grasp
PALM_1= ADC_Serial2(muestras);
PALM_2= ADC_Serial2(muestras);
PALM_3= ADC_Serial2(muestras);
PALM_4= ADC_Serial2(muestras);

%grasp tip grasp
TIP_1= ADC_Serial2(muestras);
TIP_2= ADC_Serial2(muestras);
TIP_3= ADC_Serial2(muestras);
TIP_4= ADC_Serial2(muestras);

%Grasp trippod grasp
DITSTIP_1= ADC_Serial2(muestras);
DITSTIP_2= ADC_Serial2(muestras);
DITSTIP_3= ADC_Serial2(muestras);
DITSTIP_4= ADC_Serial2(muestras);

%Grasp lateral grasp
LATERAL_1 = ADC_Serial2(muestras);
LATERAL_2 = ADC_Serial2(muestras);
LATERAL_3 = ADC_Serial2(muestras);
LATERAL_4 = ADC_Serial2(muestras);

%Grasp Power Grasp
POWER_1 = ADC_Serial2(muestras);
POWER_2 = ADC_Serial2(muestras);
POWER_3 = ADC_Serial2(muestras);
POWER_4 = ADC_Serial2(muestras);

%nivell Basal pre muscle activation
BASAL_PRE_1 = ADC_Serial2(muestras);
BASAL_PRE_2 = ADC_Serial2(muestras);
BASAL_PRE_3 = ADC_Serial2(muestras);
BASAL_PRE_4 = ADC_Serial2(muestras);

%nivell basal post muscle activation
BASAL_POST_1 = ADC_Serial2(muestras);

```

```

BASAL_POST_2 = ADC_Serial2(muestras);
BASAL_POST_3 = ADC_Serial2(muestras);
BASAL_POST_4 = ADC_Serial2(muestras);

% wrist extension
EXT_1 = ADC_Serial2(muestras);
EXT_2 = ADC_Serial2(muestras);
EXT_3 = ADC_Serial2(muestras);
EXT_4 = ADC_Serial2(muestras);

plot(PALM_1(20:500), 'b');
hold on
plot(TIP_1(20:500), 'r');
hold on
plot(DITSTIP_1(20:500), 'g');
hold on
plot(LATERAL_1(20:500), 'y');
hold on
plot(POWER_1(20:500), 'b');
hold on
plot(BASAL_PRE_1(20:500), 'm');
hold on

plot(PALM_2(20:500), 'b');
hold on
plot(TIP_2(20:500), 'r');
hold on
plot(DITSTIP_2(20:500), 'g');
hold on
plot(LATERAL_2(20:500), 'y');
hold on
plot(POWER_2(20:500), 'k');
hold on
plot(BASAL_PRE_2(20:500), 'm');
hold on

plot(PALM_3(20:500), 'b');
hold on
plot(TIP_3(20:500), 'r');
hold on
plot(DITSTIP_3(20:500), 'g');
hold on
plot(LATERAL_3(20:500), 'y');
hold on
plot(POWER_3(20:500), 'k');
hold on
plot(BASAL_PRE_3(20:500), 'm');
hold on

plot(PALM_4(20:500), 'b');
hold on
plot(TIP_4(20:500), 'r');
hold on
plot(DITSTIP_4(20:500), 'g');
hold on
plot(LATERAL_4(20:500), 'y');
hold on
plot(POWER_4(20:500), 'k');
hold on
plot(BASAL_PRE_4(20:500), 'm');
hold on

```

```

hold on

%Av sample 1
mitjana_POWER_1= mean(POWER_1(20:500));
mitjana_PALM_1 = mean(PALM_1(20:500));
mitjana_DITSTIP_1 = mean(DITSTIP_1(20:500));
mitjana_TIP_1 = mean(TIP_1(20:500));
mitjana_LATERAL_1 = mean(LATERAL_1(20:500));
mitjana_BASAL_PRE_1 = mean(BASAL_PRE_1(20:500));

%STD sample 1
STD_POWER_1 = std(POWER_1(20:500));
STD_PALM_1 = std(PALM_1(20:500));
STD_DITSTIP_1 = std(DITSTIP_1(20:500));
STD_TIP_1 = std(TIP_1(20:500));
STD_LATERAL_1 = std(LATERAL_1(20:500));
STD_BASAL_PRE_1 = std(BASAL_PRE_1(20:500));

%Av sample 2
mitjana_POWER_2 = mean(POWER_2(20:500));
mitjana_PALM_2 = mean(PALM_2(20:500));
mitjana_DITSTIP_2 = mean(DITSTIP_2(20:500));
mitjana_TIP_2 = mean(TIP_2(20:500));
mitjana_LATERAL_2 = mean(LATERAL_2(20:500));
mitjana_BASAL_PRE_2 = mean(BASAL_PRE_2(20:500));

%STD sample 2
STD_POWER_2 = std(POWER_2(20:500));
STD_PALM_2 = std(PALM_2(20:500));
STD_DITSTIP_2 = std(DITSTIP_2(20:500));
STD_TIP_2 = std(TIP_2(20:500));
STD_LATERAL_2 = std(LATERAL_2(20:500));
STD_BASAL_PRE_2 = std(BASAL_PRE_2(20:500));

%Av sampls 3
mitjana_POWER_3 = mean(POWER_3(20:500));
mitjana_PALM_3 = mean(PALM_3(20:500));
mitjana_DITSTIP_3 = mean(DITSTIP_3(20:500));
mitjana_TIP_3 = mean(TIP_3(20:500));
mitjana_LATERAL_3 = mean(LATERAL_3(20:500));

%STD sample 3
STD_POWER_3 = std(POWER_3(20:500));
STD_PALM_3 = std(PALM_3(20:500));
STD_DITSTIP_3 = std(DITSTIP_3(20:500));
STD_TIP_3 = std(TIP_3(20:500));
STD_LATERAL_3 = std(LATERAL_3(20:500));

%Av sample 4
mitjana_POWER_4 = mean(POWER_4(20:500));
mitjana_PALM_4 = mean(PALM_4(20:500));
mitjana_DITSTIP_4 = mean(DITSTIP_4(20:500));
mitjana_TIP_4 = mean(TIP_4(20:500));
mitjana_LATERAL_4 = mean(LATERAL_4(20:500));

%STD sample 4
STD_POWER_4 = std(POWER_4(20:500));
STD_PALM_4 = std(PALM_4(20:500));
STD_DITSTIP_4 = std(DITSTIP_4(20:500));
STD_TIP_4 = std(TIP_4(20:500));

```

```

STD_LATERAL_4 = std(LATERAL_4(20:500));

%Globals Av

mitjana_POWER =
(mitjana_POWER_1+mitjana_POWER_2+mitjana_POWER_3+mitjana_POWER_4)/4;
mitjana_PALM = (mitjana_PALM_1+mitjana_PALM_2+mitjana_PALM_3+mitjana_PALM_4)/4;
mitjana_DITSTIP =
(mitjana_DITSTIP_1+mitjana_DITSTIP_2+mitjana_DITSTIP_3+mitjana_DITSTIP_4)/4;
mitjana_TIP = (mitjana_TIP_1+mitjana_TIP_2+mitjana_TIP_3+mitjana_TIP_4)/4;
mitjana_LATERAL =
(mitjana_LATERAL_1+mitjana_LATERAL_2+mitjana_LATERAL_3+mitjana_LATERAL_4)/4;
mitjana_BASAL_PRE = (mitjana_BASAL_PRE_1+mitjana_BASAL_PRE_2)/2;

%Values to vectors

sd_power = [STD_POWER_1,STD_POWER_2,STD_POWER_3,STD_POWER_4];
sd_palm = [STD_PALM_1,STD_PALM_2,STD_PALM_3,STD_PALM_4];
sd_ditstip = [STD_DITSTIP_1,STD_DITSTIP_2,STD_DITSTIP_3,STD_DITSTIP_4];
sd_tip = [STD_TIP_1,STD_TIP_2,STD_TIP_3,STD_TIP_4];
sd_lateral = [STD_LATERAL_1,STD_LATERAL_2,STD_LATERAL_3,STD_LATERAL_4];
sd_basal = [STD_BASAL_PRE_1,STD_BASAL_PRE_2];

%Maximum of STD
max_sd_power = max(sd_power);
max_sd_palm = max(sd_palm);
max_sd_ditstip = max(sd_ditstip);
max_sd_tip = max(sd_tip);
max_sd_lateral = max(sd_lateral);
max_sd_basal = max(sd_basal);

for n = 1:20
    m_basal (n) = mitjana_BASAL_PRE;
    m_lateral (n) = mitjana_LATERAL;
    m_tip (n) = mitjana_TIP;
    m_ditstip (n) = mitjana_DITSTIP;
    m_palm (n) = mitjana_PALM;
    m_power (n) = mitjana_POWER;
end

for n = 1:20
    SD_basal (n) = mitjana_BASAL_PRE+max_sd_basal;
    SD_lateral (n) = mitjana_LATERAL+max_sd_lateral;
    SD_tip_pos (n) = mitjana_TIP+max_sd_tip;
    SD_ditstip (n) = mitjana_DITSTIP+max_sd_ditstip;
    SD_palm (n) = mitjana_PALM+max_sd_palm;
    SD_power (n) = mitjana_POWER +max_sd_power;
end

for n = 1:20
    SD_basal_n (n) = mitjana_BASAL_PRE-max_sd_basal;
    SD_lateral_n (n) = mitjana_LATERAL-max_sd_lateral;
    SD_tip_pos_n (n) = mitjana_TIP-max_sd_tip;
    SD_ditstip_n (n) = mitjana_DITSTIP-max_sd_ditstip;
    SD_palm_n (n) = mitjana_PALM-max_sd_palm;
    SD_power_n (n) = mitjana_POWER-max_sd_power;
end

```

Design and development of a 6 DOF, 3D printable, open source bionic hand

```
%Plot
plot(m_basal,'m');
hold on
plot(SD_basal,'m');
hold on
plot(SD_basal_n,'m');
hold on
plot(m_lateral,'y');
hold on
plot(SD_lateral,'y');
hold on
plot(SD_lateral_n,'y');
hold on
plot(m_ditstip,'g');
hold on
plot(SD_ditstip,'g');
hold on
plot(SD_ditstip_n,'g');
hold on
plot(m_palm,'b');
hold on
plot(SD_palm,'b');
hold on
plot(SD_palm_n,'b');
hold on
plot(m_power,'k');
hold on
plot(SD_power,'k');
hold on
plot(SD_power_n,'k');
hold on
plot(m_tip,'r');
hold on
plot(sd_tip_pos,'r');
hold on
plot(SD_tip_pos_n,'r');
hold on

legend('mbasal','mlateral','mditstip','mpalm','mpower','mtip');
```

APPENDIX L: Matlab script to plot the Solidworks kinematics simulation.

```
clc
clear all

% IMPORT FROM .xlsx SOLIDWORKS MOTION STUDY GENERATED FILES %

index = 'index.xlsx';
middle = 'middle.xlsx';
ring = 'ring.xlsx';
pinky = 'pinky.xlsx';
thumb1 = 'thumb_1mm.xlsx';
thumb2 = 'thumb_10mm.xlsx';
thumb3 = 'thumb_20mm.xlsx';
thumb4 = 'thumb_18mm.xlsx';
thumb5 = 'thumb_16mm.xlsx';
thumb6 = 'thumb_14mm.xlsx';
thumb7 = 'thumb_12mm.xlsx';
thumb8 = 'thumb_8mm.xlsx';
thumb9 = 'thumb_6mm.xlsx';
```

```
thumb10 = 'thumb_4mm.xlsx';
thumb11 = 'thumb_2mm.xlsx';

sheet1 = 1;
range1 = 'D3:D29';
range2 = 'E3:E29';
range3 = 'F3:F29';

range12 = 'D3:D37';
range22 = 'E3:E37';
range32 = 'F3:F37';

% Variables for index finger

index_x = xlsread(index,sheet1,range1);
index_y = xlsread(index,sheet1,range2);
index_z = xlsread(index,sheet1,range3);

% Variables for middle finger

middle_x = xlsread(middle,sheet1,range1);
middle_y = xlsread(middle,sheet1,range2);
middle_z = xlsread(middle,sheet1,range3);

% Variables for ring finger

ring_x = xlsread(ring,sheet1,range1);
ring_y = xlsread(ring,sheet1,range2);
ring_z = xlsread(ring,sheet1,range3);

% Variables for pinky finger

pinky_x = xlsread(pinky,sheet1,range1);
pinky_y = xlsread(pinky,sheet1,range2);
pinky_z = xlsread(pinky,sheet1,range3);

% Variables for thumb

thumb1_x = xlsread(thumb1,sheet1,range12);
thumb1_y = xlsread(thumb1,sheet1,range22);
thumb1_z = xlsread(thumb1,sheet1,range32);

thumb2_x = xlsread(thumb2,sheet1,range12);
thumb2_y = xlsread(thumb2,sheet1,range22);
thumb2_z = xlsread(thumb2,sheet1,range32);

thumb3_x = xlsread(thumb3,sheet1,range12);
thumb3_y = xlsread(thumb3,sheet1,range22);
thumb3_z = xlsread(thumb3,sheet1,range32);

thumb4_x = xlsread(thumb4,sheet1,range12);
thumb4_y = xlsread(thumb4,sheet1,range22);
thumb4_z = xlsread(thumb4,sheet1,range32);

thumb5_x = xlsread(thumb5,sheet1,range12);
thumb5_y = xlsread(thumb5,sheet1,range22);
thumb5_z = xlsread(thumb5,sheet1,range32);
```

```

thumb6_x = xlsread(thumb6,sheet1,range12);
thumb6_y = xlsread(thumb6,sheet1,range22);
thumb6_z = xlsread(thumb6,sheet1,range32);

thumb7_x = xlsread(thumb7,sheet1,range12);
thumb7_y = xlsread(thumb7,sheet1,range22);
thumb7_z = xlsread(thumb7,sheet1,range32);

thumb8_x = xlsread(thumb8,sheet1,range12);
thumb8_y = xlsread(thumb8,sheet1,range22);
thumb8_z = xlsread(thumb8,sheet1,range32);

thumb9_x = xlsread(thumb9,sheet1,range12);
thumb9_y = xlsread(thumb9,sheet1,range22);
thumb9_z = xlsread(thumb9,sheet1,range32);

thumb10_x = xlsread(thumb10,sheet1,range12);
thumb10_y = xlsread(thumb10,sheet1,range22);
thumb10_z = xlsread(thumb10,sheet1,range32);

thumb11_x = xlsread(thumb11,sheet1,range12);
thumb11_y = xlsread(thumb11,sheet1,range22);
thumb11_z = xlsread(thumb11,sheet1,range32);

% 3D plots

scatter3(index_x,index_y,index_z,'m','MarkerFaceColor','m')
hold on
scatter3(middle_x,middle_y,middle_z,'r','MarkerFaceColor','r')
hold on
scatter3(ring_x,ring_y,ring_z,'b','MarkerFaceColor','b')
hold on
scatter3(pinky_x,pinky_y,pinky_z,'y','MarkerFaceColor','y')
hold on
scatter3(thumb1_x,thumb1_y,thumb1_z,'g','MarkerFaceColor','g')
hold on
scatter3(thumb2_x,thumb2_y,thumb2_z,'g','MarkerFaceColor','g')
hold on
scatter3(thumb2_x,thumb2_y,thumb2_z,'g','MarkerFaceColor','g')
hold on
scatter3(thumb3_x,thumb3_y,thumb3_z,'g','MarkerFaceColor','g')
hold on
scatter3(thumb4_x,thumb4_y,thumb4_z,'g','MarkerFaceColor','g')
hold on
scatter3(thumb5_x,thumb5_y,thumb5_z,'g','MarkerFaceColor','g')
hold on
scatter3(thumb6_x,thumb6_y,thumb6_z,'g','MarkerFaceColor','g')
hold on
scatter3(thumb7_x,thumb7_y,thumb7_z,'g','MarkerFaceColor','g')
hold on
scatter3(thumb8_x,thumb8_y,thumb8_z,'g','MarkerFaceColor','g')
hold on
scatter3(thumb9_x,thumb9_y,thumb9_z,'g','MarkerFaceColor','g')
hold on
scatter3(thumb10_x,thumb10_y,thumb10_z,'g','MarkerFaceColor','g')
hold on
scatter3(thumb11_x,thumb11_y,thumb11_z,'g','MarkerFaceColor','g')
hold on

xlabel('x (mm)')
ylabel('y (mm)')

```

```

zlabel('z (mm)')
legend('Thumb')
legend('boxoff')

xlabel('x (mm)')
ylabel('y (mm)')
zlabel('z (mm)')
legend('Index', 'Middle', 'Ring', 'Little', 'Thumb')
legend('boxoff')

```

APPENDIX M: Tables of finger speed values for the index finger.

Actuator displacement (mm)	x (mm)	y (mm)	Samples	time	dx/dt	dy/dt	Tan	angle(rad)	angle(deg)
4.00	-124.06	-29.99	0.00	0.00	3.26	-9.86	-3.03	2.82	161.72
4.60	-123.93	-30.38	1.00	0.04	9.83	-28.22	-2.87	2.81	160.80
5.20	-123.54	-31.51	2.00	0.08	16.96	-44.25	-2.61	2.78	159.03
5.80	-122.86	-33.28	3.00	0.12	25.04	-57.70	-2.30	2.73	156.54
6.40	-121.86	-35.59	4.00	0.16	34.22	-68.44	-2.00	2.68	153.44
7.00	-120.49	-38.33	5.00	0.20	44.45	-76.43	-1.72	2.61	149.82
7.60	-118.71	-41.38	6.00	0.24	55.58	-81.68	-1.47	2.54	145.76
8.20	-116.49	-44.65	7.00	0.28	67.37	-84.19	-1.25	2.47	141.33
8.80	-113.79	-48.02	8.00	0.32	79.49	-83.99	-1.06	2.38	136.58
9.40	-110.61	-51.38	9.00	0.36	91.59	-81.11	-0.89	2.30	131.53
10.00	-106.95	-54.62	10.00	0.40	103.26	-75.61	-0.73	2.20	126.21
10.60	-102.82	-57.65	11.00	0.44	114.05	-67.61	-0.59	2.11	120.66
11.20	-98.26	-60.35	12.00	0.48	123.50	-57.29	-0.46	2.01	114.89
11.80	-93.32	-62.64	13.00	0.52	131.12	-44.92	-0.34	1.90	108.91
12.40	-88.07	-64.44	14.00	0.56	136.42	-30.90	-0.23	1.79	102.76
13.00	-82.62	-65.68	15.00	0.60	138.95	-15.75	-0.11	1.68	96.47
13.60	-77.06	-66.31	16.00	0.64	138.30	-0.17	0.00	1.57	90.07
14.20	-71.53	-66.31	17.00	0.68	134.16	14.98	0.11	1.46	83.63
14.80	-66.16	-65.71	18.00	0.72	126.36	28.66	0.23	1.35	77.22
15.40	-61.11	-64.57	19.00	0.76	114.87	39.63	0.35	1.24	70.96
16.00	-56.51	-62.98	20.00	0.80	99.87	46.52	0.47	1.13	65.02
16.60	-52.52	-61.12	21.00	0.84	81.74	47.91	0.59	1.04	59.62
17.20	-49.25	-59.20	22.00	0.88	60.96	42.60	0.70	0.96	55.06
17.80	-46.81	-57.50	23.00	0.92	38.00	30.03	0.79	0.90	51.68
18.40	-45.29	-56.30	24.00	0.96	13.10	11.05	0.84	0.87	49.85
19.00	-44.77	-55.86	25.00	1.00	0.00	0.00	1.25	0.68	38.71

APPENDIX N: Matlab script to compare the index finger of Grasp and the model hand.

```

clc
clear all

% variables

xi = [];
yi = [];

l1 = 40;
l2 = 22;
l3 = 25;

q1 = [0:1:90];
q2 = [0:1:90];
q3 = [0:1:90];

cxi = -51.5;
cy = -15;
zi = ones(1,90).*33;

n = 90;

% Ideal index values

for i=1:n

xi(i) = cxi + l1* cosd(q1(i))+l2*cosd(q1(i)+q2(i))+l3*cosd(q1(i)+q2(i)+q3(i));
yi(i) = cy - l1* sind(q1(i))+l2*sind(q1(i)+q2(i))+l3*sind(q1(i)+q2(i)+q3(i));

end

index = 'index.xlsx';

sheet1 = 1;
range1 = 'D3:D29';
range2 = 'E3:E29';
range3 = 'F3:F29';

% Variables for the grasp index finger

index_x = xlsread(index,sheet1,range1);
index_y = xlsread(index,sheet1,range2);
index_z = xlsread(index,sheet1,range3);

% A rotation in the x and y axis is applied respectively
index_y = index_y*-1;
index_x = index_x*-1;
% A translation in the y and r axis is applied respectively
index_y = index_y-44.98;
index_x = index_x-88.06;

% Plot
scatter3(xi,yi,zi,'r','filled');
hold on
scatter3(index_x,index_y,index_z,'b','MarkerFaceColor','b')
hold on
title('Model index finger and Grasp finger trajectories')
xlabel('x(mm)')
ylabel('y(mm)')

```

```
zlabel('z (mm)')
```

APPENDIX O: Real values of fingers speed.

	Sample	Angle (°)	t0(s)	tf(s)	t(s)	Angular velocity (°/s)	Mean (°/s)	Std (°/s)
Finger flexion	Finger 1	85	0.3	1.66	1.36		62.50	
	Finger 2	84	0.84	2.29	1.45		57.93	59.45
	Finger 3	84	0.5	1.95	1.45		57.93	2.64
Thumb opposition	Thumb 1	99	0.06	0.66	0.6		165.00	
	Thumb 2	102	1.24	2.05	0.81		125.93	143.45
	Thumb 3	99	0.7	1.41	0.71		139.44	19.84
Finger extension	Finger 1	85	2.56	3.43	0.87		97.70	
	Finger 2	84	2.69	3.8	1.11		75.68	84.46
	Finger 3	84	2.89	3.94	1.05		80.00	11.67
Thumb retroposition	Thumb 1	99	1.16	1.53	0.37		267.57	
	Thumb 2	102	2.76	3.19	0.43		237.21	248.75
	Thumb 3	99	1.91	2.32	0.41		241.46	16.44

APPENDIX P: Hand control program.

```
// Include the Servo.h library
#include <Servo.h>

const float max_EMG = 200;

// Declare the digital pin D2 for the pushbutton
const int pushbutton = 2;

// Declare the servos
Servo index;
Servo middle;
Servo ring;
Servo small;
Servo thumb_flexion;
Servo thumb_opposition;

// Declare the buttonstate variable
int buttonstate = 0;
```

```
void setup()
{
    // Set the serial communication at 9600 bauds
    Serial.begin(9600);

    //Declare the pushbutton digital port as an input
    pinMode(pushbutton, INPUT_PULLUP);

    // Declare the digital pins where the linear servos are attached
    index.attach(6);
    middle.attach(5);
    ring.attach(10);
    small.attach(9);
    thumb_flexion.attach(3);
    thumb_opposition.attach(11);
}

void loop()
{
    // Increase the buttonstate value if the pushbutton is HIGH
    if (digitalRead(pushbutton) == HIGH)
    {
        buttonstate = (buttonstate + 1) % 6;
        delay(200);
    }

    // Read the analog EMG signal from the port A0
    int flexion2= analogRead(A0);
    //Convert the flexion sensor (calibration function)
    float flexion3 = (-107/max_EMG) * flexion2 + 145;
    int flexion4 = int(flexion3);

    // Repeat the last 3 steps for the thumb opposition
```

Design and development of a 6 DOF, 3D printable, open source bionic hand

```
int opposition2= analogRead(A0);  
float opposition3 = (90/max_EMG) * opposition2 + 60;  
int opposition4 = int(opposition3);  
  
// Change across the different types of grasps when the buttonstate changes  
// calling their functions in each case  
  
switch (buttonstate) {  
    case 0:  
        tip_grasp(flexion4,opposition4);  
        break;  
    case 1:  
        trippod_grasp(flexion4,opposition4);  
        break;  
    case 2:  
        lateral_grasp(flexion4,opposition4);  
        break;  
    case 3:  
        hook_grasp(flexion4,opposition4);  
        break;  
    case 4:  
        spherical_grasp(flexion4,opposition4);  
        break;  
    case 5:  
        cylindrical_grasp(flexion4,opposition4);  
        break;  
}  
}  
  
// Tip grasp function
```

```
void tip_grasp(int flexion3, int opposition3)  
{  
    index.write(flexion3);
```

```
thumb_opposition.write(140);
thumb_flexion.write(70);
}

// Trippod grasp function
void trippod_grasp(int flexion3, int opposition3)
{
    index.write(flexion3);
    middle.write(flexion3);
    thumb_opposition.write(140);
    thumb_flexion.write(70);
}

// Lateral grasp function
void lateral_grasp(int flexion3, int opposition3)
{
    index.write(flexion3);
    middle.write(flexion3);
    ring.write(flexion3);
    small.write(flexion3);
    thumb_opposition.write(60);
    thumb_flexion.write(flexion3);
}

// Hook grasp function
void hook_grasp(int flexion3, int opposition3)
{
    index.write(flexion3);
    middle.write(flexion3);
    ring.write(flexion3);
    small.write(flexion3);
    thumb_opposition.write(60);
    thumb_flexion.write(120);
}
```

```
// Spherical grasp function
void spherical_grasp (int flexion3, int opposition3)
{
    index.write(flexion3);
    middle.write(flexion3);
    ring.write(flexion3);
    small.write(flexion3);
    thumb_opposition.write(140);
    thumb_flexion.write(flexion3);
}

// Cylindrical grasp function
void cylindrical_grasp (int flexion3, int opposition3)
{
    index.write(flexion3);
    middle.write(flexion3);
    ring.write(flexion3);
    small.write(flexion3);
    thumb_opposition.write(140);
    thumb_flexion.write(flexion3);
}
```

APPENDIX Q: Graphical user interface code.

Matlab GUI editor:

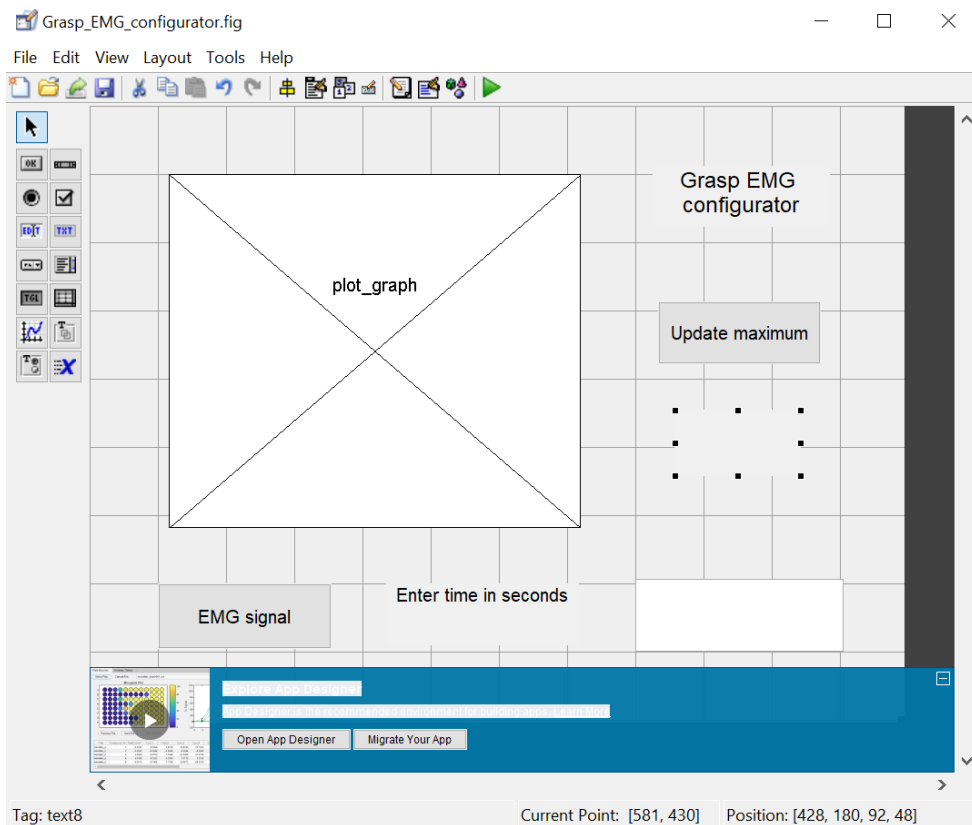


Figure 149: Image of the Matlab GUI editor.

Functions behind the GUI widgets:

```
function varargout = Grasp_EMG_configurator(varargin)
%GRASP_EMG_CONFIGURATOR MATLAB code file for Grasp_EMG_configurator.fig
%   GRASP_EMG_CONFIGURATOR, by itself, creates a new GRASP_EMG_CONFIGURATOR or
% raises the existing
%      singleton*.
%
%      H = GRASP_EMG_CONFIGURATOR returns the handle to a new
GRASP_EMG_CONFIGURATOR or the handle to
%      the existing singleton*.
%
%      GRASP_EMG_CONFIGURATOR('Property','Value',...) creates a new
GRASP_EMG_CONFIGURATOR using the
%      given property value pairs. Unrecognized properties are passed via
%      varargin to Grasp_EMG_configurator_OpeningFcn. This calling syntax
produces a
%      warning when there is an existing singleton*.
%
%      GRASP_EMG_CONFIGURATOR('CALLBACK') and
GRASP_EMG_CONFIGURATOR('CALLBACK',hObject,...) call the
%      local function named CALLBACK in GRASP_EMG_CONFIGURATOR.M with the given
input
%      arguments.
%
```

```
% *See GUI Options on GUIDE's Tools menu. Choose "GUI allows only one
% instance to run (singleton)".
%
% See also: GUIDE, GUIDATA, GUIHANDLES

% Edit the above text to modify the response to help Grasp_EMG_configurator

% Last Modified by GUIDE v2.5 07-May-2019 19:25:07

% Begin initialization code - DO NOT EDIT
gui_Singleton = 1;
gui_State = struct('gui_Name',         mfilename, ...
                   'gui_Singleton',    gui_Singleton, ...
                   'gui_OpeningFcn',   @Grasp_EMG_configurator_OpeningFcn, ...
                   'gui_OutputFcn',    @Grasp_EMG_configurator_OutputFcn, ...
                   'gui_LayoutFcn',    [], ...
                   'gui_Callback',     []);
if nargin && ischar(varargin{1})
    gui_State.gui_Callback = str2func(varargin{1});
end

if nargout
    [varargout{1:nargout}] = gui_mainfcn(gui_State, varargin{:});
else
    gui_mainfcn(gui_State, varargin{:});
end
% End initialization code - DO NOT EDIT

% --- Executes just before Grasp_EMG_configurator is made visible.
function Grasp_EMG_configurator_OpeningFcn(hObject, eventdata, handles, varargin)
% This function has no output args, see OutputFcn.
% hObject    handle to figure
% eventdata   reserved - to be defined in a future version of MATLAB
% handles    structure with handles and user data (see GUIDATA)
% varargin   unrecognizedPropertyName/PropertyValue pairs from the
%             command line (see VARARGIN)

% Choose default command line output for Grasp_EMG_configurator
handles.output = hObject;

% Update handles structure
guidata(hObject, handles);

% Remove the data from the port
delete(instrfind({'PORT'}, {'COM5'}));
clear all;
clc;
% Define a global variable a
global a ;
% Assign the variable a to the arduino board
a=arduino('com5','Nano3');

image = imread ('logo.gif');
handles.plot_graph=imshow(image);

% UIWAIT makes Grasp_EMG_configurator wait for user response (see UIRESUME)
% uiwait(handles.figure1);
```

```
% --- Outputs from this function are returned to the command line.
function varargout = Grasp_EMG_configurator_OutputFcn(hObject, eventdata,
handles)
% varargout cell array for returning output args (see VARARGOUT);
% hObject handle to figure
% eventdata reserved - to be defined in a future version of MATLAB
% handles structure with handles and user data (see GUIDATA)

% Get default command line output from handles structure
varargout{1} = handles.output;

% --- Executes on button press in EMG.
function EMG_Callback(hObject, eventdata, handles)
% hObject handle to EMG (see GCBO)
% eventdata reserved - to be defined in a future version of MATLAB
% handles structure with handles and user data (see GUIDATA)

% Define two global variables a and i
global a i M;

% initialize the x variable
x=0;

% For 1 to the time introduced by the user:
for i = 1:1:handles.time
    % Assign the voltage of the Analog input 0 to the h variable
    h=a.readVoltage('A0');
    % Convert the voltage signal to a value between 0 and 1023
    h=h*1023/5;
    x=[x,h];
    M = max(x)
    % Plot the x variable
    plot(x); grid on;
    axis([0,handles.time 0 1100]);
    % delay
    pause(.0001);
end

% --- Executes on button press in update_max.
function update_max_Callback(hObject, eventdata, handles)
% hObject handle to update_max (see GCBO)
% eventdata reserved - to be defined in a future version of MATLAB
% handles structure with handles and user data (see GUIDATA)

% Define again the global variable M
global M;

% Set on static text (text8) the converted value of M to a string
set(handles.text8,'string',num2str(M));

function time_value_Callback(hObject, eventdata, handles)
% hObject handle to time_value (see GCBO)
% eventdata reserved - to be defined in a future version of MATLAB
% handles structure with handles and user data (see GUIDATA)

% Hints: get(hObject,'String') returns contents of time_value as text
% str2double(get(hObject,'String')) returns contents of time_value as a
double

% Get the value of time introduced by the user
```

```

handles.data1=get(hObject,'string');
% Convert the value into a string
handles.time=str2double(handles.data1);
%Save th value on the GUI data
guidata(hObject,handles);

% --- Executes during object creation, after setting all properties.
function time_value_CreateFcn(hObject, eventdata, handles)
% hObject    handle to time_value (see GCBO)
% eventdata   reserved - to be defined in a future version of MATLAB
% handles    empty - handles not created until after all CreateFcns called

% Hint: edit controls usually have a white background on Windows.
%       See ISPC and COMPUTER.
if ispc && isequal(get(hObject,'BackgroundColor'),
get(0,'defaultUicontrolBackgroundColor'))
    set(hObject,'BackgroundColor','white');
end


function maximum_value_Callback(hObject, eventdata, handles)
% hObject    handle to maximum_value (see GCBO)
% eventdata   reserved - to be defined in a future version of MATLAB
% handles    structure with handles and user data (see GUIDATA)

% Hints: get(hObject,'String') returns contents of maximum_value as text
%        str2double(get(hObject,'String')) returns contents of maximum_value as a
double

% --- Executes during object creation, after setting all properties.
function maximum_value_CreateFcn(hObject, eventdata, handles)
% hObject    handle to maximum_value (see GCBO)
% eventdata   reserved - to be defined in a future version of MATLAB
% handles    empty - handles not created until after all CreateFcns called

% Hint: edit controls usually have a white background on Windows.
%       See ISPC and COMPUTER.
if ispc && isequal(get(hObject,'BackgroundColor'),
get(0,'defaultUicontrolBackgroundColor'))
    set(hObject,'BackgroundColor','white');
end

```